

BOUNDARY CORRELATIONS IN PLANAR LERW AND UST

ALEX KARRILA

`alex.karrila@aalto.fi`

Department of Mathematics and Systems Analysis
P.O. Box 11100, FI-00076 Aalto University, Finland

KALLE KYTÖLÄ

`kalle.kytola@aalto.fi`

Department of Mathematics and Systems Analysis
P.O. Box 11100, FI-00076 Aalto University, Finland
<https://math.aalto.fi/~kkytola/>

EVELIINA PELTOLA

`eveliina.peltola@unige.ch`

Section de Mathématiques, Université de Genève
2–4 rue du Lièvre, Case Postale 64, 1211 Genève 4, Switzerland

ABSTRACT. We find explicit formulas for the probabilities of general boundary visit events for planar loop-erased random walks, as well as connectivity events for branches in the uniform spanning tree. We show that both probabilities, when suitably renormalized, converge in the scaling limit to conformally covariant functions which satisfy partial differential equations of second and third order, as predicted by conformal field theory. The scaling limit connectivity probabilities also provide formulas for the pure partition functions of multiple SLE_κ at $\kappa = 2$.

CONTENTS

1. Introduction	2
1.1. Boundary visit probabilities of the loop-erased random walk	3
1.2. Connectivity probabilities of boundary branches in the uniform spanning tree	5
1.3. Steps of the proof(s)	7
1.4. Multiple SLE_2	8
1.5. Beyond the present work: conformal blocks and q -deformations	8
1.6. Organization of the article	9
2. Combinatorics of link patterns and the parenthesis reversal relation	9
2.1. Combinatorial objects and bijections	10
2.2. Partial order and the parenthesis reversal relation	11
2.3. Dyck tilings and inversion of weighted incidence matrices	14
2.4. Wedges, slopes, and link removals	19

2.5. Cascades of weighted incidence matrices	24
2.6. Inverse Fomin type sums	26
3. Uniform spanning trees and loop-erased random walks	30
3.1. Graphs embedded in a planar domain	30
3.2. The planar uniform spanning tree	31
3.3. Relation between uniform spanning trees and loop-erased random walks	34
3.4. Fomin's formula	37
3.5. Solution of the connectivity partition functions	39
3.6. Random spanning trees on weighted graphs	41
3.7. Scaling limits	41
3.8. Generalizations of the main results	44
4. Relation to multiple SLEs	47
4.1. Multiple SLEs	48
4.2. Proof of Theorem 4.1	51
5. Boundary visit probabilities and third order PDEs	54
5.1. Scaling limit of boundary visit probabilities	55
5.2. Third order partial differential equations through fusion	59
5.3. Proof of Theorem 3.17	65
5.4. Asymptotics of the scaling limits of the boundary visit probabilities	65
Appendix A. Example boundary visit formulas	69
A.1. One boundary visit	69
A.2. Two boundary visits	69
References	70

1. INTRODUCTION

In this article, we consider the planar loop-erased random walk (LERW) and a closely related model, the planar uniform spanning tree (UST). We find explicit expressions for probabilities of certain connectivity and boundary visit events in these models, and prove that, in the scaling limit as the lattice spacing tends to zero, these observables converge to conformally covariant functions, which satisfy systems of second and third order partial differential equations (PDEs) predicted by conformal field theory (CFT) [BPZ84b, BSA88, BB03, BBK05, KP19, Dub15a, Dub15b, JJK16]. As a byproduct, we also obtain formulas for the pure partition functions of multiple Schramm-Loewner evolutions (SLEs), and the existence of all extremal local multiple SLEs at the specific parameter value $\kappa = 2$ corresponding to these models [BBK05, Dub07, KP16].

We now give a brief overview of the main results of this article. The detailed formulations of the statements made here are given in the bulk of the article, as referred to below.

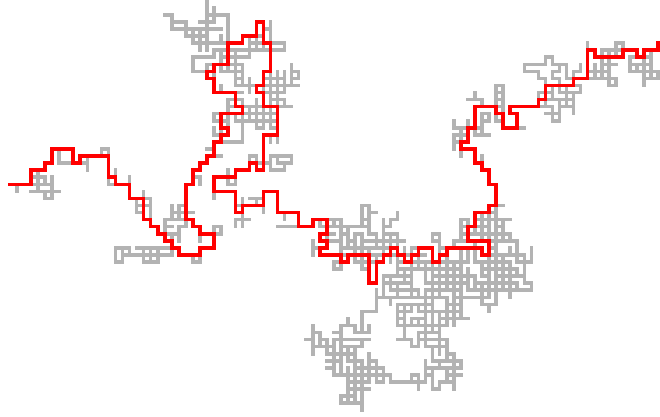


FIGURE 1.1. A loop-erased random walk on the square grid and the underlying random walk (in grey).

1.1. Boundary visit probabilities of the loop-erased random walk. Throughout, we let $\mathcal{G} = (\mathcal{V}, \mathcal{E})$ be a finite connected graph with a distinguished non-empty subset $\partial\mathcal{V} \subset \mathcal{V}$ of vertices, called boundary vertices. We assume that \mathcal{G} is a planar graph embedded in a Jordan domain $\Lambda \subset \mathbb{C}$ such that the boundary vertices $\partial\mathcal{V}$ lie on the Jordan curve $\partial\Lambda$. We denote by $\partial\mathcal{E} \subset \mathcal{E}$ the set of edges $e = \langle e^\partial, e^\circ \rangle$ which connect a boundary vertex $e^\partial \in \partial\mathcal{V}$ to an interior vertex $e^\circ \in \mathcal{V}^\circ := \mathcal{V} \setminus \partial\mathcal{V}$.

Our scaling limit results are valid in any setup where the random walk excursion kernels and their discrete derivatives on the graphs converge to the Brownian excursion kernels and their derivatives. To be specific, we present the results in the following square grid approximations (see Figure 3.7). We fix a Jordan domain Λ and a number of boundary points p_1, p_2, \dots and $\hat{p}_1, \hat{p}_2, \dots$ on horizontal or vertical parts of the boundary $\partial\Lambda$. For any small $\delta > 0$, we let $\mathcal{G}^\delta = (\mathcal{V}^\delta, \mathcal{E}^\delta)$ be a subgraph of the square lattice $\delta\mathbb{Z}^2$ of mesh size δ naturally approximating the domain Λ (as detailed in Section 3). We also let $e_j^\delta \in \partial\mathcal{E}^\delta$ be the boundary edge nearest to p_j , and let $\hat{e}_s^\delta \in \mathcal{E}^\delta$ be the edge at unit graph distance from the boundary nearest to \hat{p}_s . By scaling limits we mean limits of our quantities of interest as $\delta \rightarrow 0$ in this setting.

Generally, a loop-erased random walk (LERW) is a simple path on the graph obtained by erasing loops from a random walk in their order of appearance — see Figure 1.1 for illustration and Section 3 for the precise definitions. Choose two boundary edges $e_{\text{in}} = \langle e_{\text{in}}^\partial, e_{\text{in}}^\circ \rangle$ and $e_{\text{out}} = \langle e_{\text{out}}^\partial, e_{\text{out}}^\circ \rangle$. By the LERW λ on \mathcal{G} from e_{in} to e_{out} we mean the loop-erasure of a random walk started from the vertex e_{in}° and conditioned to reach the boundary via the edge e_{out} . In the present article, we find an explicit formula for the probability of the event that the LERW λ passes through given edges $\hat{e}_1, \dots, \hat{e}_{N'}$ at unit distance from the boundary, as illustrated in Figure 1.2. Moreover, we prove that this probability converges in the scaling limit to a conformally covariant function ζ , which satisfies a system of second and third order partial differential equations, as has been previously predicted based on conformal field theory.

Theorem (Theorem 3.17). *Let \mathcal{G}^δ with $e_{\text{in}}^\delta, e_{\text{out}}^\delta \in \partial\mathcal{E}^\delta$ and $\hat{e}_1^\delta, \dots, \hat{e}_{N'}^\delta \in \mathcal{E}^\delta$ be a square grid approximation of a domain Λ with marked boundary points $p_{\text{in}}, p_{\text{out}}, \hat{p}_1, \dots, \hat{p}_{N'}$. The probability that the LERW λ^δ on \mathcal{G}^δ from e_{in}^δ to e_{out}^δ passes through the edges $\hat{e}_1^\delta, \dots, \hat{e}_{N'}^\delta$ has the following conformally covariant scaling limit:*

$$\frac{1}{\delta^{3N'}} \mathbb{P}_{e_{\text{in}}^\delta, e_{\text{out}}^\delta} [\lambda^\delta \text{ uses } \hat{e}_1^\delta, \dots, \hat{e}_{N'}^\delta] \xrightarrow{\delta \rightarrow 0} \prod_{s=1}^{N'} |\phi'(\hat{p}_s)|^3 \times \frac{\zeta(\phi(p_{\text{in}}); \phi(\hat{p}_1), \dots, \phi(\hat{p}_{N'}); \phi(p_{\text{out}}))}{(\phi(p_{\text{out}}) - \phi(p_{\text{in}}))^{-2}},$$

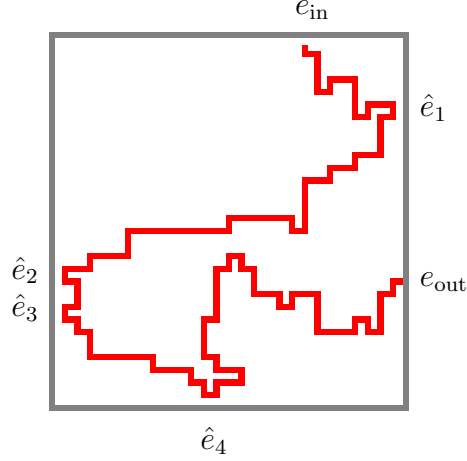


FIGURE 1.2. Illustration of a loop-erased random walk passing through edges at unit distance from the boundary. We study the probabilities of such boundary visit events.

where $\phi: \Lambda \rightarrow \mathbb{H}$ is a conformal map from the domain Λ to the upper half-plane $\mathbb{H} = \{z \in \mathbb{C} \mid \Im(z) > 0\}$. The function $\zeta(x_{\text{in}}; \hat{x}_1, \dots, \hat{x}_{N'}; x_{\text{out}})$ is a positive function of the real points $x_{\text{in}}, \hat{x}_1, \dots, \hat{x}_{N'}, x_{\text{out}}$, satisfying the following system of linear partial differential equations: the N' third order PDEs

$$\begin{aligned} & \left[\frac{\partial^3}{\partial \hat{x}_s^3} + \frac{8}{x_{\text{in}} - \hat{x}_s} \frac{\partial^2}{\partial x_{\text{in}} \partial \hat{x}_s} - \frac{8}{(x_{\text{in}} - \hat{x}_s)^2} \frac{\partial}{\partial \hat{x}_s} - \frac{12}{(x_{\text{in}} - \hat{x}_s)^2} \frac{\partial}{\partial x_{\text{in}}} + \frac{24}{(x_{\text{in}} - \hat{x}_s)^3} \right. \\ & + \frac{8}{x_{\text{out}} - \hat{x}_s} \frac{\partial^2}{\partial x_{\text{out}} \partial \hat{x}_s} - \frac{8}{(x_{\text{out}} - \hat{x}_s)^2} \frac{\partial}{\partial \hat{x}_s} - \frac{12}{(x_{\text{out}} - \hat{x}_s)^2} \frac{\partial}{\partial x_{\text{out}}} + \frac{24}{(x_{\text{out}} - \hat{x}_s)^3} \\ & \left. + \sum_{\substack{1 \leq t \leq N' \\ t \neq s}} \left(\frac{8}{\hat{x}_t - \hat{x}_s} \frac{\partial^2}{\partial \hat{x}_t \partial \hat{x}_s} - \frac{24}{(\hat{x}_t - \hat{x}_s)^2} \frac{\partial}{\partial \hat{x}_s} - \frac{12}{(\hat{x}_t - \hat{x}_s)^2} \frac{\partial}{\partial \hat{x}_t} + \frac{72}{(\hat{x}_t - \hat{x}_s)^3} \right) \right] \zeta = 0 \end{aligned}$$

for $s = 1, \dots, N'$, as well as the second order PDE

$$\left[\frac{\partial^2}{\partial x_{\text{in}}^2} + \frac{2}{x_{\text{out}} - x_{\text{in}}} \frac{\partial}{\partial x_{\text{out}}} - \frac{2}{(x_{\text{out}} - x_{\text{in}})^2} + \sum_{t=1}^{N'} \frac{2}{\hat{x}_t - x_{\text{in}}} \frac{\partial}{\partial \hat{x}_t} - \sum_{t=1}^{N'} \frac{6}{(\hat{x}_t - x_{\text{in}})^2} \right] \zeta = 0$$

and another second order PDE obtained by interchanging the roles of x_{in} and x_{out} above.

We make some remarks concerning the above result.

The scaling limit of the LERW path λ^δ above is a conformally invariant random curve called the chordal SLE_κ with parameter $\kappa = 2$, by some of the earliest of the celebrated works showing convergence of lattice model interfaces to SLEs [LSW04, Zha08], see also [CS11, YY11].

The scaling limit of the probability that a LERW uses one particular edge in the interior of the domain has been studied in [Ken00, Law14], see also [KW15]. The most accurate results currently known [BLV16] state that this probability divided by $\delta^{3/4}$ converges in the scaling limit to a conformally covariant expression known as the SLE Green's function at $\kappa = 2$. This has been recently used to prove the convergence of the LERW to the chordal SLE_κ with $\kappa = 2$ in a sense that includes parametrization [LV16]. In contrast to the probability of visiting an interior edge, our scaling limit results concern probabilities of visits to an arbitrary number of edges at unit distance from the boundary.

The scaling exponent 3 appearing in the renormalization by $\delta^{3N'}$ and the conformal covariance factors $|\phi'(\hat{p}_j)|^3$ of the above theorem is the conformal weight $h_{1,3}$ in the Kac table for a CFT with central charge $c = -2$, i.e., $h_{1,3} = 3$ is a highest weight for a degenerate highest weight representation of the Virasoro algebra [Kac78, FF90, IK11]. Among the most remarkable predictions of CFT are partial differential equations of order rs for the correlation functions of any primary field whose Virasoro representation

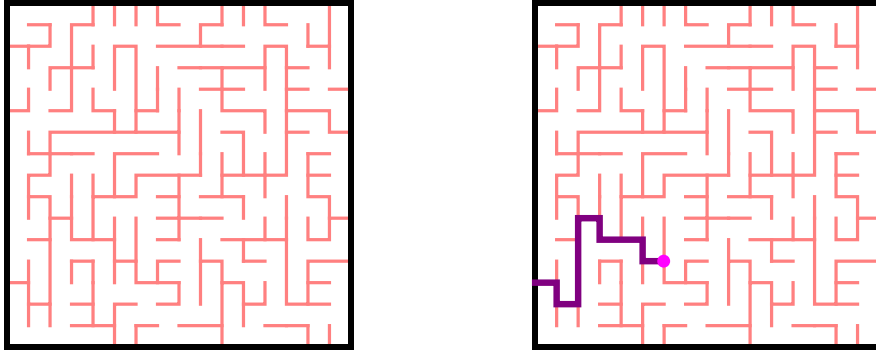


FIGURE 1.3. A uniform spanning tree with wired boundary conditions in a 15×15 square grid graph, and its boundary branch from one given interior vertex.

has highest weight $h_{r,s}$ and an appropriate degeneracy. The third order PDEs in our theorem are exactly the degeneracy equations predicted by CFT. Conformal field theory PDEs of higher than second order have recently appeared in the context of SLEs [Dub15b, LV19], but to our knowledge, the only earlier rigorous scaling limit result for a lattice model establishing such equations is Watts' formula for percolation [Dub06b, SW11]. Conformal field theory PDEs of second order, on the other hand, are well known to arise from Itô calculus in the growth process description of SLEs, and they have been established for the scaling limits of various lattice models — often as a step towards the proof of convergence of interfaces to SLE. The second order PDEs in our theorem are of this more familiar type.

In this article we in fact treat a refinement of the boundary visit probabilities, in which the contribution of each possible order of visits is isolated from the rest. The scaling limit contribution $\zeta_\omega(x_{\text{in}}; \hat{x}_1, \dots, \hat{x}_N; x_{\text{out}})$ of a given visit order ω has a particular asymptotic behavior as its arguments approach each other, as was argued by considerations of CFT fusion channels in [BB03, JJK16], and as we prove in Section 5.4. Such asymptotic behavior is believed to specify the solution to the PDEs up to a multiplicative constant. Admitting this, our formulas coincide with the SLE boundary zig-zag amplitude prediction of [JJK16, KP16].

1.2. Connectivity probabilities of boundary branches in the uniform spanning tree. The proof of the above theorem is based on careful analysis of explicit formulas for probabilities of certain connectivity events in another related model, the uniform spanning tree on \mathcal{G} . Formulas of this type were discovered by Kenyon and Wilson in [KW11a, KW11b]. In this article, we also present a derivation of these formulas based on Fomin's formulas [Fom01], develop combinatorial tools for their detailed analysis, and prove that the probabilities converge in the scaling limit to explicit functions, which satisfy the PDEs of second order predicted by CFT.

A uniform spanning tree (UST) \mathcal{T} on \mathcal{G} is a uniformly randomly chosen connected subgraph of \mathcal{G} which contains all vertices \mathcal{V} and has no cycles. We impose wired boundary conditions, by which we mean that the boundary $\partial\mathcal{V}$ is thought of as a single vertex. For any interior vertex $v \in \mathcal{V}^\circ$, there exists a unique path γ_v in the tree \mathcal{T} from v to $\partial\mathcal{V}$, see Figure 1.3. This path is called the boundary branch of \mathcal{T} from v , and it is distributed like a loop-erased random walk [Pem91, Wil96], as we recall in Section 3. For two boundary edges $e_{\text{in}}, e_{\text{out}} \in \partial\mathcal{E}$, we denote by $\{e_{\text{in}} \rightsquigarrow e_{\text{out}}\}$ the event that the boundary branch $\gamma_{e_{\text{in}}^\circ}$ of \mathcal{T} from e_{in}° reaches the boundary via the edge e_{out} , see Figure 1.4(left). Conditioned on this event, the boundary branch $\gamma_{e_{\text{in}}^\circ}$ has the distribution of a LERW from e_{in} to e_{out} .

We will study probabilities of connectivity events concerning several boundary branches, depicted in Figure 1.4(right). More precisely, let $e_1, \dots, e_{2N} \in \partial\mathcal{E}$ be boundary edges appearing in counterclockwise order along the boundary. We consider connectivity events $\bigcap_{\ell=1}^N \{e_{a_\ell} \rightsquigarrow e_{b_\ell}\}$, where $a_1, \dots, a_N, b_1, \dots, b_N$ is some indexing of the boundary edges by $1, 2, \dots, 2N$. The possible topological connectivities of the

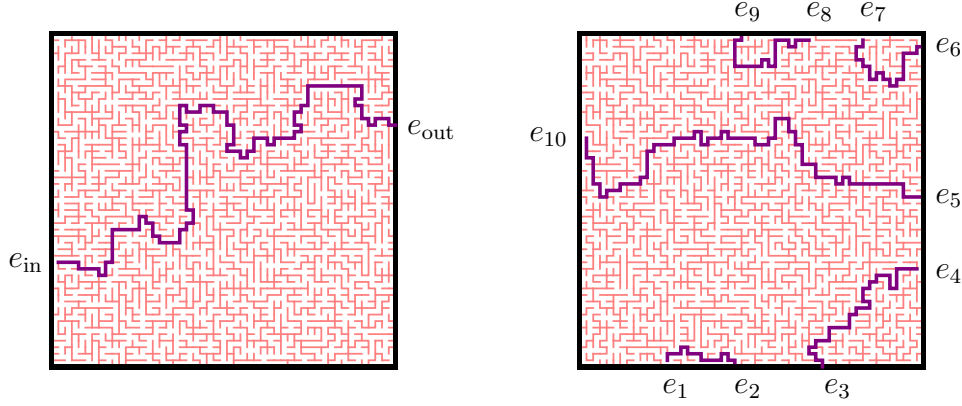


FIGURE 1.4. Uniform spanning trees with wired boundary conditions in a 50×50 square grid graph. The left figure depicts a boundary branch of the UST from e_{in} to e_{out} . The right figure depicts a connectivity event containing several boundary branches, $\{e_1 \rightsquigarrow e_2\} \cap \{e_4 \rightsquigarrow e_3\} \cap \{e_{10} \rightsquigarrow e_5\} \cap \{e_7 \rightsquigarrow e_6\} \cap \{e_8 \rightsquigarrow e_9\}$.

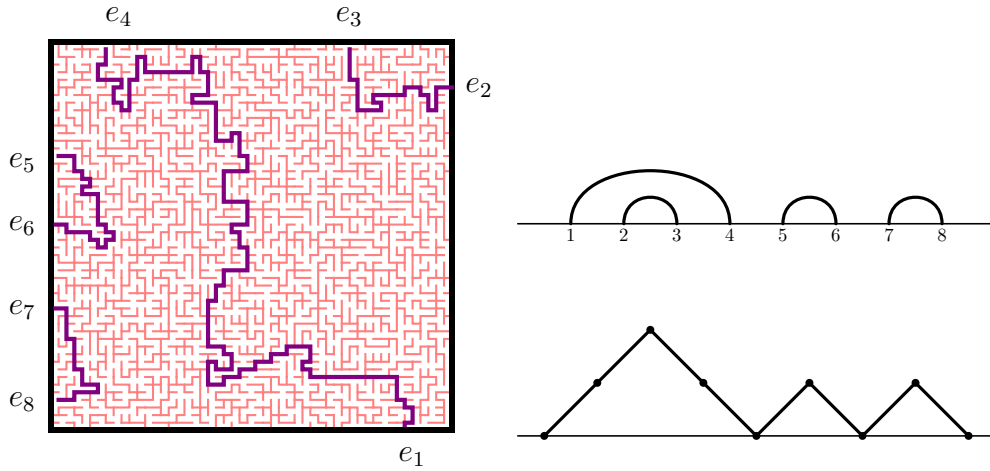


FIGURE 1.5. The connectivity event $\{e_4 \rightsquigarrow e_1\} \cap \{e_3 \rightsquigarrow e_2\} \cap \{e_5 \rightsquigarrow e_6\} \cap \{e_8 \rightsquigarrow e_7\}$ of the boundary branches in a UST, depicted in the left figure, has the same probability that the event $\{e_1 \rightsquigarrow e_4\} \cap \{e_2 \rightsquigarrow e_3\} \cap \{e_5 \rightsquigarrow e_6\} \cap \{e_7 \rightsquigarrow e_8\}$. This connectivity event can be encoded in a planar pair partition $\alpha = \{\{1, 4\}, \{2, 3\}, \{5, 6\}, \{7, 8\}\}$, or, equivalently, a Dyck path also denoted by α , depicted in the right figure.

branches are described by planar pair partitions $\alpha = \{\{a_1, b_1\}, \dots, \{a_N, b_N\}\}$ of $2N$ points, that tell which edges should be connected by boundary branches in the UST, see Figure 1.5. The number of such possible connectivities is the Catalan number $C_N = \frac{1}{N+1} \binom{2N}{N}$.

In the expressions for the UST connectivity probabilities, we use determinants of matrices formed of random walk excursion kernels, like in Fomin's formulas for loop-erased random walks [Fom01]. Let $K(e_1, e_2)$ denote the excursion kernel of the symmetric random walk on \mathcal{G} between the boundary edges e_1 and e_2 , that is, the discrete harmonic measure of e_2 seen from e_1° (see Section 3 for details). With a suitable renormalization, the kernel K converges in the scaling limit to the Brownian excursion kernel \mathcal{K}_Λ , in regular enough approximations \mathcal{G}^δ of Λ . In the upper half-plane \mathbb{H} , the Brownian excursion kernel is simply a constant multiple of

$$\mathcal{K}(x_1, x_2) = \frac{1}{(x_2 - x_1)^2} \quad \text{for } x_1, x_2 \in \mathbb{R}, x_1 \neq x_2.$$

For any planar pair partition β of $2N$ points and marked boundary edges $e_1, \dots, e_{2N} \in \partial\mathcal{E}$, we define in Section 3 a determinant $\Delta_\beta^K(e_1, \dots, e_{2N})$ of an $N \times N$ matrix whose entries are the excursion kernels K evaluated at pairs of marked edges determined by β — see Equation (3.7) for the precise definition. We also define a similar determinant $\Delta_\beta^K(x_1, \dots, x_{2N})$ of an $N \times N$ matrix whose entries are instead the kernels K evaluated at pairs of points among $x_1 < \dots < x_{2N}$.

Theorem (Theorem 3.12). *For the UST with wired boundary conditions, the probability of the connectivity described by the planar pair partition $\alpha = \{\{a_1, b_1\}, \dots, \{a_N, b_N\}\}$, as illustrated in Figure 1.5, equals*

$$\mathbb{P}\left[\bigcap_{\ell=1}^N \{e_{a_\ell} \rightsquigarrow e_{b_\ell}\}\right] = \sum_{\beta} \mathcal{M}_{\alpha, \beta}^{-1} \Delta_\beta^K(e_1, \dots, e_{2N}),$$

where the sum is over planar pair partitions β , and, for each β , the coefficient $\mathcal{M}_{\alpha, \beta}^{-1}$ is the number of cover-inclusive Dyck tilings of a skew shape between the Young diagrams associated to the two Dyck paths of α and β (the precise definitions are given in Section 2).

In fact, the numbers $\mathcal{M}_{\alpha, \beta}^{-1}$ are entries of the inverse matrix \mathcal{M}^{-1} of a signed incidence matrix \mathcal{M} of a binary relation on Dyck paths, introduced by Kenyon and Wilson [KW11a, KW11b] and Shigechi and Zinn-Justin [SZ12]. These matrices are given explicitly in Example 2.10 in Section 2. Combinatorics related to the binary relation were furthermore recently used by Poncelet [Pon18] to generalize Schramm's passage probability formula to multiple LERWs.

Theorem (Theorems 3.16 and 4.1). *Let \mathcal{G}^δ with $e_1^\delta, \dots, e_{2N}^\delta \in \partial\mathcal{E}^\delta$ be a square grid approximation of a domain Λ with marked boundary points p_1, \dots, p_{2N} appearing in counterclockwise order along the boundary. Then, the UST connectivity probability has the following conformally covariant scaling limit:*

$$\frac{1}{\delta^{2N}} \mathbb{P}\left[\bigcap_{\ell=1}^N \{e_{a_\ell}^\delta \rightsquigarrow e_{b_\ell}^\delta\}\right] \xrightarrow{\delta \rightarrow 0} \frac{1}{\pi^N} \times \prod_{j=1}^{2N} |\phi'(p_j)| \times \mathcal{Z}_\alpha(\phi(p_1), \dots, \phi(p_{2N})),$$

where $\phi: \Lambda \rightarrow \mathbb{H}$ is a conformal map, and, for $x_1 < \dots < x_{2N}$, the function \mathcal{Z}_α is given explicitly by

$$\mathcal{Z}_\alpha(x_1, \dots, x_{2N}) = \sum_{\beta} \mathcal{M}_{\alpha, \beta}^{-1} \Delta_\beta^K(x_1, \dots, x_{2N}).$$

The function \mathcal{Z}_α is positive and it satisfies the following system of $2N$ second order PDEs:

$$\left[\frac{\partial^2}{\partial x_j^2} + \sum_{i \neq j} \left(\frac{2}{x_i - x_j} \frac{\partial}{\partial x_i} - \frac{2}{(x_i - x_j)^2} \right) \right] \mathcal{Z}_\alpha = 0 \quad \text{for all } j = 1, \dots, 2N.$$

1.3. Steps of the proof(s). The proof of Theorem 3.12, concerning the connectivity probabilities in the discrete UST model, consists of the relatively well known Wilson's algorithm and Fomin's formulas combined with combinatorics of Dyck tilings. Then, Theorem 3.16 about the scaling limits of the connectivity probabilities follows from scaling limit results for random walk excursion kernels, and the PDEs in Theorem 4.1 are directly verified from the explicit formulas.

The proof of our main theorem about the boundary visit probabilities of LERW (Theorem 3.17) uses the expressions from Theorems 3.12 and 3.16. Namely, we first observe that the (order-refined) boundary visit probability can be written as

$$\mathbb{P}_{e_{\text{in}}, e_{\text{out}}}[\gamma \text{ uses } \hat{e}_1, \dots, \hat{e}_{N'} \text{ in this order}] = \sum_{\beta} \mathcal{M}_{\alpha, \beta}^{-1} \frac{\Delta_\beta^K(e_1, \dots, e_{2N})}{K(e_{\text{in}}, e_{\text{out}})},$$

for a suitably chosen connectivity α and boundary edges e_1, \dots, e_{2N} , with $N = N' + 1$. The key steps then are to show cancellations in the leading terms of the explicit determinantal formulas in the $\delta \rightarrow 0$ limit, and an exchange of limits property for the subleading terms, detailed in Section 5. Our proofs of both of these properties rely heavily on combinatorics of cover-inclusive Dyck tilings. The cancellations

and exchange of limits eventually allow us also to establish the asserted third order partial differential equations by a fusion argument similar to the recent work of Dubédat [Dub15b].

1.4. Multiple SLE_2 . Collections of several branches of the UST are expected to converge to multiple SLE_κ curves at $\kappa = 2$ [BBK05, Dub06a, Dub07, KL07, KW11a, KP16], as stated in more detail in Conjecture 4.3.¹ In general, a multiple SLE_κ , for $\kappa > 0$, is a process of random conformally invariant curves in a simply connected planar domain, connecting marked boundary points p_1, \dots, p_{2N} pairwise without crossing. The possible topological connectivities of the curves can be described by planar pair partitions α similarly as in the discrete case (see Figure 1.5). To construct a (local) multiple SLE_κ , one uses as an input a positive function $\mathcal{Z}(x_1, \dots, x_{2N})$, defined for $x_1 < \dots < x_{2N}$, called a multiple SLE partition function. This function is subject to the requirements of positivity, Möbius covariance (COV), and $2N$ partial differential equations of second order (PDE), recalled explicitly in Section 4.

Consider a chosen connectivity pattern α . It has been argued in [BBK05, KP16] that the multiple SLE_κ in which the random curves form this deterministic connectivity α has a particular partition function $\mathcal{Z}_\alpha^{(\kappa)}$ determined by certain asymptotic boundary conditions (ASY), given in Section 4. In [KP16], solutions $\mathcal{Z}_\alpha^{(\kappa)}$ satisfying the required covariance, PDEs and asymptotics are constructed for the generic parameter values $\kappa \in (0, 8) \setminus \mathbb{Q}$. These functions are called the multiple SLE_κ pure partition functions.

In the present article, we show that the pure partition functions of the local multiple SLE_2 can be obtained as the scaling limits of the probabilities of the connectivity events $\bigcap_{\ell=1}^N \{e_{a_\ell} \rightsquigarrow e_{b_\ell}\}$ of the UST boundary branches.² Importantly, we can conclude the existence of local multiple SLE_κ at $\kappa = 2$, with the pure partition functions \mathcal{Z}_α .

Theorem (Theorems 4.1 and 4.2). *For any planar pair partition α , the function $\mathcal{Z}_\alpha = \sum_\beta \mathcal{M}_{\alpha,\beta}^{-1} \Delta_\beta^\kappa$ is a positive, Möbius covariant solution to the $2N$ second order PDEs required from the multiple SLE_2 partition functions. In particular, there exists a local multiple SLE_2 with partition function \mathcal{Z}_α .*

In fact, for each $\alpha \in \text{LP}_N$, the function \mathcal{Z}_α is the unique solution which satisfies the asymptotic boundary conditions (ASY), when solutions with at most power-law growth are considered, see Section 4.

1.5. Beyond the present work: conformal blocks and q -deformations. Many of the delicate properties of the scaling limits of connectivity probabilities of UST branches and boundary visit probabilities of LERWs rely heavily on remarkable combinatorial structures. Some key aspects of the combinatorics are captured by a certain binary relation on planar pair partitions, and Fomin's formulas lie at the very heart of the applications to the UST and LERW. Fomin's formulas certainly seem specific to the loop-erased random walks, and one could thus be lead to suspect that the remarkable combinatorics in our scaling limit results might also be specific to SLEs at $\kappa = 2$ and conformal field theories at the corresponding central charge $c = -2$. Somewhat surprisingly, however, it turns out that versions of the combinatorial structures in fact persist at generic κ and c . The generic parameter analogues of the results relate the multiple SLE pure partition functions $\mathcal{Z}_\alpha^{(\kappa)}$ not to determinant functions Δ_α^κ as in Fomin's formulas, but rather to the conformal block functions of conformal field theories. Some combinatorial enumerations will have to be replaced by appropriate q -analogues, where the deformation parameter q depends on κ . This generalization is the topic of a companion paper [KKP19].

¹See also the update below the conjecture for recent progress.

²This is the first proof of the existence of *positive* pure partition functions of multiple SLEs, implying in particular the existence of the extremal (local) multiple SLEs. After the present work, the existence of positive pure partition functions for $\kappa \in (0, 6]$ has been proven by SLE methods [PW19, Wu18], which however do not yield explicit formulas.

1.6. Organization of the article. The roles of the remaining four sections can be roughly summarized as follows. The main probabilistic content is in Sections 3–5. Section 2 has a crucial but auxiliary role for the main content: the other sections repeatedly rely on the combinatorial results there. A recommended approach is to read Sections 3–5, while consulting Section 2 as it is needed.

More precisely, the combinatorics of Section 2 will be employed in the rest of the article as follows. The results from Sections 2.1–2.3 will be needed in Section 3.5 and the follow-up work [KKP19]. The results in Sections 2.4–2.5 are mainly for the purpose of the follow-up [KKP19]. The results in Sections 2.4 and 2.6 are used in Sections 4.2.3, 5.1, and 5.4.

Section 3 constitutes the derivation of the explicit formulas for the connectivity and boundary visit probabilities, as well as the convergence proof for the connectivity probabilities in the scaling limit. Sections 3.1–3.2 introduce the uniform spanning tree with wired boundary conditions and its boundary branches, and contain elementary observations about their connectivity and boundary visit events. Sections 3.3 and 3.4 review two well-known but essential tools for the uniform spanning tree and loop-erased random walk: Wilson’s algorithm and Fomin’s formula. In Section 3.5, our solution to the connectivity and boundary visit probabilities is presented for the discrete models. Scaling limits are addressed in Section 3.7. Some generalizations of our main results, in particular pertaining to the uniform spanning tree with free boundary conditions, are discussed in Section 3.8.

The topic of Section 4 is the relation of the scaling limit connectivity probabilities to multiple SLE processes. Multiple SLE_κ is introduced in Section 4.1. In Section 4.2, we prove the second order partial differential equations, positivity, and asymptotics for the functions \mathcal{Z}_α , and as a consequence get that each of these functions can be used to construct a local multiple SLE_κ at $\kappa = 2$.

Section 5 contains the proof of the scaling limit results for the boundary visit probabilities. In Section 5.1, we prove the existence of the scaling limit and obtain a formula for it which allows us to interchange two limits. Section 5.2 contains a fusion argument by which the third order partial differential equations can be proven after the two limits have been exchanged. Section 5.3 then summarizes the proof of the main scaling limit result for the boundary visit probabilities. We finish in Section 5.4 by proving asymptotics properties for the limit of boundary visit probabilities.

Acknowledgments: We thank Christian Hagendorf for useful discussions, and in particular for drawing our attention to the results of [KW11a, KW11b, KW15]. We also thank Dmitry Chelkak, Steven Flores, Christophe Garban, Konstantin Izyurov, Richard Kenyon, Marcin Lis, Wei Qian, David Radnell, Fredrik Viklund, David Wilson, and Hao Wu for interesting and helpful discussions.

A.K. and K.K. are supported by the Academy of Finland project “Algebraic structures and random geometry of stochastic lattice models”. During this work, E.P. was supported by Vilho, Yrjö and Kalle Väisälä Foundation and later by the ERC AG COMPASP, the NCCR SwissMAP, and the Swiss NSF.

2. COMBINATORICS OF LINK PATTERNS AND THE PARENTHESIS REVERSAL RELATION

In this section, we introduce combinatorial objects and present needed results about them.

The first sections 2.1 and 2.2 introduce basic definitions and tools. The first fundamental combinatorial result is Theorem 2.9 in Section 2.3, which gives a formula for the inverse of a weighted incidence matrix of a certain binary relation. This formula will be instrumental in Section 3 when solving for the probabilities of connectivity events for multiple branches of the uniform spanning tree, as well as the probabilities of boundary visit events for the loop-erased random walk. It will also be used in the companion paper [KKP19] to obtain a change of basis matrix from the pure partition functions of multiple SLEs to the basis of conformal blocks of CFT. For the latter purpose, we present the theorem in a generality which allows for weighted incidence matrices.

In the rest of this section, we give some further combinatorial tools that are needed in analyzing the asymptotics and scaling limits of the probabilistic observables of interest. These pertain to what we call

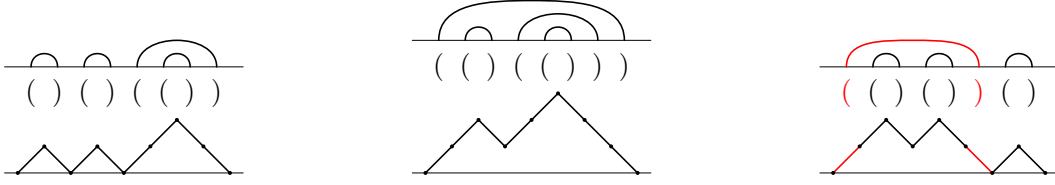


FIGURE 2.1. Illustration of the bijections between LP_4 , BPE_4 , and DP_4 , and the correspondence of links, matching pairs of parentheses, and opposite slopes.

cascade properties, which describe the behavior of multiple SLEs when reducing the number of curves. Section 2.4 introduces the basic notations and definitions. In Section 2.5, we show that cascade properties uniquely determine certain weighted incidence matrices, such as those encountered in [KKP19]. In Section 2.6, we develop concrete combinatorial tools which will be relied on in all further analysis of the UST connectivity and LERW boundary visit pattern probabilities.

2.1. Combinatorial objects and bijections. The *Catalan numbers* $C_N = \frac{1}{N+1} \binom{2N}{N}$ are typically introduced as the number of different planar pair partitions of $2N$ points. Planar pair partitions naturally appear as different connectivity patterns or configurations of interfaces in various planar random models, and in this context they are usually called link patterns. It is convenient to identify planar pair partitions with yet other families of combinatorial objects, since each interpretation makes some of our combinatorial considerations easier or more transparent. We will work interchangeably with the following three families, illustrated in Figure 2.1.

Link patterns (planar pair partitions) with N links are partitions

$$(2.1) \quad \alpha = \{\{a_1, b_1\}, \dots, \{a_N, b_N\}\}$$

of the set $\{1, \dots, 2N\}$ into N pairs, called *links*, such that the points a_ℓ and b_ℓ , for $\ell = 1, \dots, N$, can be connected by non-intersecting paths in the upper half-plane, see Figure 1.5. The family of all link patterns with N links is denoted by LP_N . By convention, we set $LP_0 := \{\emptyset\}$.

Dyck paths are non-negative walks w of $2N$ up- or down-steps starting and ending at zero,

$$DP_N := \{w : \{0, \dots, 2N\} \rightarrow \mathbb{Z}_{\geq 0} \mid w(0) = w(2N) = 0, \text{ and } |w(j) - w(j-1)| = 1 \text{ for all } j\}.$$

Balanced parenthesis expressions are sequences of $2N$ parentheses “(” and “)”, balanced in the conventional sense of parentheses. More precisely, given a sequence α of $2N$ parentheses, denote by $o_j(\alpha)$ the number of opening parentheses (among the j first parentheses from the left, and by $c_j(\alpha)$ the number of closing parentheses). Then, α is a balanced parenthesis expression if and only if $c_j(\alpha) \leq o_j(\alpha)$ for all j and $c_{2N}(\alpha) = o_{2N}(\alpha) = N$. This is equivalent to $j \mapsto o_j(\alpha) - c_j(\alpha)$ being a Dyck path. The family of all balanced parenthesis expressions with N pairs of parentheses is denoted by BPE_N , and it is in bijective correspondence with DP_N . By a slight abuse of notation, we thus identify a balanced parenthesis expression $\alpha \in BPE_N$ with the Dyck path also denoted by $\alpha \in DP_N$,

$$\alpha(j) = o_j(\alpha) - c_j(\alpha).$$

In a balanced parenthesis expression α , an opening parenthesis (at position j and a closing parenthesis) at position i , with $j < i$, are said to be a *matching pair* if the subexpression Y consisting of the parentheses at $j+1, \dots, i-1$ is also a balanced parenthesis expression, so that $\alpha = X(Y)Z$, where X and Z are (not necessarily balanced) sequences of parentheses. In terms of the Dyck path α , the j :th and i :th steps of α are the opposite slopes at equal height of a single mountain silhouette, as illustrated in Figure 2.1. There are N matching pairs in a balanced parenthesis expression $\alpha \in BPE_N$, and these determine a link pattern. Thus the sets BPE_N and LP_N are in bijection, and by a slight abuse of notation we again interpret α interchangeably as either a balanced parenthesis expression or a link pattern.



FIGURE 2.2. The minimal (left) and maximal (right) elements \sqcap_N and \sqcup_N .

Via the bijections above, we identify the three sets LP_N , DP_N , and BPE_N , and an element of them will be denoted by the same symbol. With the identifications, the j :th index of $\alpha \in \text{LP}_N$ is a left (resp. right) endpoint of a link, if and only if the j :th parenthesis of $\alpha \in \text{BPE}_N$ is an opening (resp. closing) parenthesis, if and only if the j :th step of $\alpha \in \text{DP}_N$ is an up-step (resp. down-step). The Dyck path $\alpha(j) = o_j(\alpha) - c_j(\alpha)$ tells how many pairs of parentheses (or links) remain open after reading the first j parentheses (or link endpoints) from the left in α . This measures how nested the link pattern or parenthesis expression α is at j .

2.2. Partial order and the parenthesis reversal relation.

Definition 2.1. A partial order \preceq on the set DP_N of $2N$ -step Dyck paths is defined by setting $\alpha \preceq \beta$ if and only if $\alpha(j) \leq \beta(j)$ for all $0 \leq j \leq 2N$.

This also naturally defines a partial order on the sets of link patterns LP_N and parenthesis expressions BPE_N , where we have $\alpha \preceq \beta$ if and only if β is more nested than α at every position j . This partial order has unique minimal and maximal elements, denoted by \sqcap_N and \sqcup_N , respectively, and illustrated in Figure 2.2. Figure 2.3 illustrates the partial order \preceq .

The following relation was introduced in [KW11b] and [SZ12].

Definition 2.2. The parenthesis reversal relation $\stackrel{\circ}{\leftarrow}$ on the set BPE_N is defined by setting $\alpha \stackrel{\circ}{\leftarrow} \beta$ if and only if α can be obtained from β by choosing a subset B of parentheses in β such that the matching pair of each parenthesis in the set B also belongs to B , and then reversing all the parentheses in B .

Note that the relation $\alpha \stackrel{\circ}{\leftarrow} \beta$ implies $\alpha \preceq \beta$, since the reversal of a matching pair shifts the opening parenthesis to the right. In fact, the relation \preceq is the transitive closure of the non-transitive relation $\stackrel{\circ}{\leftarrow}$, see [KW11b]. We also use the binary relation $\stackrel{\circ}{\leftarrow}$ on the sets LP_N and DP_N , and in Lemmas 2.5 and 2.7 below, we characterize the relation in terms of link patterns and Dyck paths, respectively.

It is often preferable to reverse matching pairs of parentheses one at a time, and with the following convention for the order of reversals. Suppose that $\alpha \stackrel{\circ}{\leftarrow} \beta$, and let B be the collection of the reversed matching pairs of β . By the *nested chain of reversals* from β to α we mean the sequence of intermediate steps $\beta = \beta_0, \beta_1, \dots, \beta_m = \alpha$, where β_n is obtained from β_{n-1} by reversing the matching pair in B whose opening parenthesis is the n :th from the left. The term nested refers to the following property of the sequence $\beta_0, \beta_1, \dots, \beta_m$: if any two matching pairs to be reversed are nested, one inside the other, then the reversal of the outer is performed before the inner.

Example 2.3. We have the following parenthesis reversal relation

$$(())(())(())(()) \stackrel{\circ}{\leftarrow} ((([]]))([])),$$

where we have emphasized the subset B of reversed matching pairs by square brackets. Starting from the latter balanced parenthesis expression $((([]]))([]))$ and reversing one pair at a time with the above convention, each reversal turns out to yield a parenthesis reversal relation as follows

$$(())(())(())(()) \stackrel{\circ}{\leftarrow} (())(())([]) \stackrel{\circ}{\leftarrow} ([]([]))(()) \stackrel{\circ}{\leftarrow} ((([]]))(()).$$

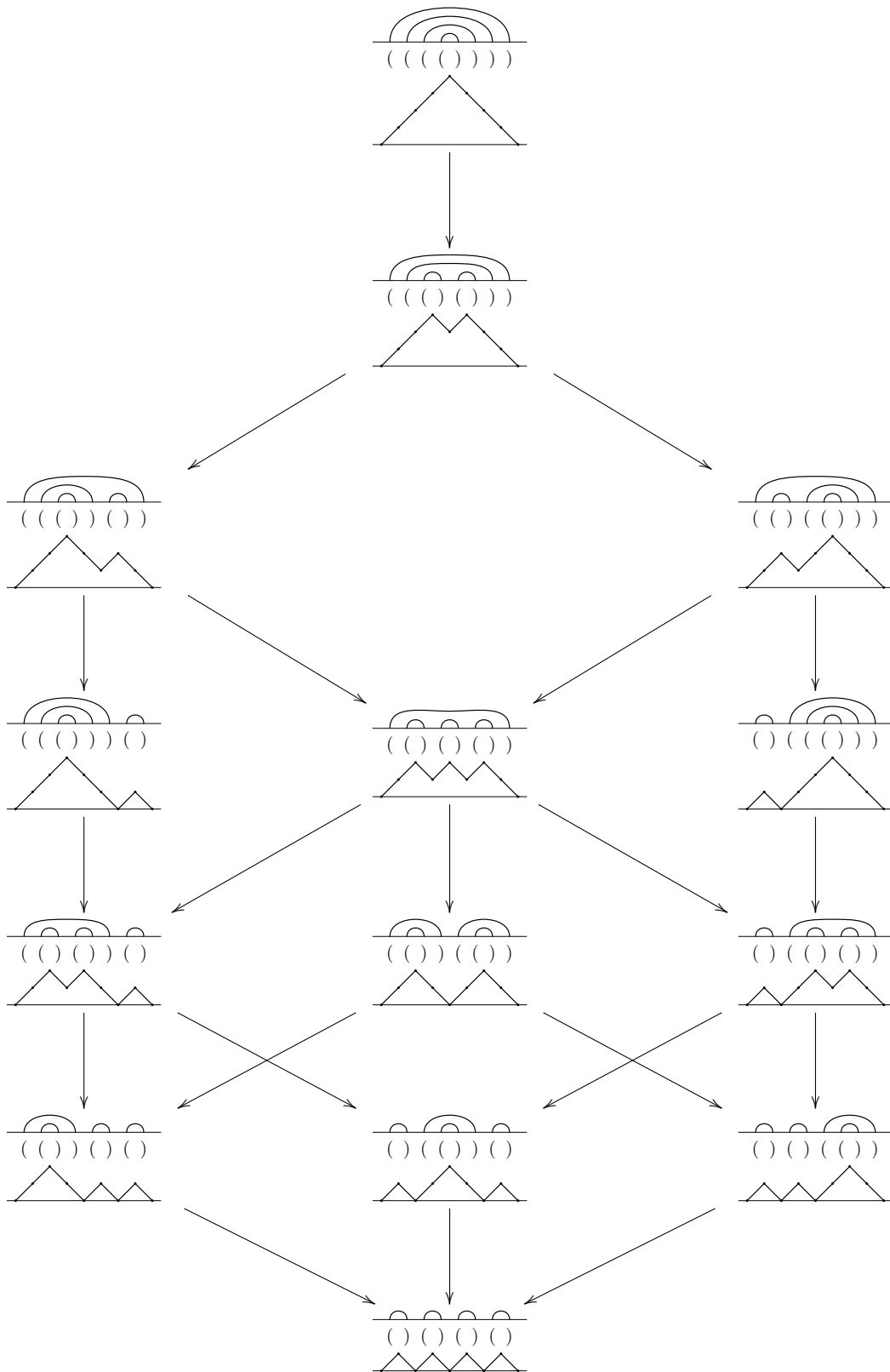


FIGURE 2.3. The partially ordered set LP_4 of link patterns with four links, and the corresponding Dyck paths and balanced parenthesis expressions.

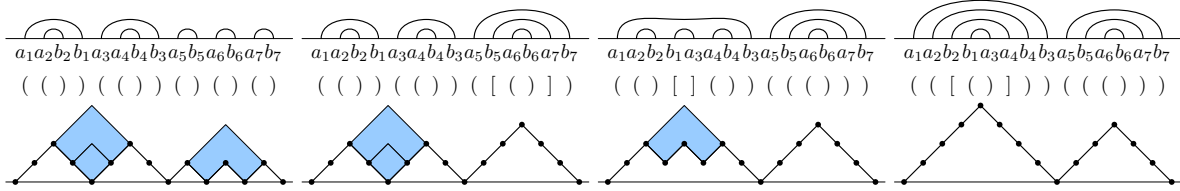


FIGURE 2.4. The nested chain of Example 2.3, with the interpretations in terms of link patterns and Dyck paths, given by Lemmas 2.5 and 2.7, respectively.

The following lemma asserts that the example above featured a general phenomenon.

Lemma 2.4. *Let $\alpha \xleftarrow{\circ} \beta$, and let $\beta = \beta_0, \beta_1, \dots, \beta_m = \alpha$ be the nested chain of reversals from β to α . Then we have $\beta_n \in \text{BPE}_N$ for all $n = 0, \dots, m$, and the following parenthesis reversal relations hold:*

$$\alpha = \beta_m \xleftarrow{\circ} \beta_{m-1} \xleftarrow{\circ} \dots \xleftarrow{\circ} \beta_1 \xleftarrow{\circ} \beta_0 = \beta.$$

Moreover, for all n , we have the relation $\alpha \xleftarrow{\circ} \beta_n$ with the nested chain $\beta_n, \beta_{n+1}, \dots, \beta_m = \alpha$.

Proof. Since α is a balanced parenthesis expression, we have $o_j(\alpha) \geq c_j(\alpha)$ for all j . Because a reversal of a matching pair always shifts the opening parenthesis to the right, we see that

$$o_j(\beta_n) \geq o_j(\alpha) \geq c_j(\alpha) \geq c_j(\beta_n) \quad \text{for all } j \text{ and } n, \text{ and} \quad c_{2N}(\beta_n) = o_{2N}(\beta_n) = N \quad \text{for all } n.$$

This shows that the intermediate steps β_n are balanced parenthesis expressions. By the chosen order of reversals in a nested chain, each matching pair of β to be reversed remains matching in the intermediate steps β_n until that pair is reversed. This implies the relations $\beta_{n+1} \xleftarrow{\circ} \beta_n$ and $\alpha \xleftarrow{\circ} \beta_n$. The reversals in the subchain $\beta_n, \beta_{n+1}, \dots, \beta_m = \alpha$ are still ordered by their opening parentheses from the left. \square

We next characterize the parenthesis reversal relation in terms of (oriented) link patterns, depicted in Figure 2.4. This characterization will be crucial in Section 3 for recovering the uniform spanning tree connectivity probabilities from Fomin's formulas.

We frequently need to refine the link patterns with choices of orientation. Recall from (2.1) that a link pattern α is an unordered collection of unordered pairs $\alpha = \{\{a_1, b_1\}, \dots, \{a_N, b_N\}\}$. An ordered collection of ordered pairs $((a_\ell, b_\ell))_{\ell=1}^N$ is called an *orientation* of α . The points a_ℓ are then called *entrances* and b_ℓ *exits*. As a standard reference orientation of a link pattern α , we will use the *left-to-right orientation*, defined by the conditions $a_\ell < b_\ell$ for all ℓ , and $a_1 < \dots < a_N$.

Lemma 2.5. *Let $((a_\ell, b_\ell))_{\ell=1}^N$ be the left-to-right orientation of a link pattern $\alpha \in \text{LP}_N$. The following statements are equivalent.*

- (a): *A link pattern $\beta \in \text{LP}_N$ connects every entrance of $((a_\ell, b_\ell))_{\ell=1}^N$ to an exit, that is, there exists a permutation $\sigma \in \mathfrak{S}_N$ such that $\beta = \{\{a_1, b_{\sigma(1)}\}, \dots, \{a_N, b_{\sigma(N)}\}\}$.*
- (b): *We have $\alpha \xleftarrow{\circ} \beta$.*

Moreover, we then have $\text{sgn}(\sigma) = (-1)^m$, where m is the number of matching pairs of parentheses reversed in the nested chain from β to α .

Proof. To prove that (a) implies (b), let $\beta \in \text{LP}_N$ be a link pattern connecting entrances of the left-to-right oriented α to exits. Let B consist of those matching pairs of parentheses in β whose opening parenthesis (corresponds to a left link endpoint labeled as an exit $b_{\sigma(\ell)}$. Since β connects entrances to exits, all closing parentheses) in B correspond to entrances a_ℓ . Reversing the parentheses in B , we obtain the balanced parenthesis expression of α , so $\alpha \xleftarrow{\circ} \beta$. This shows that (a) implies (b).

To prove that (b) implies (a), we show that the links of β_n connect entrances $(a_\ell)_{\ell=1}^N$ of α to exits $(b_\ell)_{\ell=1}^N$ of α in any intermediate step β_n of the nested chain $\beta = \beta_0, \beta_1, \dots, \beta_m = \alpha$ of reversals from β to α .

Recall from Lemma 2.4 that the nested chain has subchains of the form $\alpha = \beta_m \stackrel{\circ}{\leftarrow} \beta_{m-1} \stackrel{\circ}{\leftarrow} \cdots \stackrel{\circ}{\leftarrow} \beta_{m-k}$. We perform an induction on the length k of the subchain. In the base case $k = 0$, each entrance a_ℓ connects to the corresponding exit b_ℓ , since $\beta_m = \alpha$. We then assume that in β_{m-k} , entrances of α connect to exits, and we show that β_{m-k-1} also satisfies this property. Since $\beta_{m-k} \stackrel{\circ}{\leftarrow} \beta_{m-k-1}$, we can write $\beta_{m-k-1} = \cdots (\mathbf{X}(\mathbf{Y})\mathbf{Z}) \cdots$ and $\beta_{m-k} = \cdots (\mathbf{X})\mathbf{Y}(\mathbf{Z}) \cdots$, where the parentheses written out explicitly denote matching pairs, and $\mathbf{X}, \mathbf{Y}, \mathbf{Z}$, and the ellipses denote parenthesis expressions that are identical in β_{m-k-1} and β_{m-k} ; see also Figure 2.5. By the induction assumption, it suffices to show that the matching parentheses written explicitly in $\beta_{m-k-1} = \cdots (\mathbf{X}(\mathbf{Y})\mathbf{Z}) \cdots$ connect entrances of α to exits. Lemma 2.4 also guarantees that

$$\alpha = \beta_m \stackrel{\circ}{\leftarrow} \cdots \stackrel{\circ}{\leftarrow} \underbrace{\beta_{m-k}}_{\cdots (\mathbf{X})\mathbf{Y}(\mathbf{Z}) \cdots} \stackrel{\circ}{\leftarrow} \underbrace{\beta_{m-k-1}}_{\cdots (\mathbf{X}(\mathbf{Y})\mathbf{Z}) \cdots}$$

is a nested chain of reversals. By the order of reversals in the nested chain from $\beta_{m-k-1} = \cdots (\mathbf{X}(\mathbf{Y})\mathbf{Z}) \cdots$ to α , the parentheses written out explicitly in $\beta_{m-k} = \cdots (\mathbf{X})\mathbf{Y}(\mathbf{Z}) \cdots$ are not reversed in the subchain $\beta_{m-k}, \beta_{m-k+1}, \dots, \beta_m = \alpha$. Therefore, these two matching pairs of parentheses of β_{m-k} correspond to links $\{a_\ell, b_\ell\}$ and $\{a_s, b_r\}$ as in Figure 2.5(left), so the corresponding matching pairs of β_{m-k-1} also connect entrances of α to exits, as desired — see Figure 2.5(right). This finishes the induction step, and proves that (b) implies (a).

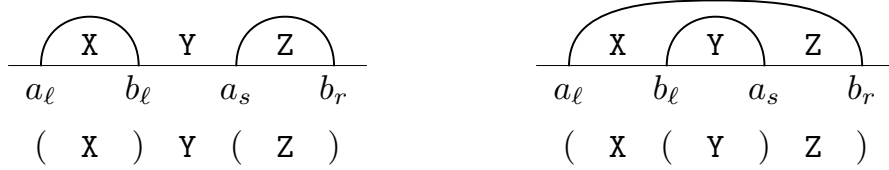


FIGURE 2.5. The balanced subexpressions and sub-link patterns of β_{m-k} (left) and β_{m-k-1} (right) of the proof of Lemma 2.5.

The last assertion follows by noticing that each reversal in the nested chain from β to α corresponds to a transposition exchanging two exits of α , see Figure 2.5. The permutation σ is a composition of m such transpositions and we have $\text{sgn}(\sigma) = (-1)^m$. This concludes the proof. \square

2.3. Dyck tilings and inversion of weighted incidence matrices. Dyck paths only take two kinds of steps, given by the vectors $(1,1)$ and $(1,-1)$ — the paths live on the tilted square lattice generated by these vectors. In particular, the area between any two Dyck paths $\alpha \preceq \beta$ is a union of the atomic squares of this lattice that lie between the highest and lowest Dyck paths $\underline{\alpha}_N$ and $\underline{\beta}_N$, illustrated in Figure 2.6(left). The squares between α and β with $\alpha \preceq \beta$ form a *skew Young diagram*, denoted by α/β .

We consider tilings of skew Young diagrams by so called Dyck tiles. A *Dyck tile* is a nonempty union of atomic squares, where the midpoints of the squares form a shifted Dyck path (possibly a zero-step path). A *Dyck tiling* T of a skew Young diagram α/β is a collection of non-overlapping tiles, whose union is the diagram: $\bigcup T = \alpha/\beta$. Figure 2.6 depicts some Dyck tiles and a Dyck tiling.

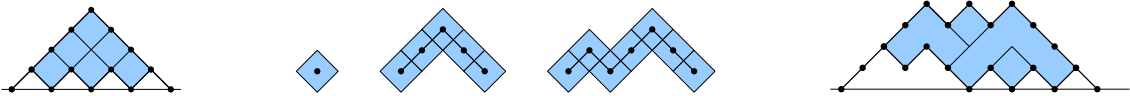


FIGURE 2.6. From the left: the atomic squares of DP_4 , three different Dyck tile shapes, and a Dyck tiling of a skew Young diagram.

In our applications, skew Young diagrams, Dyck tilings, and Dyck tiles have a shape and placement. By skew shapes we mean the shift equivalence classes of skew Young diagrams. Similarly, the shape of

a Dyck tile t is the underlying Dyck path whose bottom left position is at $(0, 0)$. The placement of t is the applied shift, i.e., the integer coordinates (x_t, h_t) of the bottom left position of t . We need four notions related to the horizontal and vertical placement of Dyck tiles. If the coordinates of the bottom left and bottom right positions of t are (x_t, h_t) and (x'_t, h_t) , then we say that the *height* of t is $h_t \in \mathbb{Z}_{>0}$, the *horizontal extent* of t is the closed interval $[x_t, x'_t] \subset \mathbb{R}$, and the *shadow* of t is the open interval $(x_t - 1, x'_t + 1) \subset \mathbb{R}$, see Figure 2.7. A Dyck tile t_1 is said to *cover* a Dyck tile t_2 if t_1 contains an atomic square which is an upward vertical translation of some atomic square of t_2 .

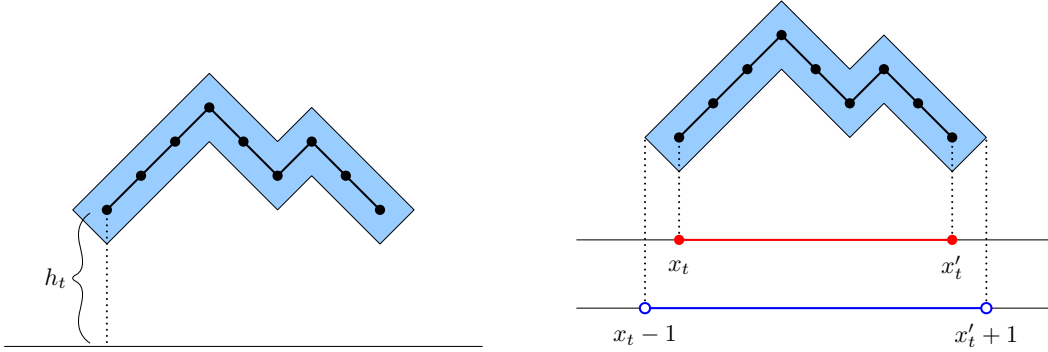


FIGURE 2.7. The vertical position of a Dyck tile t is described by the integer height h_t . The horizontal extent $[x_t, x'_t]$ (in red) and shadow $(x_t - 1, x'_t + 1)$ (in blue) are intervals that describe the horizontal position.

We will use two special types of Dyck tilings, *nested Dyck tilings* (Definition 2.6) and *cover-inclusive Dyck tilings* (Definition 2.8).

Definition 2.6. A Dyck tiling T is *nested* if the shadows of any two distinct tiles of T are either disjoint or one contained in the other, and in the latter case the tile with the larger shadow covers the other.

Nested Dyck tilings can always be described as follows, see Figures 2.8 and 2.9 for illustration. The top layer of each connected component of the skew shape α/β must form a single tile in a nested tiling of

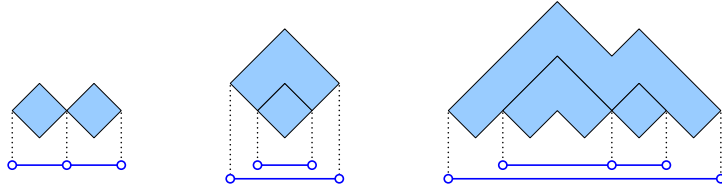


FIGURE 2.8. Nested Dyck tilings of a skew Young diagram, with shadows illustrated.

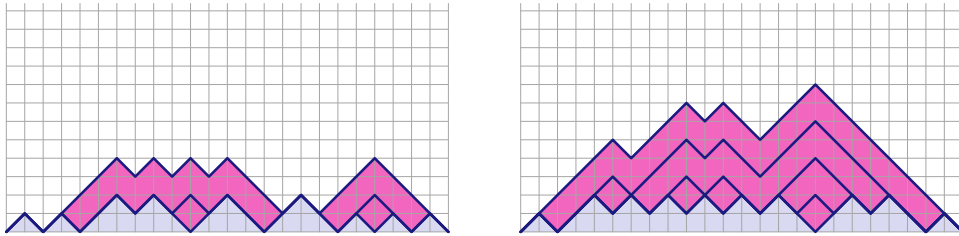


FIGURE 2.9. Nested Dyck tilings of skew Young diagrams.

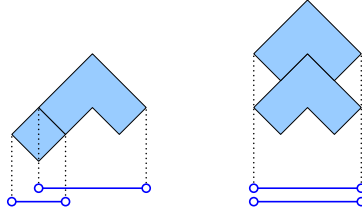


FIGURE 2.10. A non-nested tiling and a non-skew shape, with shadows illustrated.

α/β (if any exists), since breaking the top layer to more than one tile would lead to non-disjoint shadows without the containment property. Recursively, after removing these top layer tiles, the new top layers of the remaining components form again single tiles. This shows first of all that there is at most one nested Dyck tiling of any given skew Young diagram α/β , which we then denote by $T_0(\alpha/\beta)$. Moreover, in a nested Dyck tiling, the containment of the shadows is always strict, since the unique leftmost and rightmost atomic squares of a component are contained in its top layer. The following lemma shows that the existence of a nested tiling characterizes the parenthesis reversal relation for Dyck paths. See also Figure 2.4.

Lemma 2.7. *Let $\alpha, \beta \in \text{DP}_N$. The following statements are equivalent.*

- (a): *We have $\alpha \preceq \beta$ and the skew Young diagram α/β admits a nested Dyck tiling.*
- (b): *We have $\alpha \xleftarrow{\circ} \beta$.*

Moreover, in this case the number of matching pairs of parentheses reversed in the nested chain from β to α is the number of tiles in the unique nested Dyck tiling $T_0(\alpha/\beta)$.

Proof. To prove that (b) implies (a), we assume that $\alpha \xleftarrow{\circ} \beta$ and we consider the nested chain of reversals $\beta = \beta_0, \beta_1, \dots, \beta_m = \alpha$ of matching pairs of parentheses from β to α . The area between the consecutive intermediate steps $\beta_n \xleftarrow{\circ} \beta_{n-1}$ forms a Dyck tile, and these tiles form a Dyck tiling of α/β . The tiling is nested because if any two matching pairs of parentheses to be reversed are one inside the other, then the reversal of the outer is performed before the inner.

To prove that (a) implies (b), consider the nested Dyck tiling $T_0(\alpha/\beta)$ of the skew Young diagram α/β . The endpoints of each tile $t \in T_0(\alpha/\beta)$ correspond to a matching pair of parentheses in the balanced parenthesis expression β . The reversal of these matching pairs of β produces α .

The remaining part of the statement is clear. □

In a nested Dyck tiling, wide tiles are on the top. Conversely, in a *cover-inclusive Dyck tiling*, wide tiles are on the bottom.

Definition 2.8. *A Dyck tiling T is cover-inclusive if for any two distinct tiles of T , either the horizontal extents are disjoint, or the tile that covers the other has horizontal extent contained in the horizontal extent of the other.*

The property of being cover-inclusive is illustrated in Figures 2.11 and 2.12. Any skew Young diagram admits a cover-inclusive Dyck tiling at least with atomic square tiles. We denote by $\mathcal{C}(\alpha/\beta)$ the family of all cover-inclusive tilings of α/β . Note that the disjointness of horizontal extents is less restrictive than the disjointness of shadows, which is essentially why there are more cover-inclusive Dyck tilings than nested Dyck tilings.

The cover-inclusive tilings are a key ingredient in the following theorem, which gives an explicit inversion formula for weighted incidence matrices. Allowing for the weights makes this theorem a slight generalization of a result of Kenyon and Wilson [KW11b, Theorem 1.5]. The unit weight case will be used in

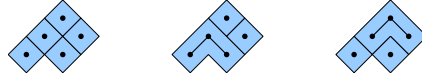


FIGURE 2.11. All the Dyck tilings of a small skew shape. The two first ones (from the left) are cover-inclusive. The third one is neither cover-inclusive nor nested.

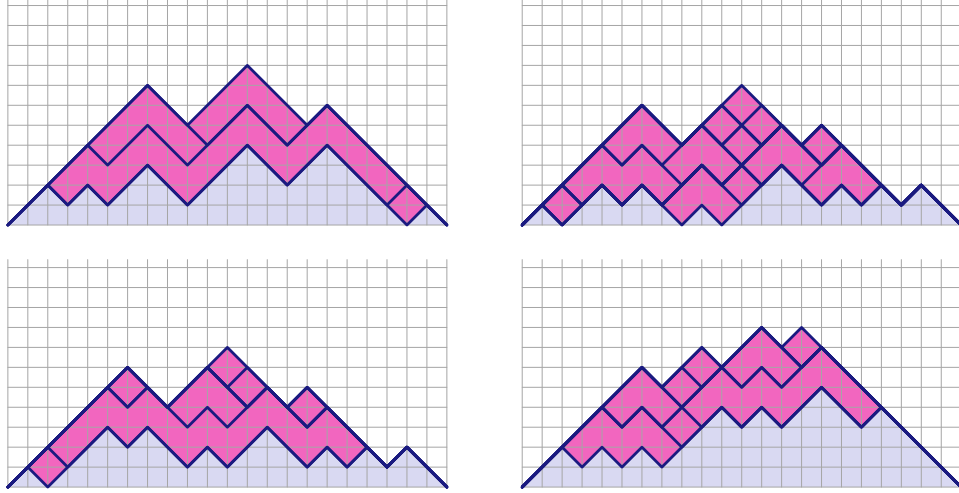


FIGURE 2.12. Cover-inclusive Dyck tilings of skew Young diagrams.

Section 3, whereas a nontrivially weighted case will be needed in [KKP19]. We give the beginning of the proof up to a point where the reduction to the results of Kenyon and Wilson is clear.

Theorem 2.9. *Assign weights $w(t) \in \mathbb{C}$ to all Dyck tiles t (with shape and placement). Let $M \in \mathbb{C}^{\text{DP}_N \times \text{DP}_N}$ be the weighted incidence matrix*

$$(2.2) \quad M_{\alpha, \beta} := \begin{cases} \prod_{t \in T_0(\alpha/\beta)} (-w(t)) & \text{if } \alpha \stackrel{\circ}{\leftarrow} \beta \\ 0 & \text{otherwise} \end{cases}$$

of the parenthesis reversal relation $\stackrel{\circ}{\leftarrow}$, where $T_0(\alpha/\beta)$ is the unique nested tiling of the skew Young diagram α/β . Then M is invertible, and the entries of the inverse matrix M^{-1} are given by the weighted sums

$$(2.3) \quad M_{\alpha, \beta}^{-1} = \begin{cases} \sum_{T \in \mathcal{C}(\alpha/\beta)} \prod_{t \in T} w(t) & \text{if } \alpha \preceq \beta \\ 0 & \text{otherwise} \end{cases}$$

over the sets $\mathcal{C}(\alpha/\beta)$ of cover-inclusive Dyck tilings of the skew Young diagrams α/β .

Proof. Since $\alpha \stackrel{\circ}{\leftarrow} \beta$ implies $\alpha \preceq \beta$, the matrix M is upper-triangular with respect to the partial order \preceq . The diagonal entries are all ones, $M_{\alpha, \alpha} = 1$. Thus M is invertible, and also M^{-1} is upper-triangular with ones on the diagonal: $M_{\alpha, \beta}^{-1} = 0$ unless $\alpha \preceq \beta$, and $M_{\alpha, \alpha}^{-1} = 1$.

It remains to compute the entries $M_{\alpha, \beta}^{-1}$ when $\alpha \preceq \beta$ and $\beta \neq \alpha$. We then have

$$\sum_{\lambda \in \text{DP}_N} M_{\alpha, \lambda}^{-1} M_{\lambda, \beta} = \delta_{\alpha, \beta} = 0,$$

and with the knowledge of the zero entries of M and M^{-1} , we can restrict the summation to obtain

$$\sum_{\substack{\lambda \in \text{DP}_N \\ \lambda \stackrel{\circ}{\leftarrow} \beta \text{ \& } \alpha \preceq \lambda}} M_{\alpha, \lambda}^{-1} M_{\lambda, \beta} = 0.$$

By Lemma 2.7, instead of λ , the summation can be indexed by the nested Dyck tilings $S = T_0(\lambda/\beta)$, whose upper boundary is a subpath of β and which are contained in the skew Young diagram between α and β , i.e., $\bigcup S \subseteq \alpha/\beta$. With the notation $\lambda = \beta \downarrow S$, we then have

$$\sum_{\substack{\text{nested Dyck tilings } S \text{ of } \bigcup S \subseteq \alpha/\beta \\ \text{with upper boundary in } \beta}} M_{\alpha, \beta \downarrow S}^{-1} M_{\beta \downarrow S, \beta} = 0.$$

Using the definition of M , from the equation above we solve $M_{\alpha, \beta}^{-1}$ in terms of $M_{\alpha, \gamma}^{-1}$, where $\alpha \preceq \gamma \preceq \beta$:

$$M_{\alpha, \beta}^{-1} = \sum_{\substack{\text{nested Dyck tilings } S \text{ of } \bigcup S \subseteq \alpha/\beta, \\ S \neq \emptyset, \text{ with upper boundary in } \beta}} -(-1)^{|S|} \left(\prod_{t \in S} w(t) \right) M_{\alpha, \beta \downarrow S}^{-1},$$

where $|S|$ denotes the number of Dyck tiles in S . This formula combined with the initial condition $M_{\alpha, \alpha}^{-1} = 1$ can be used to find $M_{\alpha, \beta}^{-1}$ recursively for all β . Inductively, we now first deduce that $M_{\alpha, \beta}^{-1}$ is a sum of weights of Dyck tilings of α/β , that is, there exist coefficients c_T that are independent of the weight function w , such that we have

$$M_{\alpha, \beta}^{-1} = \sum_{\text{Dyck tilings } T \text{ of } \alpha/\beta} c_T \left(\prod_{t \in T} w(t) \right).$$

The remaining task is to find the coefficients c_T . Here we rely on results of Kenyon and Wilson: it follows from [KW11b, Theorem 1.6.] that

$$c_T = \begin{cases} 1 & \text{if } T \text{ is cover-inclusive} \\ 0 & \text{otherwise.} \end{cases}$$

□

The next example gives the special case of the above theorem that will be employed in the present article, with all tiles having weights $w(t) = 1$. This case will be needed in Section 3 in order to solve for the UST connectivity probabilities, and it is very closely related to the original choice of Kenyon and Wilson [KW11b], which can be recovered by setting $w(t) = -1$ instead. More general choices of weights will be needed in the follow-up work [KKP19].

Example 2.10. Let $\mathcal{M} \in \mathbb{C}^{\text{DP}_N \times \text{DP}_N}$ be the unit weight incidence matrix of the parenthesis reversal relation, obtained by choosing the weight function $w(t) = 1$ for all tiles t ,

$$\mathcal{M}_{\alpha, \beta} = \begin{cases} (-1)^{|T_0(\alpha/\beta)|} & \text{if } \alpha \stackrel{\circ}{\leftarrow} \beta \\ 0 & \text{otherwise,} \end{cases}$$

where $|T_0(\alpha/\beta)|$ is the number of Dyck tiles in the nested tiling $T_0(\alpha/\beta)$. Let $((a_\ell, b_\ell))_{\ell=1}^N$ denote the left-to-right orientation of the link pattern α . Lemmas 2.5 and 2.7 show that the relation $\alpha \stackrel{\circ}{\leftarrow} \beta$ is equivalent to the existence of a unique permutation $\sigma \in \mathfrak{S}_N$ of the exits $(b_\ell)_{\ell=1}^N$ of α such that $\beta = \{\{a_1, b_{\sigma(1)}\} \dots \{a_N, b_{\sigma(N)}\}\}$, and then $(-1)^{|T_0(\alpha/\beta)|} = \text{sgn}(\sigma)$ is the sign of that permutation. Hence, we can equivalently write

$$(2.4) \quad \mathcal{M}_{\alpha, \beta} = \begin{cases} \text{sgn}(\sigma) & \text{if } \beta = \{\{a_1, b_{\sigma(1)}\} \dots \{a_N, b_{\sigma(N)}\}\} \text{ for some } \sigma \in \mathfrak{S}_N \\ 0 & \text{otherwise.} \end{cases}$$

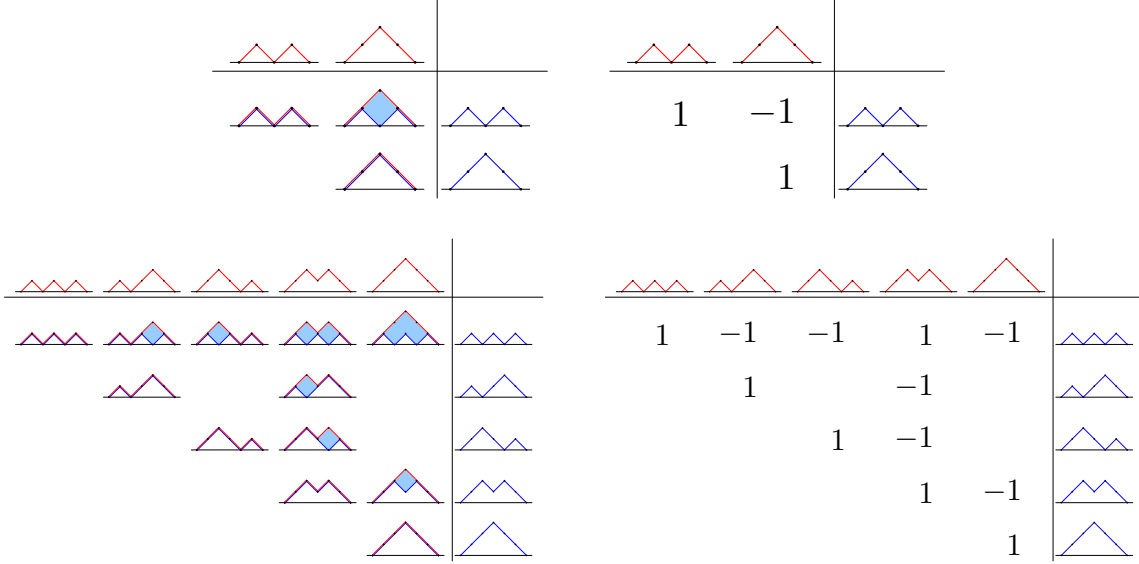


FIGURE 2.13. The nested Dyck tilings of all skew Young diagrams for $N = 2$ and $N = 3$ and the corresponding signed incidence matrices \mathcal{M} defined in Equation (2.4).

Theorem 2.9 shows that \mathcal{M} has inverse with entries counting the cover-inclusive Dyck tilings,

$$(2.5) \quad \mathcal{M}_{\alpha, \beta}^{-1} = \begin{cases} \#\mathcal{C}(\alpha/\beta) & \text{if } \alpha \preceq \beta \\ 0 & \text{otherwise.} \end{cases}$$

In particular, the entries $\mathcal{M}_{\alpha, \beta}^{-1}$ are non-negative integers, and positive precisely when $\alpha \preceq \beta$.

For concreteness, the matrices \mathcal{M} and \mathcal{M}^{-1} as well as the illustrations of all cover-inclusive and nested Dyck tilings of each skew shape are given explicitly for $N = 2, 3, 4$ in Figures 2.13–2.17.

2.4. Wedges, slopes, and link removals. A recurrent topic in this article is cascade properties of random interface models (branches in the uniform spanning tree in Section 3 and multiple SLEs in Section 4), with the following interpretation. Suppose that N interfaces connect $2N$ boundary points p_1, \dots, p_{2N} in a planar domain according to a link pattern $\alpha \in \text{LP}_N$, which contains a link $\{j, j+1\} \in \alpha$ between two consecutive points. If we let the endpoints p_j and p_{j+1} of the corresponding curve approach each other, then the other $N-1$ random curves are described by the random interface model in which the curves connect the remaining points $p_1, \dots, p_{j-1}, p_{j+2}, \dots, p_{2N}$ according to a link pattern obtained from α by removing the link $\{j, j+1\}$. The rest of this section considers the combinatorics of such link removals.

If a link pattern $\alpha \in \text{LP}_N$ has a link $\{j, j+1\} \in \alpha$ of the above kind, then in the corresponding balanced parenthesis expression $\alpha \in \text{BPE}_N$, the j :th and $(j+1)$:st parentheses form a matching pair, i.e., we have $\alpha = \mathbf{X}() \mathbf{Y}$ for some parenthesis sequences \mathbf{X} and \mathbf{Y} of lengths $j-1$ and $2N-j-1$. Then, we denote by $\alpha \setminus \wedge^j = \mathbf{X} \mathbf{Y} \in \text{BPE}_{N-1}$ the balanced parenthesis expression with this one matching pair removed. As usual, we use the same notation for link patterns and Dyck paths, and call the operation $\alpha \mapsto \alpha \setminus \wedge^j$ the link removal of α . Figure 2.18 illustrates this with all three equivalent combinatorial objects.

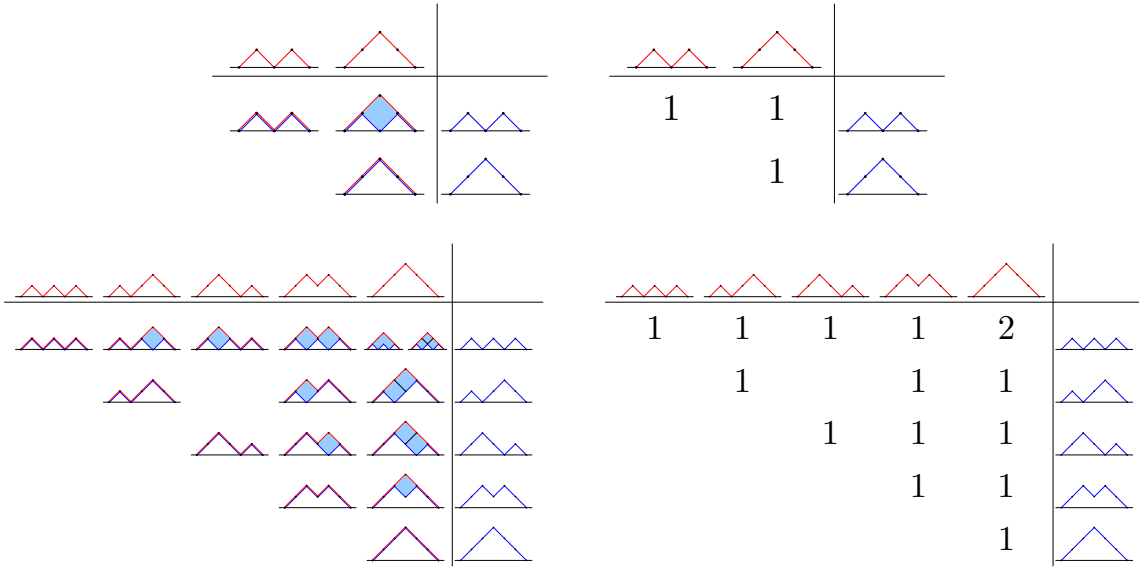


FIGURE 2.14. The cover-inclusive Dyck tilings of all skew Young diagrams for $N = 2$ and $N = 3$ and the corresponding matrices \mathcal{M}^{-1} , whose entries count the number of such tilings according to Equation (2.5).

We usually formulate our combinatorial results in terms of Dyck paths. Then, a link between j and $j + 1$ corresponds with an up-step followed by a down-step, so $\{j, j + 1\} \in \alpha \in \text{LP}_N$ is equivalent to j being a local maximum of the Dyck path $\alpha \in \text{DP}_N$. In this situation, we say that α has an *up-wedge* at j and denote $\wedge^j \in \alpha$. *Down-wedges* \vee_j are defined analogously, and an unspecified local extremum is called a *wedge* \diamond_j . Otherwise, we say that α has a *slope* at j , denoted by $\times_j \in \alpha$.

For Dyck paths, the link removal $\alpha \mapsto \alpha \setminus \wedge^j$ could alternatively be called an up-wedge removal, and one can define a completely analogous down-wedge removal $\alpha \mapsto \alpha \setminus \vee_j$. Occasionally, it is not important to specify the type of wedge that is removed, so whenever α has either type of local extremum at j , we denote by $\alpha \setminus \diamond_j \in \text{DP}_{N-1}$ the two steps shorter Dyck path obtained by removing the two steps around that local extremum. Wedge removals are depicted in Figure 2.19.

Finally, when α has a down-wedge, $\vee_j \in \alpha$, we define the *wedge-lifting operation* $\alpha \mapsto \alpha \uparrow \diamond_j$ by letting $\alpha \uparrow \diamond_j$ be the Dyck path obtained by converting the down-wedge \vee_j in α into an up-wedge \wedge^j . Note that for the balanced parenthesis expression α , the property $\vee_j \in \alpha$ is equivalent to that the j :th and $(j + 1)$:st parentheses are $) ($, and a wedge-lift converts them to a matching pair $()$.

The following two lemmas will be needed later in this section.

Lemma 2.11. *Assume that $\wedge^j \notin \alpha$ and $\vee_j \in \beta$. Then, we have $\alpha \preceq \beta$ if and only if $\alpha \preceq \beta \uparrow \diamond_j$.*

Proof. Drawing the Dyck paths, the assertion is immediate. \square

A useful reinterpretation of the above lemma is that if we have $\wedge^j \notin \alpha$, then the Dyck paths β such that $\beta \succeq \alpha$ and $\diamond_j \in \beta$ come in pairs, one containing an up-wedge and the other a down-wedge at j .

The next lemma states in what sense the parenthesis reversal relation is preserved under wedge removals.

Lemma 2.12. *Assume that $\wedge^j \in \beta$. Then, we have $\alpha \stackrel{0}{\leftarrow} \beta$ if and only if $\diamond_j \in \alpha$ and $\alpha \setminus \diamond_j \stackrel{0}{\leftarrow} \beta \setminus \wedge^j$.*

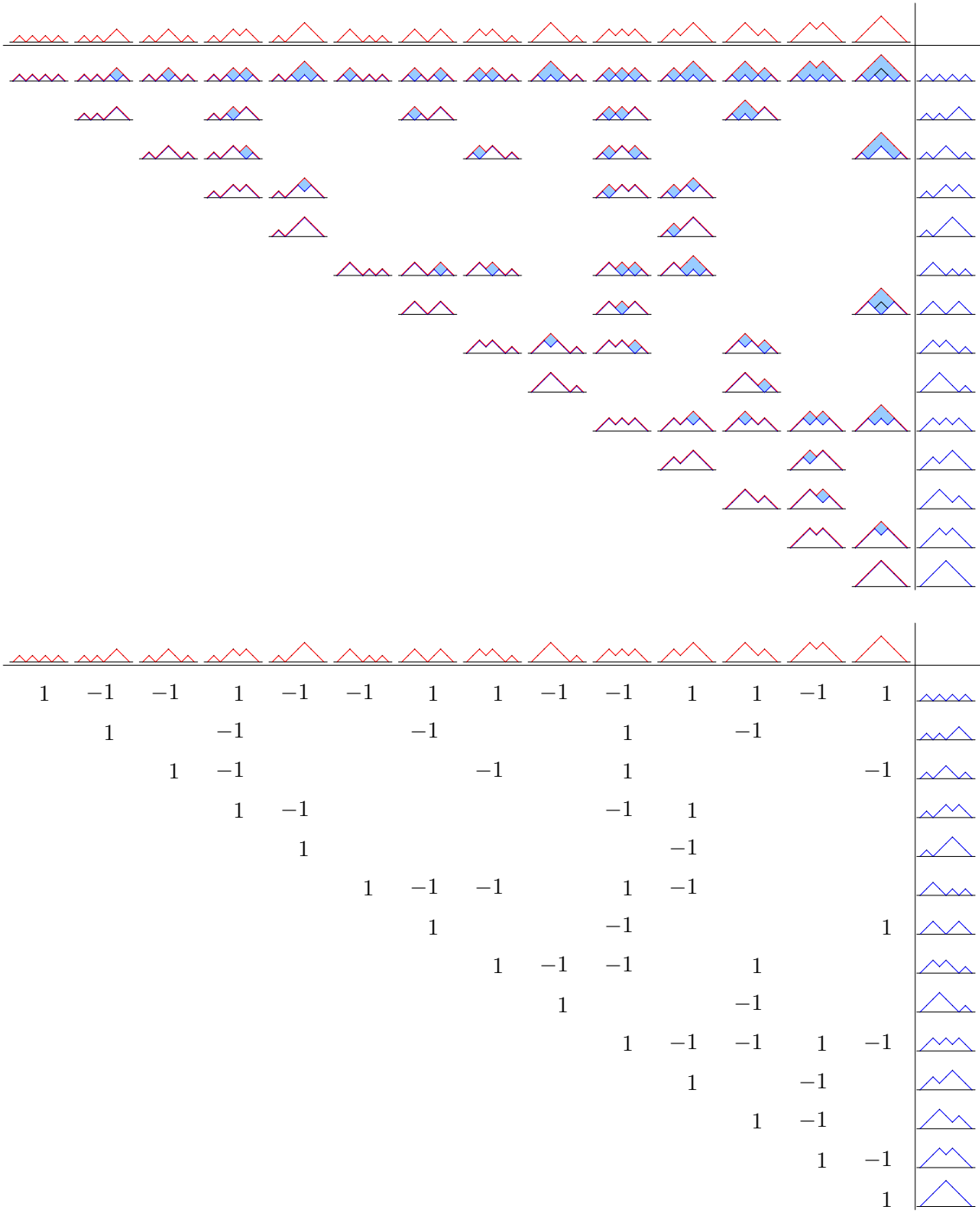


FIGURE 2.15. The nested Dyck tilings of all skew Young diagrams for $N = 4$ and the corresponding signed incidence matrix \mathcal{M} .

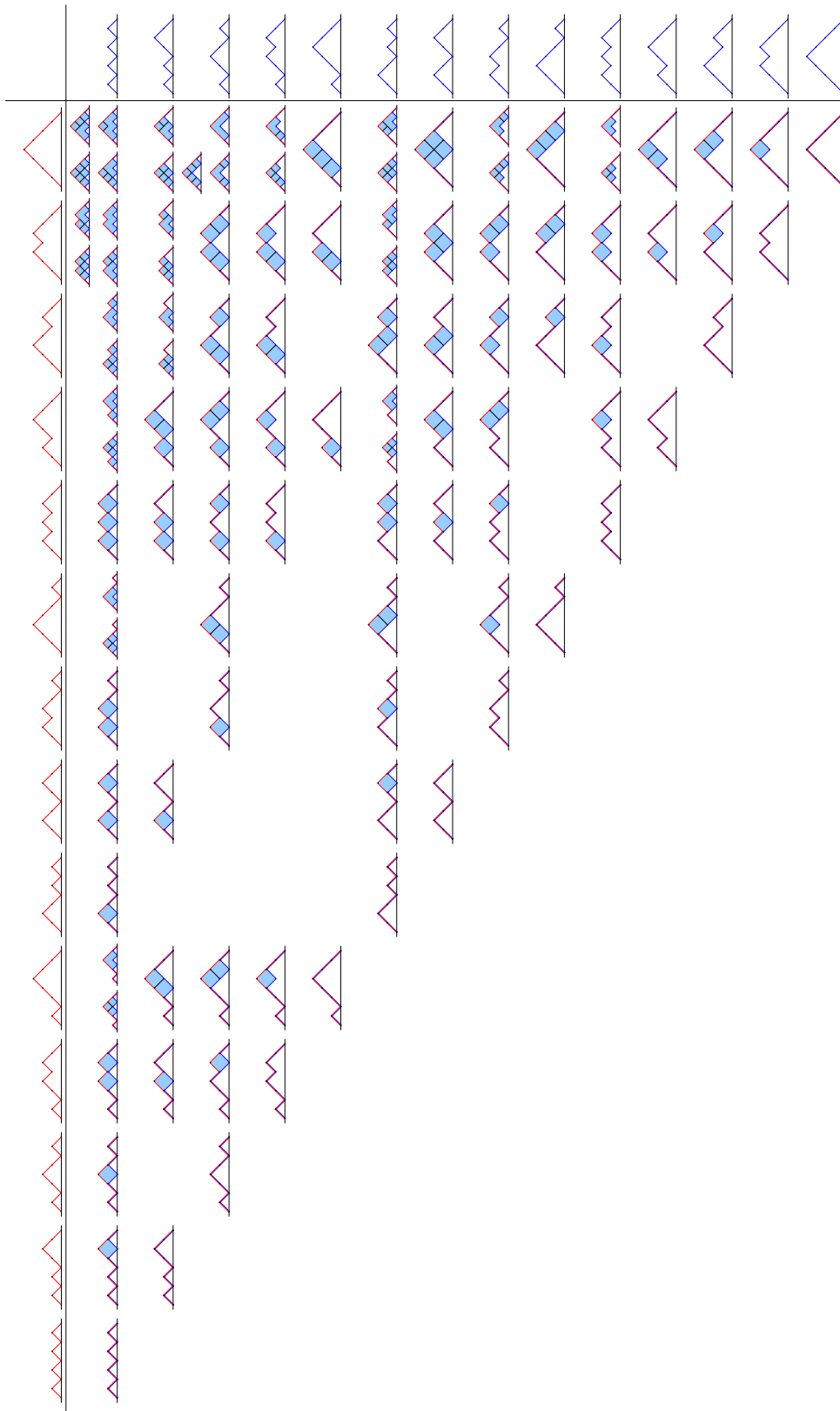


FIGURE 2.16. The cover-inclusive Dyck tilings of all skew Young diagrams for $N = 4$.


















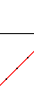


















																		
1	1	1	1	1	1	1	1	1	2	1	2	1	2	2	4	4		
	1		1	1	1		1		1	1		1	1	2	2	2		
		1	1	1		1		1	1	1	1	1	1	1	3	3		
			1	1				1	1	1		1	1		2	2		
				1					1		1		1		1	1		
					1	1	1		1	1	1	1	2	1	2	2		
						1			1	1		1	1	1	1	1		
							1					1	1					
								1	1	1	1	1	1	1	1	1		

FIGURE 2.17. The matrix \mathcal{M}^{-1} counting the cover-inclusive Dyck tilings in Figure 2.16.

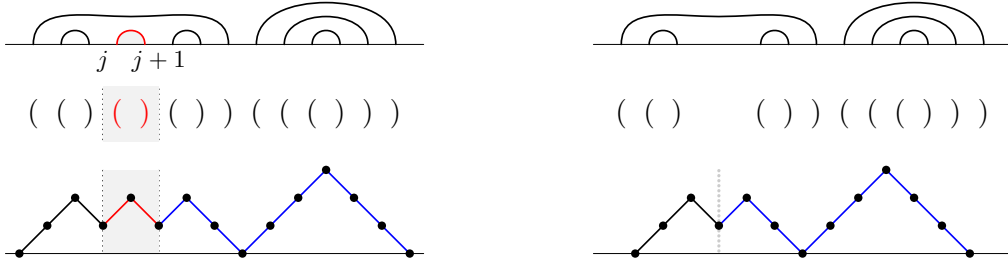


FIGURE 2.18. Link removal and its interpretation in terms of parentheses and Dyck paths.

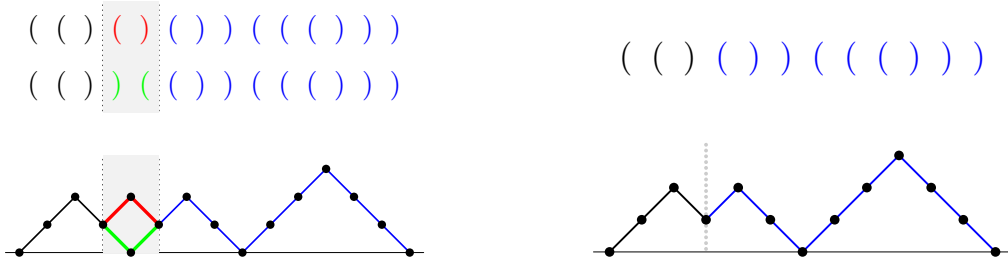


FIGURE 2.19. Wedge removal.

Proof. The j :th and $(j+1)$:st parentheses are a matching pair $()$ in β . When $\alpha \xleftarrow{0} \beta$, then the reversal of matching pairs either leaves the j :th and $(j+1)$:st parentheses unchanged as $()$, or reverses them to $)()$. In both cases, α contains the wedge \diamond_j and $\alpha \setminus \diamond_j$ can be defined. All other matching pairs of parentheses in β correspond bijectively with the matching pairs of $\beta \setminus \wedge^j$. \square

2.5. Cascades of weighted incidence matrices. In this section, we establish a characterization of weighted incidence matrices by a recursion property under wedge removals, that will be needed in [KKP19]. This property holds whenever the weights $w(t)$ of the Dyck tiles t only depend on the height h_t of the tile: $w(t) = f(h_t)$ for some function $f: \mathbb{Z}_+ \rightarrow \mathbb{C}$.

Cascade Recursion (2.6) captures how weighted incidence matrix elements change under the removal of a wedge. Note that, for fixed $j \in \{1, \dots, 2N-1\}$, the wedge removal gives rise to the natural bijection $\beta \mapsto \beta \setminus \wedge^j$ between the elements of DP_N containing the up-wedge \wedge^j , and the elements of DP_{N-1} . Furthermore, by Lemma 2.12, the parenthesis reversal relation is preserved under wedge removals: if $\hat{\alpha} = \alpha \setminus \diamond_j$ and $\hat{\beta} = \beta \setminus \wedge^j$ are the wedge removals of α and β , then $\alpha \xleftarrow{0} \beta$ if and only if $\hat{\alpha} \xleftarrow{0} \hat{\beta}$. The Cascade Recursion expresses the incidence matrix entry at (α, β) in terms of that at $(\hat{\alpha}, \hat{\beta})$.

Consider a collection of matrices $(M^{(N)})_{N \geq 1}$, with $M^{(N)} = (M_{\alpha, \beta}^{(N)}) \in \mathbb{C}^{\text{DP}_N \times \text{DP}_N}$. This collection is said to satisfy the *Cascade Recursion* if for any $\alpha, \beta \in \text{DP}_N$ and any $j \in \{1, \dots, 2N-1\}$ such that $\wedge^j \in \beta$, we have

$$(2.6) \quad M_{\alpha, \beta}^{(N)} = \begin{cases} 0 & \text{if } \alpha \not\xleftarrow{0} \beta \\ M_{\hat{\alpha}, \hat{\beta}}^{(N-1)} & \text{if } \alpha \xleftarrow{0} \beta \text{ and } \wedge^j \in \alpha \\ -f(\alpha(j)+1) \times M_{\hat{\alpha}, \hat{\beta}}^{(N-1)} & \text{if } \alpha \xleftarrow{0} \beta \text{ and } \forall j \in \alpha, \end{cases}$$

where we denote by $\hat{\alpha} = \alpha \setminus \diamond_j \in \text{DP}_{N-1}$ and $\hat{\beta} = \beta \setminus \wedge^j \in \text{DP}_{N-1}$.

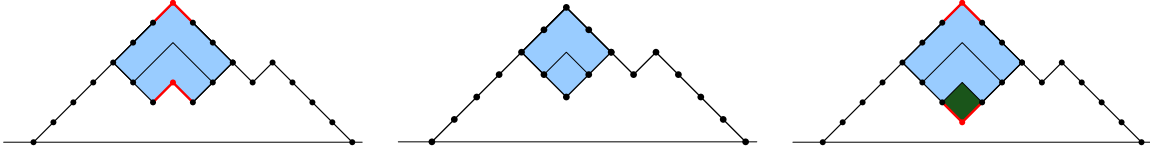


FIGURE 2.20. The nested tilings $T_0(\alpha/\beta)$ and $T_0(\hat{\alpha}/\hat{\beta})$ of the skew shapes α/β and $\hat{\alpha}/\hat{\beta}$ in the cases when $\wedge^j \in \alpha$ (left and middle figure, respectively), and $\vee_j \in \alpha$ (right and middle figure, respectively).

Lemma 2.13. *The Cascade Recursion (2.6) has a unique solution $(M^{(N)})_{N \geq 1}$ with the initial condition $M^{(1)} = 1$, given by a weighted incidence matrix with tile weights determined by heights:*

$$(2.7) \quad M_{\alpha, \beta}^{(N)} = \begin{cases} \prod_{t \in T_0(\alpha/\beta)} (-f(h_t)) & \text{if } \alpha \xleftarrow{0} \beta \\ 0 & \text{otherwise.} \end{cases}$$

Proof. Suppose first that $(M^{(N)})_{N \geq 1}$ and $(\widetilde{M}^{(N)})_{N \geq 1}$ are two solutions to the Cascade Recursion (2.6). We show by induction on N that $M^{(N)} = \widetilde{M}^{(N)}$. The case $N = 1$ is just the initial condition $M^{(1)} = 1 = \widetilde{M}^{(1)}$ of the recursion. Assume then that the matrices $M^{(N-1)} = \widetilde{M}^{(N-1)}$ coincide. Then, for any $\alpha, \beta \in \text{DP}_N$, choosing j such that $\wedge^j \in \beta$ (such j always exists), it follows from the recursion (2.6) that $M_{\alpha, \beta}^{(N)} - \widetilde{M}_{\alpha, \beta}^{(N)} = 0$. Thus, the solution to the recursion (2.6) is necessarily unique.

It remains to prove that the matrix (2.7) satisfies the recursion (2.6). The initial condition $M^{(1)} = 1$ is obviously satisfied. Fix $\alpha, \beta \in \text{DP}_N$, and let $j \in \{1, \dots, 2N-1\}$ be such that $\wedge^j \in \beta$. We may assume that $\alpha \xleftarrow{0} \beta$. Then, by Lemma 2.12, we have $\diamond_j \in \alpha$ and $\alpha \setminus \diamond_j \xleftarrow{0} \beta \setminus \wedge^j$.

Suppose first that $\wedge^j \in \alpha$. Then, the nested tilings $T_0(\alpha/\beta)$ and $T_0(\hat{\alpha}/\hat{\beta})$ of the skew shapes α/β and $\hat{\alpha}/\hat{\beta}$, respectively, contain equally many tiles and the heights of the tiles are equal as well, see Figure 2.20. From this, we immediately get the asserted recursion (2.6) in the case $\alpha \xleftarrow{0} \beta$ and $\wedge^j \in \alpha$:

$$(2.8) \quad M_{\alpha, \beta}^{(N)} = \prod_{t \in T_0(\alpha/\beta)} (-f(h_t)) = \prod_{t \in T_0(\hat{\alpha}/\hat{\beta})} (-f(h_t)) = M_{\hat{\alpha}, \hat{\beta}}^{(N-1)}.$$

Suppose then that $\vee_j \in \alpha$. In this case, the nested tiling $T_0(\alpha/\beta)$ contains an atomic square tile t_0 at position $(x_{t_0}, h_{t_0}) = (j, \alpha(j) + 1)$ at the bottom of $T_0(\alpha/\beta)$, as illustrated in Figure 2.20. Removing the tile t_0 from $T_0(\alpha/\beta)$, we obtain the nested tiling $T_0((\alpha \uparrow \diamond_j)/\beta)$ of the skew shape $(\alpha \uparrow \diamond_j)/\beta$, that is, $T_0(\alpha/\beta) = T_0((\alpha \uparrow \diamond_j)/\beta) \cup \{t_0\}$. Using this observation, the identity $h_{t_0} = \alpha(j) + 1$, and Equation (2.7), we get

$$M_{\alpha, \beta}^{(N)} = \prod_{t \in T_0(\alpha/\beta)} (-f(h_t)) = -f(h_{t_0}) \times \prod_{t \in T_0((\alpha \uparrow \diamond_j)/\beta)} (-f(h_t)) = -f(\alpha(j) + 1) \times M_{\alpha \uparrow \diamond_j, \beta}^{(N)}.$$

To obtain the asserted recursion (2.6) in the case $\alpha \xleftarrow{0} \beta$ and $\vee_j \in \alpha$, it remains to note that Equation (2.8) with $\wedge^j \in \alpha \uparrow \diamond_j$ gives

$$M_{\alpha \uparrow \diamond_j, \beta}^{(N)} = M_{\widehat{\alpha \uparrow \diamond_j}, \hat{\beta}}^{(N-1)} = M_{\hat{\alpha}, \hat{\beta}}^{(N-1)}.$$

□

The recursion (2.6) can equivalently be cast in the following form, only referring to the local structure of the Dyck paths.

Lemma 2.14. *The Cascade Recursion relations (2.6) are equivalent to the following linear recursion relations: for any N , any $\alpha, \beta \in \text{DP}_N$, and any $j \in \{1, \dots, 2N-1\}$ such that $\wedge^j \in \beta$, we have*

$$(2.9) \quad M_{\alpha, \beta}^{(N)} = \begin{cases} 0 & \text{if } \times_j \in \alpha \\ M_{\hat{\alpha}, \hat{\beta}}^{(N-1)} & \text{if } \wedge^j \in \alpha \\ -f(\alpha(j) + 1) \times M_{\hat{\alpha}, \hat{\beta}}^{(N-1)} & \text{if } \vee_j \in \alpha, \end{cases}$$

where we denote by $\hat{\alpha} = \alpha \setminus \diamond_j \in \text{DP}_{N-1}$ and $\hat{\beta} = \beta \setminus \wedge^j \in \text{DP}_{N-1}$.

Proof. If $\alpha \stackrel{0}{\leftarrow} \beta$, then $\diamond_j \in \alpha$ by Lemma 2.12, so the content of Equations (2.6) and (2.9) is the same. If $\alpha \not\stackrel{0}{\leftarrow} \beta$, it suffices to show that (2.9) implies $M_{\alpha, \beta}^{(N)} = 0$. In that case, by Lemma 2.12, we either have $\diamond_j \in \alpha$ and $\alpha \setminus \diamond_j \not\stackrel{0}{\leftarrow} \beta \setminus \wedge^j$, or $\times_j \in \alpha$. In both cases, the relations (2.9) imply $M_{\alpha, \beta}^{(N)} = 0$ — the latter case is a defining property, and the former follows by induction on N . \square

2.6. Inverse Fomin type sums. Let $\mathfrak{K}: \{1, \dots, 2N\} \times \{1, \dots, 2N\} \rightarrow \mathbb{C}$ be a symmetric kernel: $\mathfrak{K}(i, j) = \mathfrak{K}(j, i)$. Let $\beta \in \text{LP}_N$ be a link pattern and $((a_\ell, b_\ell))_{\ell=1}^N$ its left-to-right orientation, i.e., $a_1 < a_2 < \dots < a_N$ and $a_\ell < b_\ell$ for all ℓ . We define the determinant of β with the kernel \mathfrak{K} as

$$(2.10) \quad \Delta_\beta^\mathfrak{K} := \det \left(\mathfrak{K}(a_k, b_\ell) \right)_{k, \ell=1}^N.$$

This makes sense even if the diagonal entries $\mathfrak{K}(i, i)$ of the kernel are not defined, since they do not appear in the determinants. For a link pattern α , we set

$$(2.11) \quad \mathfrak{Z}_\alpha^\mathfrak{K} := \sum_{\beta \succeq \alpha} \# \mathcal{C}(\alpha/\beta) \Delta_\beta^\mathfrak{K},$$

where $\# \mathcal{C}(\alpha/\beta)$ is the number of cover-inclusive Dyck tilings of the skew Young diagram α/β . We call $\mathfrak{Z}_\alpha^\mathfrak{K}$ the *inverse Fomin type sum* associated to α . We will see in Section 3 that sums of this type give connectivity probabilities in the uniform spanning tree as well as boundary visit probabilities of the loop-erased random walk, ultimately by virtue of Fomin’s formula [Fom01]. In the rest of this section, we prove properties of the inverse Fomin type sums (2.11) for the later purpose of analyzing the asymptotics and scaling limits of these probabilities.

We first prove that the coefficients $\# \mathcal{C}(\alpha/\beta)$ of the determinants $\Delta_\beta^\mathfrak{K}$ in the inverse Fomin type sum $\mathfrak{Z}_\alpha^\mathfrak{K}$ have the same value for the pairs of Dyck paths described after Lemma 2.11.

Lemma 2.15. *Assume that $\wedge^j \notin \alpha$, $\vee_j \in \beta$, and $\alpha \preceq \beta$. Then we have $\# \mathcal{C}(\alpha/\beta) = \# \mathcal{C}(\alpha/(\beta \uparrow \diamond_j))$.*

Proof. The equality of the cardinalities is shown by giving a bijection between the sets $\mathcal{C}(\alpha/\beta)$ and $\mathcal{C}(\alpha/(\beta \uparrow \diamond_j))$ of cover-inclusive Dyck tilings of the two skew Young diagrams. The only difference between the diagrams is that $\alpha/(\beta \uparrow \diamond_j)$ contains exactly one atomic square more than α/β . The bijection is defined by adding to a tiling of α/β the tile formed by this atomic square.

Clearly such extensions of tilings in $\mathcal{C}(\alpha/\beta)$ produce $\# \mathcal{C}(\alpha/\beta)$ distinct elements of the set $\mathcal{C}(\alpha/(\beta \uparrow \diamond_j))$, so it remains to prove that all cover-inclusive tilings of $\alpha/(\beta \uparrow \diamond_j)$ must have an atomic square tile at the lifted square. Consider a Dyck tiling S of $\alpha/(\beta \uparrow \diamond_j)$ not satisfying this property. Then, the tile covering the lifted square contains at least a “three-square Λ -shape” growing down from the lifted square. In order for S to be cover-inclusive, also all tiles below the “three-square Λ -shape” would have to contain a lowered “three-square Λ -shape”. Stacking such shapes until they touch α as in Figure 2.21, we notice that S could only be cover-inclusive if $\wedge^j \in \alpha$, which is ruled out by our assumption $\wedge^j \notin \alpha$. \square

We then prove that the determinants $\Delta_\beta^\mathfrak{K}$ in the inverse Fomin type sum (2.11) do not change too much in the wedge-lifting operation either.

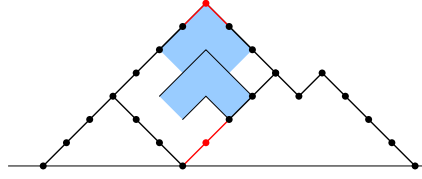


FIGURE 2.21. Illustration of a situation in the proof of Lemma 2.15 where a Dyck tiling of the skew-shape $\alpha/(\beta \uparrow \diamond_j)$ would not have an atomic square tile at the lifted square. The Dyck tiling cannot be cover-inclusive, because $\wedge^j \notin \alpha$.

Lemma 2.16. Let $((a_\ell, b_\ell))_{\ell=1}^N$ be the left-to-right orientation of the link pattern $\beta \in \text{LP}_N$, and let $\vee_j \in \beta$, so that $j = b_s$ and $j+1 = a_r$ for some $s < r$. Let $((a'_\ell, b'_\ell))_{\ell=1}^N$ be the left-to-right orientation of $\beta \uparrow \diamond_j$. Then we have

$$a'_k = \begin{cases} a_k & \text{for } k \neq r \\ b_s & \text{for } k = r \end{cases} \quad \text{and} \quad b'_\ell = \begin{cases} b_\ell & \text{for } \ell \neq r, s \\ a_r & \text{for } \ell = r \\ b_r & \text{for } \ell = s \end{cases}.$$

Proof. In terms of parenthesis expressions, the j :th and $(j+1)$:st parentheses of β read $) ($. Writing out their matching pairs, we see that β contains the balanced subexpression $(X)(Y)$, which converts to $(X(X)Y)$ in $\beta \uparrow \diamond_j$, while everything else remains unchanged. Recalling that matching pairs of a parenthesis expression correspond to links of a link pattern, the assertion is immediate from Figure 2.22.

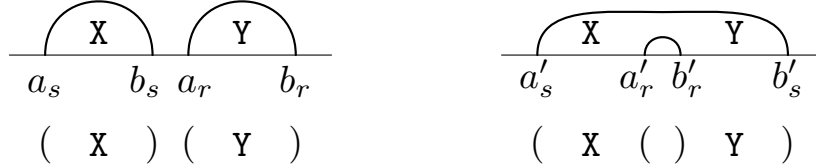


FIGURE 2.22. The s :th and r :th links in left-to-right orientations before and after a wedge-lift.

□

Remark 2.17. This lemma has an important interpretation in terms of the determinants with a symmetric kernel \mathfrak{K} . Compare the two determinants $\Delta_{\beta}^{\mathfrak{K}}$ and $\Delta_{\beta \uparrow \diamond_j}^{\mathfrak{K}}$, and interchange the r :th and s :th columns in the matrix in the determinant $\Delta_{\beta \uparrow \diamond_j}^{\mathfrak{K}}$. Then, the resulting matrix and the matrix in $\Delta_{\beta}^{\mathfrak{K}}$ only differ in the r :th row and the s :th column, containing the kernel entries depending on j and $j+1$. Explicitly, the resulting determinants read

$$\Delta_{\beta}^{\mathfrak{K}} = \det \begin{pmatrix} \ddots & \mathfrak{K}(a_k, j)_{k=1}^{r-1} & \ddots \\ \mathfrak{K}(j+1, b_\ell)_{\ell=1}^{s-1} & \mathfrak{K}(j+1, j) & \mathfrak{K}(j+1, b_\ell)_{\ell=s+1}^N \\ \ddots & \mathfrak{K}(a_k, j)_{k=r+1}^N & \ddots \end{pmatrix}$$

and

$$\Delta_{\beta \uparrow \diamond_j}^{\mathfrak{K}} = - \det \begin{pmatrix} \ddots & \mathfrak{K}(a_k, j+1)_{k=1}^{r-1} & \ddots \\ \mathfrak{K}(j, b_\ell)_{\ell=1}^{s-1} & \mathfrak{K}(j, j+1) & \mathfrak{K}(j, b_\ell)_{\ell=s+1}^N \\ \ddots & \mathfrak{K}(a_k, j+1)_{k=r+1}^N & \ddots \end{pmatrix},$$

where the ellipses stand for submatrices which are identical in both cases. Notice also that, by the symmetry of \mathfrak{K} , the entries in the middle are equal: $\mathfrak{K}(j, j+1) = \mathfrak{K}(j+1, j)$.

The determinants $\Delta_\beta^{\mathfrak{K}}$ and the inverse Fomin type sums $\mathfrak{Z}_\alpha^{\mathfrak{K}}$, defined in (2.10) and (2.11), are polynomials in the entries $\mathfrak{K}(i, j)$ of the kernel \mathfrak{K} . The kernels are symmetric and the diagonal kernel entries $\mathfrak{K}(i, i)$ do not appear in $\Delta_\beta^{\mathfrak{K}}$ and $\mathfrak{Z}_\alpha^{\mathfrak{K}}$, so we can view the entries $\mathfrak{K}(i, j)$, for $i < j$, as the independent variables of these polynomials. For notational convenience, for any j , we let $\mathfrak{K}(\cdot, j) = \mathfrak{K}(j, \cdot)$ stand for the collection of independent variables $(\mathfrak{K}(1, j), \mathfrak{K}(2, j), \dots, \mathfrak{K}(j-1, j), \mathfrak{K}(j, j+1), \dots, \mathfrak{K}(j, 2N))$ that involve the index j . For any j , the determinants $\Delta_\beta^{\mathfrak{K}}$ are linear in the collection $\mathfrak{K}(\cdot, j) = \mathfrak{K}(j, \cdot)$, i.e., they are of the form

$$\Delta_\beta^{\mathfrak{K}} = \sum_{\substack{1 \leq i \leq 2N \\ i \neq j}} [\Delta_\beta^{\mathfrak{K}}]_{i,j} \mathfrak{K}(i, j),$$

where $[\Delta_\beta^{\mathfrak{K}}]_{i,j}$ is a polynomial in the variables other than $\mathfrak{K}(i, \cdot)$ and $\mathfrak{K}(\cdot, j)$. Below, by the coefficient of $\mathfrak{K}(i, j)$ in $\Delta_\beta^{\mathfrak{K}}$ we mean $[\Delta_\beta^{\mathfrak{K}}]_{i,j}$. Note that we have $[\Delta_\beta^{\mathfrak{K}}]_{i,j} = [\Delta_\beta^{\mathfrak{K}}]_{j,i}$. Similarly, we may define the coefficient $[\mathfrak{Z}_\alpha^{\mathfrak{K}}]_{i,j}$ of $\mathfrak{K}(i, j)$ in the inverse Fomin type sum $\mathfrak{Z}_\alpha^{\mathfrak{K}}$, by noting that $\mathfrak{Z}_\alpha^{\mathfrak{K}}$ is a linear combination of determinants $\Delta_\beta^{\mathfrak{K}}$.

Proposition 2.18. *Let $\alpha \in \text{LP}_N$ be a link pattern, and suppose that $j \in \{1, \dots, 2N-1\}$ is such that $\wedge^j \notin \alpha$. Then, the following statements hold.*

- (a): *The inverse Fomin type sum \mathfrak{Z}_α is antisymmetric under interchanging the kernel entries at j and $j+1$ in the following sense: if*

$$\begin{cases} \widetilde{\mathfrak{K}}(j, \cdot) = \mathfrak{K}(j+1, \cdot) & \text{and} & \widetilde{\mathfrak{K}}(j+1, \cdot) = \mathfrak{K}(j, \cdot) \\ \widetilde{\mathfrak{K}}(i, k) = \mathfrak{K}(i, k), & \text{for all other indices } (i, k), \end{cases}$$

then for the inverse Fomin type sums $\mathfrak{Z}_\alpha^{\mathfrak{K}}$ and $\mathfrak{Z}_\alpha^{\widetilde{\mathfrak{K}}}$ with kernels $\widetilde{\mathfrak{K}}$ and \mathfrak{K} , respectively, we have

$$\mathfrak{Z}_\alpha^{\widetilde{\mathfrak{K}}} = -\mathfrak{Z}_\alpha^{\mathfrak{K}}.$$

- (b): *If the collections $\mathfrak{K}(j, \cdot)$ and $\mathfrak{K}(j+1, \cdot)$ are identical, then $\mathfrak{Z}_\alpha^{\mathfrak{K}} = 0$.*

- (c): *The coefficient of $\mathfrak{K}(j, j+1)$ in $\mathfrak{Z}_\alpha^{\mathfrak{K}}$ is zero: $[\mathfrak{Z}_\alpha^{\mathfrak{K}}]_{j,j+1} = 0$. In particular, the replacement*

$$\begin{cases} \mathfrak{K}_0(j, j+1) = \mathfrak{K}_0(j+1, j) = 0 \\ \mathfrak{K}_0(i, k) = \mathfrak{K}(i, k), & \text{for all other indices } (i, k), \end{cases}$$

of the $(j, j+1)$ entries by zero does not affect the inverse Fomin-type sum: $\mathfrak{Z}_\alpha^{\mathfrak{K}_0} = \mathfrak{Z}_\alpha^{\mathfrak{K}}$.

Remark 2.19. Parts (a) and (c) are often applied iteratively: the modified kernels $\widetilde{\mathfrak{K}}$ and \mathfrak{K}_0 are themselves symmetric kernels, and the above replacement rules continue to hold for them.

Proof. Parts (b) and (c) will be obtained as rather straightforward consequences of part (a). We prove the antisymmetry rule of part (a) by regrouping the terms of the inverse Fomin type sum (2.11) into antisymmetric groups. Recall from the discussion after Lemma 2.11 that Dyck paths having a wedge at j appear in the sum (2.11) in pairs: if β is a Dyck path with a down-wedge, $\forall_j \in \beta$, and $\beta \uparrow \diamond_j$ its wedge-lift, then $\beta \succeq \alpha$ is equivalent to $\beta \uparrow \diamond_j \succeq \alpha$. By Lemma 2.15, the coefficients corresponding to β and $\beta \uparrow \diamond_j$ in the inverse Fomin type sum (2.11) are equal: $\#\mathcal{C}(\alpha/\beta) = \#\mathcal{C}(\alpha/(\beta \uparrow \diamond_j))$. Thus, we split the sum as

$$\mathfrak{Z}_\alpha^{\mathfrak{K}} = \sum_{\substack{\beta \succeq \alpha \\ \forall_j \in \beta}} \#\mathcal{C}(\alpha/\beta) \left(\Delta_\beta^{\mathfrak{K}} + \Delta_{\beta \uparrow \diamond_j}^{\mathfrak{K}} \right) + \sum_{\substack{\beta \succeq \alpha \\ \times_j \in \beta}} \#\mathcal{C}(\alpha/\beta) \Delta_\beta^{\mathfrak{K}}.$$

The terms in the first sum on the right-hand side are antisymmetric under the exchange of j and $j+1$, as seen from the expressions in Remark 2.17 given for $\Delta_\beta^{\mathfrak{K}}$ and $\Delta_{\beta \uparrow \diamond_j}^{\mathfrak{K}}$. In the second sum, where $\times_j \in \beta$, the endpoints j and $j+1$ are either both exits or both entrances in the left-to-right orientation of β . For definiteness, assume that they are entrances. Then, in the matrix in $\Delta_\beta^{\mathfrak{K}}$, both collections $\mathfrak{K}(j, \cdot)$ and $\mathfrak{K}(j+1, \cdot)$ appear on a row. The determinant $\Delta_\beta^{\mathfrak{K}}$ changes sign under the exchange of these rows.

For part (b), if we have $\mathfrak{K}(j, \cdot) = \mathfrak{K}(j+1, \cdot)$, then $\widetilde{\mathfrak{K}} = \mathfrak{K}$, and $\mathfrak{Z}_\alpha^{\mathfrak{K}}$ is symmetric under interchange of indices j and $j+1$. On the other hand, it is antisymmetric by part (a), and must therefore vanish.

For part (c), recall first that the coefficient $[\mathfrak{Z}_\alpha^{\mathfrak{K}}]_{j,j+1}$ of $\mathfrak{K}(j, j+1)$ is a polynomial in the variables other than $\mathfrak{K}(j, \cdot)$ and $\mathfrak{K}(j+1, \cdot)$. Let us evaluate the polynomial $\mathfrak{Z}_\alpha^{\mathfrak{K}}$ at $\mathfrak{K}(i, j) = \delta_{i,j+1}$ and $\mathfrak{K}(i, j+1) = \delta_{i,j}$, leaving the variables of $[\mathfrak{Z}_\alpha^{\mathfrak{K}}]_{j,j+1}$ undetermined. Using part (b), we obtain

$$0 = \mathfrak{Z}_\alpha^{\mathfrak{K}} = \sum_{\substack{1 \leq i \leq 2N \\ i \neq j+1}} [\mathfrak{Z}_\alpha^{\mathfrak{K}}]_{i,j+1} \mathfrak{K}(i, j+1) = [\mathfrak{Z}_\alpha^{\mathfrak{K}}]_{j,j+1}.$$

The property $\mathfrak{Z}_{\alpha^0}^{\mathfrak{K}} = \mathfrak{Z}_\alpha^{\mathfrak{K}}$ is clear. \square

The above result details the behavior of the inverse Fomin type sum $\mathfrak{Z}_\alpha^{\mathfrak{K}}$ when $\wedge^j \notin \alpha$. We will also need the complementary case $\wedge^j \in \alpha$ where, in terms of the link pattern α , the indices j and $j+1$ are connected by a link. For this purpose, we define the wedge removal of a symmetric kernel as follows: as a matrix, let the kernel $\mathfrak{K} \setminus \diamond_j \in \mathbb{C}^{2(N-1) \times 2(N-1)}$ be obtained from $\mathfrak{K} \in \mathbb{C}^{2N \times 2N}$ by removing the rows and columns j and $j+1$. Let us first calculate the coefficients of $\mathfrak{K}(j, j+1)$ in the determinants $\Delta_\beta^{\mathfrak{K}}$.

Lemma 2.20. *The coefficient of $\mathfrak{K}(j, j+1)$ in the determinant $\Delta_\beta^{\mathfrak{K}}$ is given by*

$$(2.12) \quad [\Delta_\beta^{\mathfrak{K}}]_{j,j+1} = \begin{cases} \Delta_{\beta \setminus \wedge^j}^{\mathfrak{K} \setminus \diamond_j}, & \text{if } \wedge^j \in \beta \\ -\Delta_{\beta \setminus \vee_j}^{\mathfrak{K} \setminus \diamond_j}, & \text{if } \vee_j \in \beta \\ 0, & \text{if } \times_j \in \beta. \end{cases}$$

Proof. Assume first that $\wedge^j \in \beta$, and let $((a_\ell, b_\ell))_{\ell=1}^N$ be the left-to-right orientation of β . Since there is a link $\{j, j+1\}$ in β , we have $j = a_s$ and $j+1 = b_s$ for some s . Then, applying the subdeterminant rule in the definition of the determinant $\Delta_\beta^{\mathfrak{K}}$, we have

$$(2.13) \quad [\Delta_\beta^{\mathfrak{K}}]_{j,j+1} = (-1)^{s+s} \det \left(\mathfrak{K}(a_k, b_\ell) \right)_{\substack{k, \ell=1 \\ k, \ell \neq s}}^N = \Delta_{\beta \setminus \wedge^j}^{\mathfrak{K} \setminus \diamond_j}.$$

Assume next that $\vee_j \in \beta$. Applying the subdeterminant rule in the matrices written out in Remark 2.17, the case (2.13) above, and the fact $(\beta \uparrow \diamond_j) \setminus \wedge^j = \beta \setminus \vee_j$, we observe that

$$[\Delta_\beta^{\mathfrak{K}}]_{j,j+1} = -[\Delta_{\beta \uparrow \diamond_j}^{\mathfrak{K}}]_{j,j+1} = -\Delta_{(\beta \uparrow \diamond_j) \setminus \wedge^j}^{\mathfrak{K} \setminus \diamond_j} = -\Delta_{\beta \setminus \vee_j}^{\mathfrak{K} \setminus \diamond_j}.$$

Finally, if $\times_j \in \beta$, then $\mathfrak{K}(j, j+1)$ and $\mathfrak{K}(j+1, j)$ do not appear as entries in the matrix of $\Delta_\beta^{\mathfrak{K}}$, because either both collections $\mathfrak{K}(j, \cdot)$ and $\mathfrak{K}(j+1, \cdot)$ appear on a row, or both appear on a column. \square

We now prove a cascade property for the inverse Fomin type sums, see also Figure 2.18.

Proposition 2.21. *Assume that $\wedge^j \in \alpha$. Then, the coefficient of $\mathfrak{K}(j, j+1)$ in $\mathfrak{Z}_\alpha^{\mathfrak{K}}$ is $\mathfrak{Z}_{\alpha \setminus \wedge^j}^{\mathfrak{K} \setminus \diamond_j}$.*

Proof. By Example 2.10, the coefficients $\#\mathcal{C}(\alpha/\beta)$ in the inverse Fomin type sums (2.11) are the entries $\mathcal{M}_{\alpha, \beta}^{-1}$ of the inverse signed incidence matrix of the relation $\stackrel{\circ}{\leftarrow}$. Thus, the inverse Fomin type sums $\mathfrak{Z}_\gamma^{\mathfrak{K}}$ are uniquely determined by the system of equations

$$(2.14) \quad \Delta_\beta^{\mathfrak{K}} = \sum_{\substack{\gamma \in \text{DP}_N \\ \beta \stackrel{\circ}{\leftarrow} \gamma}} \mathcal{M}_{\beta, \gamma} \mathfrak{Z}_\gamma^{\mathfrak{K}},$$

indexed by $\beta \in \text{DP}_N$, where $\mathcal{M}_{\beta,\gamma} = (-1)^{|T_0(\beta/\gamma)|}$. Assume that $\wedge^j \in \beta$, and denote $\hat{\beta} = \beta \setminus \wedge^j$. Applying Equation (2.14) with both β and $\hat{\beta}$, and using Proposition 2.18(c) and Lemma 2.20 gives

$$(2.15) \quad \sum_{\substack{\gamma \in \text{DP}_N \\ \wedge^j \in \gamma \text{ \& } \beta \xleftarrow{0} \gamma}} \mathcal{M}_{\beta,\gamma} [\mathfrak{Z}_\gamma^{\mathfrak{R}}]_{j,j+1} = [\Delta_\beta^{\mathfrak{R}}]_{j,j+1} = \Delta_{\beta \setminus \wedge^j}^{\mathfrak{R} \setminus \diamond_j} = \sum_{\substack{\hat{\gamma} \in \text{DP}_{N-1} \\ \hat{\beta} \xleftarrow{0} \hat{\gamma}}} \mathcal{M}_{\hat{\beta},\hat{\gamma}} \mathfrak{Z}_{\hat{\gamma}}^{\mathfrak{R} \setminus \diamond_j}.$$

Next, notice that $\gamma \mapsto \gamma \setminus \wedge^j$ gives a bijection between the Dyck paths $\gamma \in \text{DP}_N$ such that $\wedge^j \in \gamma$ and DP_{N-1} , and Lemma 2.12 furthermore guarantees that $\beta \xleftarrow{0} \gamma$ is equivalent to $\hat{\beta} \xleftarrow{0} \gamma \setminus \wedge^j$. Thus, re-indexing the sum on the left-hand side of Equation (2.15) by $\hat{\gamma} = \gamma \setminus \wedge^j$ gives

$$\sum_{\substack{\gamma \in \text{DP}_{N-1} \\ \hat{\beta} \xleftarrow{0} \gamma}} \mathcal{M}_{\beta,\gamma} [\mathfrak{Z}_\gamma^{\mathfrak{R}}]_{j,j+1} = \sum_{\substack{\hat{\gamma} \in \text{DP}_{N-1} \\ \hat{\beta} \xleftarrow{0} \hat{\gamma}}} \mathcal{M}_{\hat{\beta},\hat{\gamma}} \mathfrak{Z}_{\hat{\gamma}}^{\mathfrak{R} \setminus \diamond_j}.$$

Observe that $\mathcal{M}_{\beta,\gamma} = \mathcal{M}_{\hat{\beta},\hat{\gamma}}$, by the Cascade Recursion (2.6) with tile weight 1. Since the above equations hold for all $\hat{\beta} \in \text{DP}_{N-1}$, solving the system yields $[\mathfrak{Z}_\gamma^{\mathfrak{R}}]_{j,j+1} = \mathfrak{Z}_{\hat{\gamma}}^{\mathfrak{R} \setminus \diamond_j}$ for all $\gamma \in \text{DP}_N$ such that $\wedge^j \in \gamma$. \square

3. UNIFORM SPANNING TREES AND LOOP-ERASED RANDOM WALKS

We now consider planar loop-erased random walks (LERW) and the planar uniform spanning tree (UST). The main results of this section are the following. First, we derive explicit determinantal formulas for the connectivity probabilities of boundary branches in the UST, see Theorem 3.12. These formulas are obtained using the combinatorial results of Sections 2.1–2.3 combined with Fomin’s formulas, given in Section 3.4 — hence the determinantal form. Using the connectivity probabilities and Wilson’s algorithm, we obtain formulas for boundary visit probabilities of the LERW, see Corollary 3.13.

Second, we establish results concerning scaling limits of these quantities. In Theorem 3.16, we prove that the suitably renormalized connectivity probabilities have explicit conformally covariant scaling limits. We will prove in Section 4 that these functions satisfy a system of PDEs of second order. The formula of Corollary 3.13 also enables us to prove a similar convergence result (Theorem 3.17) for the LERW boundary visit probabilities — remarkably, the scaling limit satisfies a system of PDEs of second and third order. The proof of this fact is postponed to Sections 5.1–5.3.

This section is organized as follows. In Section 3.2, we define the UST with wired boundary conditions and study connectivity and boundary visit events for its branches. Section 3.3 contains the definition of the LERW and relates it to a branch of the UST, via Wilson’s algorithm. In Section 3.4, we recall Fomin’s formulas, which are crucial tools for explicitly solving the probabilities of interest in Section 3.5. The scaling limit setup and main scaling limit results are the topic of Section 3.7. Finally, a number of further generalizations is briefly discussed in Section 3.8, including results about the uniform spanning tree with free boundary conditions.

3.1. Graphs embedded in a planar domain. We consider a finite planar graph $\mathcal{G} = (\mathcal{V}, \mathcal{E})$ with a non-empty subset of vertices $\partial\mathcal{V} \subset \mathcal{V}$ declared as *boundary vertices*. All other vertices are called *interior vertices*, and the set of them is denoted by $\mathcal{V}^\circ = \mathcal{V} \setminus \partial\mathcal{V}$. The set $\partial\mathcal{E} \subset \mathcal{E}$ of *boundary edges* consists of those edges $e = \langle e^\partial, e^\circ \rangle$ which connect a boundary vertex $e^\partial \in \partial\mathcal{V}$ to an interior vertex $e^\circ \in \mathcal{V}^\circ$. We assume that the graph is embedded inside a Jordan domain in the plane in such a way that the boundary vertices $\partial\mathcal{V}$ are embedded on the boundary of the domain. We also assume that every interior vertex is connected to some boundary vertex by a path on \mathcal{G} , see Figure 3.1.

We denote by \mathcal{G}/∂ the (multi-)graph obtained by collapsing all boundary vertices $\partial\mathcal{V}$ into a single vertex v_∂ . The vertex set of \mathcal{G}/∂ is $\mathcal{V}^\circ \cup \{v_\partial\}$, where the single vertex v_∂ represents the collapsed boundary, and the edges of \mathcal{G}/∂ are obtained from the edges of \mathcal{G} by replacing any boundary vertex by v_∂ . As

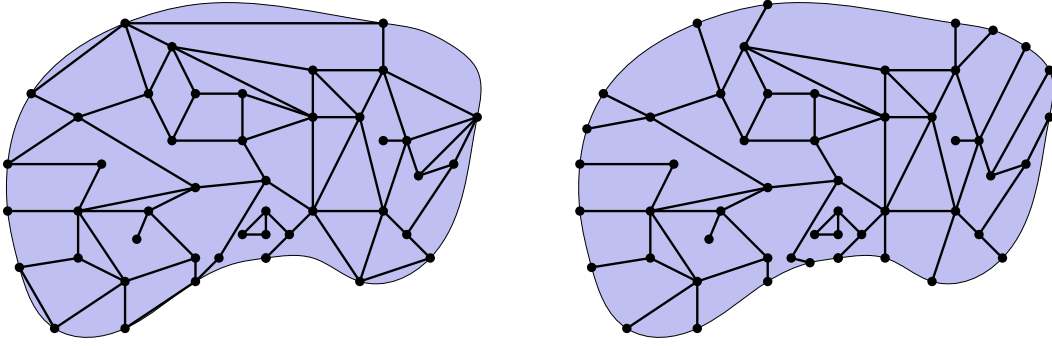


FIGURE 3.1. Planar graphs \mathcal{G}' (left) and \mathcal{G} (right) embedded in a Jordan domain. The UST and LERW models are the same in \mathcal{G}'/∂ and \mathcal{G}/∂ .

illustrated in Figure 3.1(right), we can assume that all boundary vertices of \mathcal{G} have degree one and that no edge of \mathcal{G} connects two boundary vertices, so that the boundary points of \mathcal{G} correspond one-to-one to the edges from v_∂ and the (multi-)graph \mathcal{G}/∂ has no self-loops at v_∂ .

3.2. The planar uniform spanning tree. A spanning tree of a connected graph is a subgraph which is connected and has no cycles (tree) and which contains every vertex (spanning). Let \mathcal{G} be a finite graph embedded in a planar domain as in Section 3.1 above. A uniformly randomly chosen spanning tree \mathcal{T} of the quotient graph \mathcal{G}/∂ is called a *uniform spanning tree with wired boundary conditions* on \mathcal{G} , below just referred to as a uniform spanning tree (UST). To facilitate the discussion, we occasionally view \mathcal{T} as a collection of edges of the original graph \mathcal{G} , by the obvious identification of the edges of \mathcal{G} and those of \mathcal{G}/∂ .

If $v \in \mathcal{V}^\circ$ is an interior vertex, then there exists a unique path γ_v in \mathcal{T} from v to the boundary, i.e., a sequence $\gamma_v = (v_0, v_1, \dots, v_\ell)$ of distinct vertices v_0, v_1, \dots, v_ℓ with $v_0 = v$ and $v_\ell = v_\partial$ and $\langle v_{j-1}, v_j \rangle \in \mathcal{T}$ for all $j = 1, \dots, \ell$ — for an illustration, see Figure 1.3(right). We call γ_v the *boundary branch* from the vertex v , and say that the branch reaches the boundary via the boundary edge $\langle v_{\ell-1}, v_\ell \rangle \in \partial\mathcal{E}$. For a given $e_{\text{out}} \in \partial\mathcal{E}$, we denote by $v \rightsquigarrow e_{\text{out}}$ on the event $\langle v_{\ell-1}, v_\ell \rangle = e_{\text{out}}$ that the branch γ_v from v reaches the boundary via e_{out} .

We will mostly be interested in boundary-to-boundary connectivities of the type illustrated in Figure 1.4, where the boundary branches from the interior vertices of boundary edges are considered. It is convenient to label these by the boundary edge rather than its interior vertex. For a boundary edge $e_{\text{in}} = \langle e_{\text{in}}^\partial, e_{\text{in}}^\circ \rangle$, we thus write simply $\gamma_{e_{\text{in}}}$ instead of $\gamma_{e_{\text{in}}^\circ}$, and $e_{\text{in}} \rightsquigarrow e_{\text{out}}$ instead of $e_{\text{in}}^\circ \rightsquigarrow e_{\text{out}}$.

3.2.1. The connectivity partition functions. Let $N \in \mathbb{N}$ and consider $2N$ marked distinct boundary edges $e_1, \dots, e_{2N} \in \partial\mathcal{E}$ appearing in counterclockwise order along the boundary of the domain. We are interested in the probability that the boundary branches $\gamma_{e_1}, \dots, \gamma_{e_{2N}}$ of the UST connect the marked boundary edges e_1, \dots, e_{2N} in a particular topological manner, encoded in a link pattern $\alpha \in \text{LP}_N$ — see Figure 1.5 for an example. To make precise sense of this, fix the link pattern $\alpha \in \text{LP}_N$, and choose an orientation $((a_\ell, b_\ell))_{\ell=1}^N$ of α . This selects N of the marked edges, e_{a_1}, \dots, e_{a_N} , as entrances and the other N of the marked edges, e_{b_1}, \dots, e_{b_N} , as exits. By the connectivity α we then mean that, for all $\ell = 1, \dots, N$, the boundary branch $\gamma_{e_{a_\ell}}$ from $e_{a_\ell}^\circ$ connects to the wired boundary via the edge e_{b_ℓ} (i.e., $e_{a_\ell} \rightsquigarrow e_{b_\ell}$). The partition function for the connectivity α is the probability of this event,

$$(3.1) \quad Z_\alpha(e_1, \dots, e_{2N}) := \mathbb{P} \left[\bigcap_{\ell=1}^N \{e_{a_\ell} \rightsquigarrow e_{b_\ell}\} \right].$$

A priori, the definition of the event depends on our choice of orientation of α which determines the entrance points, but we will show below in Lemma 3.1 that the probability is the same for any orientation

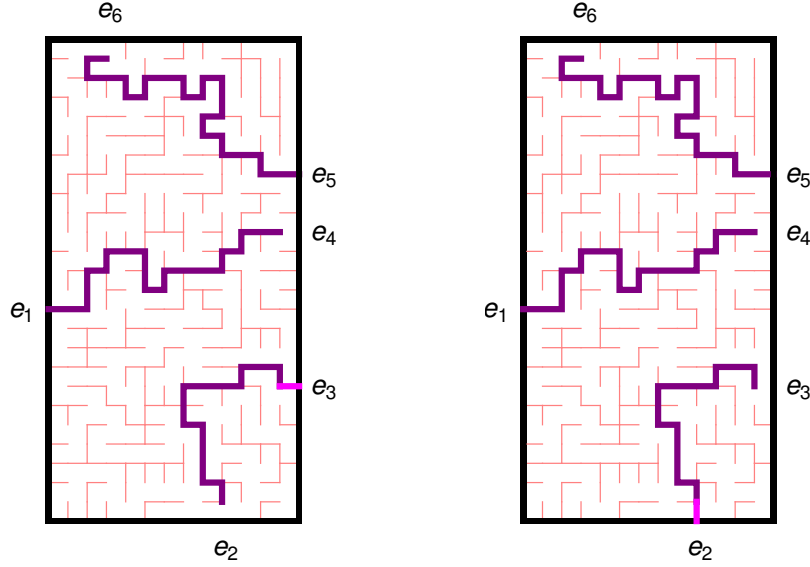


FIGURE 3.2. Illustration of the bijection used in the proof of Lemma 3.1 to show that UST boundary branch connectivity probabilities do not depend on the orientation. Both pictures have connectivities $e_4 \rightsquigarrow e_1$ and $e_6 \rightsquigarrow e_5$, but the connectivity $e_2 \rightsquigarrow e_3$ on the left is changed to the connectivity $e_3 \rightsquigarrow e_2$ on the right by deleting one edge and adding one in the tree.

of α . Note that we do not assign any connectivity unless the boundary branches from some N marked boundary edges connect to the boundary via the other N marked boundary edges. In particular, even the total partition function, defined as the sum of all connectivity probabilities

$$Z(e_1, \dots, e_{2N}) = \sum_{\alpha \in \text{LP}_N} Z_\alpha(e_1, \dots, e_{2N}),$$

is typically of small order of magnitude.

Lemma 3.1. *The connectivity probability*

$$\mathbb{P} \left[\bigcap_{\ell=1}^N \{e_{a_\ell} \rightsquigarrow e_{b_\ell}\} \right]$$

does not depend on the choice of orientation $((a_\ell, b_\ell))_{\ell=1}^N$ of the link pattern $\alpha \in \text{LP}_N$. In particular, the partition function $Z_\alpha(e_1, \dots, e_{2N})$ is well-defined by Equation (3.1).

Proof. Fix the link pattern $\alpha \in \text{LP}_N$, and let $((a_\ell, b_\ell))_{\ell=1}^N$ and $((a'_\ell, b'_\ell))_{\ell=1}^N$ be two orientations of α . The order of the links does not affect the definition of the connectivity event, so we may assume that for each ℓ , we have $\{a_\ell, b_\ell\} = \{a'_\ell, b'_\ell\}$ (in either order). Let R be the set of those link indices ℓ for which the orientation of the link is reversed, $a_\ell = b'_\ell$ and $b_\ell = a'_\ell$. Now, define the following bijection between the sets of spanning trees with these connectivities. To a tree \mathcal{T} for which the connectivity $e_{a_\ell} \rightsquigarrow e_{b_\ell}$ holds for each ℓ , we associate the tree

$$\left(\mathcal{T} \cup \{e_{a_r} \mid r \in R\} \right) \setminus \{e_{b_r} \mid r \in R\}$$

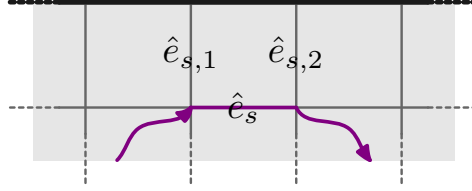


FIGURE 3.3. For an edge $\hat{e}_s \in \mathcal{E}$ at unit distance from the boundary, we associate two boundary edges $\hat{e}_{s,1}, \hat{e}_{s,2} \in \partial\mathcal{E}$. We choose them in such an order that any simple path from e_{in} to e_{out} that uses \hat{e}_s will visit $\hat{e}_{s,1}^\circ$ before $\hat{e}_{s,2}^\circ$.

obtained by deleting the exit edges and adding the entrance edges of the reversed links, as illustrated in Figure 3.2. This defines a bijection between the two connectivity events

$$\bigcap_{\ell=1}^N \{e_{a_\ell} \rightsquigarrow e_{b_\ell}\} \longrightarrow \bigcap_{\ell=1}^N \{e_{a'_\ell} \rightsquigarrow e_{b'_\ell}\}$$

and shows that the probabilities of the connectivity events for the uniform spanning tree are equal. \square

3.2.2. Boundary visit probabilities of boundary branches. Fix two boundary edges $e_{\text{in}}, e_{\text{out}} \in \partial\mathcal{E}$ of the graph \mathcal{G} . Consider the uniform spanning tree with wired boundary conditions on \mathcal{G} , conditioned on the event $\{e_{\text{in}} \rightsquigarrow e_{\text{out}}\}$ that the boundary branch $\gamma = \gamma_{e_{\text{in}}}$ from e_{in}° connects to the boundary via e_{out} . Note that the probability of the event $\{e_{\text{in}} \rightsquigarrow e_{\text{out}}\}$ on which we condition equals

$$\mathbb{P}[e_{\text{in}} \rightsquigarrow e_{\text{out}}] = Z(e_{\text{in}}, e_{\text{out}}),$$

the partition function of the unique link pattern with just one link. To make a distinction, we continue to denote by \mathbb{P} the uniform measure on spanning trees, and use $\mathbb{P}_{e_{\text{in}}, e_{\text{out}}}$ for the conditioned measure.

We are interested in the boundary visit probabilities of γ , i.e., the probabilities of the event that γ contains given edges at unit distance from the boundary, as illustrated in Figure 1.2. We say that an edge $\hat{e}_s \in \mathcal{E}$ is at unit distance from the boundary if $\hat{e}_s = \langle \hat{e}_{s,1}^\circ, \hat{e}_{s,2}^\circ \rangle$ joins the interior vertices $\hat{e}_{s,1}^\circ, \hat{e}_{s,2}^\circ$ of two boundary edges $\hat{e}_{s,1}, \hat{e}_{s,2} \in \partial\mathcal{E}$, as in Figure 3.3. Let $N' \in \mathbb{N}$ and let $\hat{e}_1, \dots, \hat{e}_{N'} \in \mathcal{E}$ be N' edges at unit distance from the boundary, and assume that the edges $e_{\text{in}}, e_{\text{out}}, \hat{e}_1, \dots, \hat{e}_{N'}$ do not have any common vertices. We will calculate the probability

$$\mathbb{P}_{e_{\text{in}}, e_{\text{out}}}[\gamma \ni \hat{e}_1, \dots, \hat{e}_{N'}],$$

and, even more specifically, the probability that the branch γ visits the edges $\hat{e}_1, \dots, \hat{e}_{N'}$ in this order, as illustrated schematically in Figure 3.4(left).

For each of the edges \hat{e}_s , choose two boundary edges $\hat{e}_{s,1}, \hat{e}_{s,2}$ so that \hat{e}_s joins their interior vertices. Note that due to planarity and the fact that these edges are at unit distance from the boundary, any simple path from e_{in} to e_{out} can only traverse \hat{e}_s in one possible direction. We assume $\hat{e}_{s,1}^\circ, \hat{e}_{s,2}^\circ$ chosen so that $\hat{e}_{s,1}^\circ$ must be visited before $\hat{e}_{s,2}^\circ$. If \hat{e}_s is on the counterclockwise boundary arc $\partial\mathcal{G}_+$ from e_{in} to e_{out} , then the directed edge from $\hat{e}_{s,1}^\circ$ to $\hat{e}_{s,2}^\circ$ is counterclockwise along the boundary, and if \hat{e}_s is on the clockwise boundary arc $\partial\mathcal{G}_-$ from e_{in} to e_{out} , then the directed edge is clockwise along the boundary, see Figure 3.4. The sequence $\omega = (\omega_1, \dots, \omega_{N'}) \in \{+, -\}^{N'}$, with $\omega_s = \pm$ if \hat{e}_s is on $\partial\mathcal{G}_\pm$, is called a *boundary visit order*: it specifies the order in which the (unordered) collection of N' edges at unit distance from the boundary is to be visited.

We now have $2N = 2N' + 2$ marked boundary edges $e_{\text{in}}, e_{\text{out}}, \hat{e}_{1,1}, \hat{e}_{1,2}, \dots, \hat{e}_{N',1}, \hat{e}_{N',2}$. We order these boundary edges counterclockwise along the boundary, to obtain a sequence of boundary edges that we denote by $e_1, \dots, e_{2N} \in \partial\mathcal{E}$ as in the previous section. By convention, we choose to start the labeling from $e_1 = e_{\text{in}}$. The boundary visit order ω determines a link pattern $\alpha(\omega) \in \text{LP}_N$ as illustrated in Figure 3.4 — see also [KP16, Section 5.2] for a more formal definition. The next result relates the probability of the boundary visits in the order ω to the partition function of the connectivity $\alpha(\omega)$.

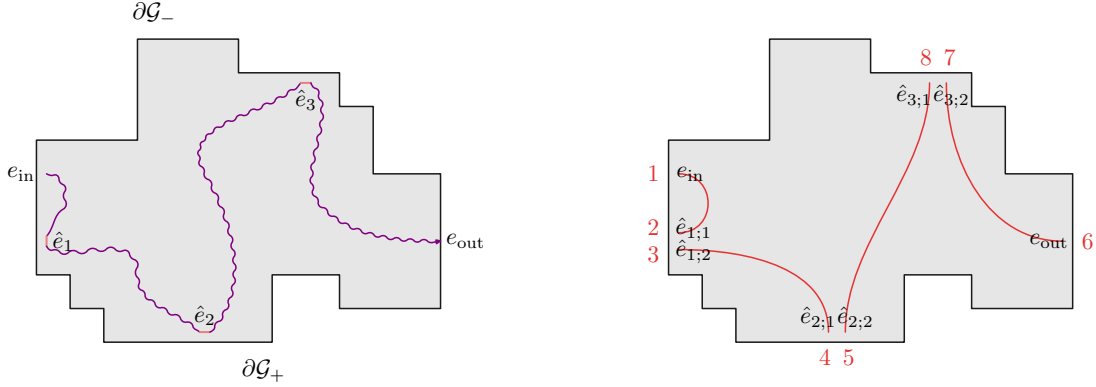


FIGURE 3.4. To any boundary visit order $\omega \in \{+, -\}^{N'}$ we associate a corresponding link pattern $\alpha(\omega) \in \text{LP}_N$ with $N = N' + 1$. For the case illustrated in the figure, we have $\omega = (+, +, -)$ and $\alpha(\omega) = \{\{1, 2\}, \{3, 4\}, \{5, 8\}, \{6, 7\}\}$.

Lemma 3.2. *Let $e_{\text{in}}, e_{\text{out}} \in \partial\mathcal{E}$ be two boundary edges and let $\hat{e}_1, \dots, \hat{e}_{N'}$ be edges at unit distance from the boundary, as above. Associate to them the boundary edges e_1, \dots, e_{2N} and the link pattern $\alpha(\omega)$, as above. Then, the boundary visit probability for the branch γ from e_{in} to e_{out} is given by the ratio*

$$\mathbb{P}_{e_{\text{in}}, e_{\text{out}}}[\gamma \text{ uses } \hat{e}_1, \dots, \hat{e}_{N'} \text{ in this order}] = \frac{Z_{\alpha(\omega)}(e_1, \dots, e_{2N})}{Z(e_{\text{in}}, e_{\text{out}})}$$

of partition functions.

Proof. Recall first that the assertion concerns the uniform spanning tree conditioned on the event $e_{\text{in}} \rightsquigarrow e_{\text{out}}$ of probability $Z(e_{\text{in}}, e_{\text{out}})$. We again use a bijection in the uniform spanning tree. To define the bijection, we use the link pattern $\alpha(\omega)$ and the orientation $((a_\ell, b_\ell))_{\ell=1}^N$ of it which naturally corresponds to the direction that the path γ travels.

Let \mathcal{T} be a tree such that we have $e_{\text{in}} \rightsquigarrow e_{\text{out}}$ and the branch γ contains the edges $\hat{e}_1, \dots, \hat{e}_{N'}$. The bijection associates to this tree the tree obtained by replacing in \mathcal{T} each edge \hat{e}_s at unit distance from the boundary by the boundary edge $\hat{e}_{s;1}$, see Figure 3.5. This transformation is bijective onto the set of spanning trees which have the connectivity $\alpha(\omega)$ for the edges e_1, \dots, e_{2N} . Therefore, we have

$$\mathbb{P}[e_{\text{in}} \rightsquigarrow e_{\text{out}} \text{ and } \gamma_{e_{\text{in}}} \text{ uses } \hat{e}_1, \dots, \hat{e}_{N'} \text{ in this order}] = \mathbb{P}\left[\bigcap_{\ell=1}^N \{e_{a_\ell} \rightsquigarrow e_{b_\ell}\}\right] = Z_{\alpha(\omega)}(e_1, \dots, e_{2N}).$$

With the conditioning, we get the asserted formula

$$\begin{aligned} \mathbb{P}_{e_{\text{in}}, e_{\text{out}}}[\gamma \text{ uses } \hat{e}_1, \dots, \hat{e}_{N'} \text{ in this order}] &= \frac{\mathbb{P}[e_{\text{in}} \rightsquigarrow e_{\text{out}} \text{ and } \gamma_{e_{\text{in}}} \text{ uses } \hat{e}_1, \dots, \hat{e}_{N'} \text{ in this order}]}{\mathbb{P}[e_{\text{in}} \rightsquigarrow e_{\text{out}}]} \\ &= \frac{Z_{\alpha(\omega)}(e_1, \dots, e_{2N})}{Z(e_{\text{in}}, e_{\text{out}})}. \end{aligned}$$

□

3.3. Relation between uniform spanning trees and loop-erased random walks. We next turn to Wilson's algorithm, introduced in [Wil96] as an efficient method of sampling a uniform spanning tree. For us, the algorithm is mainly important because with it, the relation of the uniform spanning tree to loop-erased random walks becomes apparent, see also [Pem91].

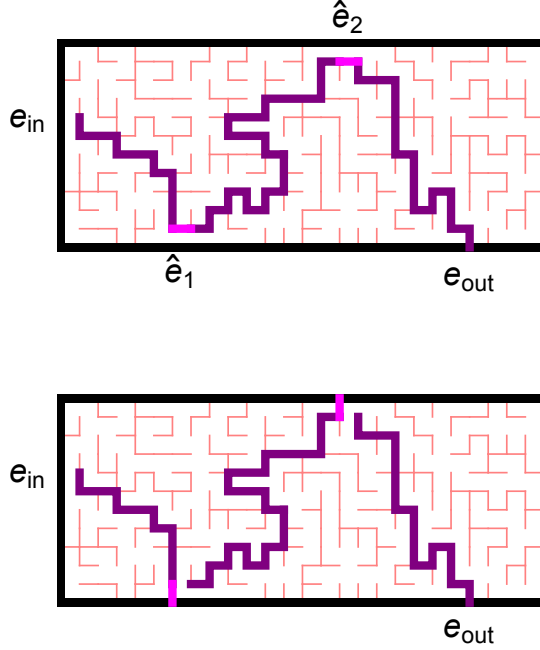


FIGURE 3.5. Illustration of the bijection used in Lemma 3.2 to obtain general boundary visit probabilities of a UST boundary branch from multiple branch connectivity probabilities.

3.3.1. Random walks. Let $\mathcal{G} = (\mathcal{V}, \mathcal{E})$ and $\partial\mathcal{V} \subset \mathcal{V}$, $\partial\mathcal{E} \subset \mathcal{E}$ be as in Section 3.1. The *symmetric random walk* (SRW) on the graph \mathcal{G} is the Markov process on the vertex set \mathcal{V} whose transition probability from $v \in \mathcal{V}$ to $w \in \mathcal{V}$ is

$$(3.2) \quad P_{v,w} = \begin{cases} \frac{1}{\deg(v)} & \text{if } \langle v, w \rangle \in \mathcal{E} \\ 0 & \text{otherwise.} \end{cases}$$

We use in particular the random walk η started from an interior vertex $\eta(0) = v \in \mathcal{V}^\circ$, and stopped at the first time τ at which it is on the boundary $\partial\mathcal{V}$. The last step of the stopped random walk $\eta = (\eta(t))_{t=0}^\tau$ is a boundary edge $\langle \eta(\tau-1), \eta(\tau) \rangle \in \partial\mathcal{E}$. For any given boundary edge $e_{\text{out}} \in \partial\mathcal{E}$, the *harmonic measure* $H_v(e_{\text{out}})$ of e_{out} seen from $v \in \mathcal{V}^\circ$ is the probability that the random walk η started from v exits via the edge e_{out} :

$$H_v(e_{\text{out}}) = \mathbb{P} \left[\langle \eta(\tau-1), \eta(\tau) \rangle = e_{\text{out}} \mid \eta(0) = v \right].$$

If $e_{\text{in}} = \langle e_{\text{in}}^\partial, e_{\text{in}}^\circ \rangle \in \partial\mathcal{E}$ and $e_{\text{out}} = \langle e_{\text{out}}^\partial, e_{\text{out}}^\circ \rangle \in \partial\mathcal{E}$ are two boundary edges, then, an easy path reversal argument shows that the harmonic measure of e_{out} seen from e_{in}° and the harmonic measure of e_{in} seen from e_{out}° coincide.

Lemma 3.3. *For any $e_{\text{in}}, e_{\text{out}} \in \partial\mathcal{E}$, we have $H_{e_{\text{in}}^\circ}(e_{\text{out}}) = H_{e_{\text{out}}^\circ}(e_{\text{in}})$.*

The *random walk excursion kernel* $K(e_{\text{in}}, e_{\text{out}})$ between e_{in} and e_{out} is either one of the above harmonic measures

$$K(e_{\text{in}}, e_{\text{out}}) := H_{e_{\text{in}}^\circ}(e_{\text{out}}) = H_{e_{\text{out}}^\circ}(e_{\text{in}}).$$

In particular, the excursion kernel is symmetric, $K(e_{\text{in}}, e_{\text{out}}) = K(e_{\text{out}}, e_{\text{in}})$.

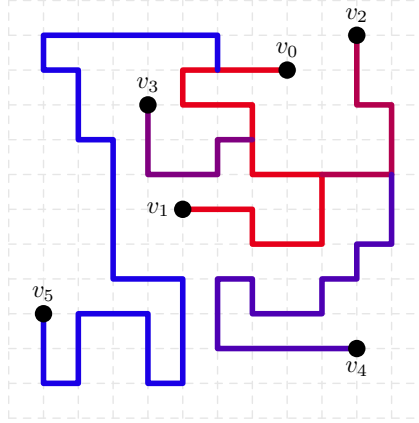


FIGURE 3.6. Wilson's algorithm (Theorem 3.4) constructs the uniform spanning tree step by step, by adding loop-erased random walks from vertices v_1, v_2, \dots

3.3.2. Loop-erased random walk and Wilson's algorithm. If $z = (z(t))_{t=0}^n$ is a finite sequence of symbols, its *loop-erasure* $\text{LE}(z)$ is defined as the sequence $(\lambda(s))_{s=0}^m$ given recursively by

$$\begin{aligned} \lambda(0) &= z(0), & \text{and for } s \geq 0 \\ \lambda(s+1) &= z(t_s + 1), & \text{where } t_s = \max \left\{ t \in \mathbb{Z}_{\geq 0} \mid t > t_{s-1} \text{ and } z(t) = \lambda(s) \right\} \end{aligned}$$

(interpret $t_{-1} = -1$), and its number of steps is the smallest m such that $t_m = n$. Note that the loop-erasure has the same first and last symbols as the original sequence, $\lambda(0) = z(0)$ and $\lambda(m) = z(n)$, and it is self-avoiding in the sense that we have $\lambda(s) \neq \lambda(s')$ whenever $s \neq s'$.

A *loop-erased random walk* is the loop-erasure of some random walk of finitely many steps. We consider a symmetric random walk η as in Section 3.3.1. The random walk η is started from an interior vertex $\eta(0) = v \in \mathcal{V}$, its transition probabilities (3.2) to all neighboring vertices are equal, and the walk is stopped at the (almost surely finite) first time τ at which the walk reaches a given non-empty set $S \subset \mathcal{V}$, for example the boundary $\partial\mathcal{V}$. We define the loop-erased random walk (LERW) λ from v to S as the loop-erasure of $\eta = (\eta(t))_{t=0}^\tau$, that is, $\lambda = \text{LE}(\eta)$. With a slight abuse of notation, we view λ alternatively as the list of its vertices $(\lambda(s))_{s=0}^m$, or as the list of edges $(\langle \lambda(s-1), \lambda(s) \rangle)_{s=1}^m$ it uses, or as the subgraph formed by these vertices and edges.

The following procedure of constructing a uniform spanning tree is known as Wilson's algorithm.

Theorem 3.4. [Wil96] *Let v_0, \dots, v_n be any enumeration of the set of vertices of a finite connected graph. Define \mathcal{T}_0 as the subgraph consisting of only the vertex v_0 , and recursively for $k = 1, \dots, n$ define \mathcal{T}_k as the union of \mathcal{T}_{k-1} and a loop-erased random walk from v_k to \mathcal{T}_{k-1} , independently for each k . Then $\mathcal{T} = \mathcal{T}_n$ is a uniform spanning tree of the original graph.*

To get a uniform spanning tree with wired boundary conditions, i.e., a uniform spanning tree of \mathcal{G}/∂ , we will make various convenient choices of enumeration of the interior vertices, but we always use the boundary as the zeroth step in the construction, $v_0 = v_\partial$.

Let us now record a few direct consequences of Wilson's algorithm.

Corollary 3.5. *For the uniform spanning tree with wired boundary conditions on \mathcal{G} , we have:*

- (a): *The boundary branch γ_v from $v \in \mathcal{V}$ has the law of a loop-erased random walk from v to $\partial\mathcal{V}$.*
- (b): *The probability that the boundary branch γ_v from $v \in \mathcal{V}$ reaches the boundary via a boundary edge $e_{\text{out}} \in \partial\mathcal{E}$ is the harmonic measure*

$$\mathbb{P}[v \rightsquigarrow e_{\text{out}}] = \mathbb{H}_v(e_{\text{out}}).$$

(c): Conditionally on the event that the boundary branch γ_v reaches the boundary via an edge $e_{\text{out}} \in \partial\mathcal{E}$, the law of the branch γ_v is the loop-erasure of a symmetric random walk from v to $\partial\mathcal{V}$ conditioned to reach $\partial\mathcal{V}$ via the edge e_{out} .

Proof. Construct the uniform spanning tree \mathcal{T} by Wilson's algorithm, using an enumeration of vertices such that $v_0 = v_\partial$ and $v_1 = v$. For part (a), note that the loop-erased random walk from $v_1 = v$ to $\mathcal{T}_0 = \{v_\partial\}$ is a path in the tree $\mathcal{T} = \mathcal{T}_n$ from v to $\partial\mathcal{V}$, and this unique path is the boundary branch γ_v . For parts (b) and (c), note that the last edge used by the random walk and its loop-erasure is the same. Therefore, the event that the branch reaches the boundary via e_{out} coincides with the event that the random walk reaches the boundary via e_{out} . \square

In particular, we can describe the boundary branch $\gamma_{e_{\text{in}}}$ from a boundary edge $e_{\text{in}} \in \partial\mathcal{E}$, by choosing $v = e_{\text{in}}^\circ$. The partition function for the connectivity of just two boundary edges $e_{\text{in}}, e_{\text{out}} \in \partial\mathcal{E}$ is the excursion kernel

$$(3.3) \quad Z(e_{\text{in}}, e_{\text{out}}) = \mathbb{P}[e_{\text{in}}^\circ \rightsquigarrow e_{\text{out}}] = H_{e_{\text{in}}^\circ}(e_{\text{out}}) = K(e_{\text{in}}, e_{\text{out}}).$$

To consider multiple branches, we will crucially use the following slight generalization. We use the notation $\mathcal{W}(u, e)$ for the set of all finite walks on the graph \mathcal{G} from an interior vertex $u \in \mathcal{V}^\circ$ to the boundary via the boundary edge $e \in \partial\mathcal{E}$, i.e.,

$$(3.4) \quad \mathcal{W}(u, e) := \left\{ (v_0, v_1, \dots, v_{\ell-1}, v_\ell) \mid \ell \in \mathbb{N}, v_0 = u, \langle v_{\ell-1}, v_\ell \rangle = e, \right. \\ \left. \text{for all } j < \ell \text{ we have } v_j \in \mathcal{V}^\circ \text{ and } \langle v_{j-1}, v_j \rangle \in \mathcal{E} \right\}.$$

Lemma 3.6. *Let $e_1, \dots, e_N \in \partial\mathcal{E}$ be distinct boundary edges, and $u_1, \dots, u_N \in \mathcal{V}^\circ$ distinct interior vertices. Let also η^1, \dots, η^N be independent symmetric random walks started from u_1, \dots, u_N , respectively, and stopped upon hitting the boundary. Then the probability that, in the uniform spanning tree, the N boundary branches from u_1, \dots, u_N connect to the boundary via the edges e_1, \dots, e_N , respectively, equals*

$$\mathbb{P}\left[\bigcap_{j=1}^N \{u_j \rightsquigarrow e_j\}\right] = \mathbb{P}\left[\eta^j \in \mathcal{W}(u_j, e_j) \text{ for all } j, \text{ and } \eta^j \cap \text{LE}(\eta^i) = \emptyset \text{ for all } i < j\right].$$

Proof. The assertion becomes clear when the uniform spanning tree is constructed by Wilson's algorithm, using an enumeration of vertices such that $v_0 = v_\partial$, $v_1 = u_1, \dots, v_N = u_N$. \square

3.4. Fomin's formula. We now recall a formula by Fomin [Fom01], which we will use for the calculation of the connectivity probabilities of UST branches.

To state the original formulation of Fomin's theorem, consider for a moment a weighted directed graph \mathcal{G} , with each directed edge (v, v') assigned a weight $w_{v, v'}$. To a finite walk $\chi = (v_0, \dots, v_\ell)$ on the graph \mathcal{G} , assign the weight $w(\chi) = \prod_{s=1}^\ell w_{(v_{s-1}, v_s)}$ given by the product of the weights of the edges used by the walk. We denote $\chi \in \mathcal{W}(u, v)$ if the path χ starts from $v_0 = u$ and ends at $v_\ell = v$ — this differs from (3.4) in that the path must end at a given vertex v rather than a given boundary edge e . The generalized Green's function is defined as the sum of weights of such (finite) walks,

$$G(u, v) = \sum_{\chi \in \mathcal{W}(u, v)} w(\chi).$$

Fomin found a formula for a determinant of Green's functions as a sum over paths, from the starting points u_1, \dots, u_N to the end points v_1, \dots, v_N in any order, subject to the requirement that later paths do not intersect the loop-erasures of the former paths. His proof was a clever generalization of a path-switching argument of Karlin and McGregor [KM59], see also Lindström [Lin73] and Gessel and Viennot [GV85].

Theorem 3.7. [Fom01, Theorem 6.1] *Let u_1, \dots, u_N and v_1, \dots, v_N be distinct vertices of a weighted directed graph. Then we have*

$$\det [G(u_i, v_j)]_{i,j=1}^N = \sum_{\sigma \in \mathfrak{S}_N} \text{sgn}(\sigma) \sum_{\substack{\chi^1, \dots, \chi^N \\ \chi^i \in \mathcal{W}(u_i, v_{\sigma(i)}) \\ \forall i < j : \chi^j \cap \text{LE}(\chi^i) = \emptyset}} w(\chi^1) \cdots w(\chi^N).$$

Note that if the weights are the transition probabilities of a random walk, $w_{v,v'} = P_{v,v'}$, then the generalized Green's function is the usual probabilistic Green's function $G(u, v) = \sum_{t \geq 0} \mathbb{P}[\eta(t) = v \mid \eta(0) = u]$. We consider the symmetric random walk of (3.2) stopped upon reaching the boundary $\partial \mathcal{V}$. For this, set

$$(3.5) \quad w_{v,v'} = \begin{cases} \frac{1}{\deg(v)} & \text{if } v \in \mathcal{V}^\circ \text{ and } \langle v, v' \rangle \in \mathcal{E} \\ 0 & \text{otherwise.} \end{cases}$$

In particular, the weights from the boundary vertices are set to zero, to correctly account for the stopping. Then the harmonic measure of the boundary edge $e \in \partial \mathcal{E}$ seen from an interior vertex $u \in \mathcal{V}^\circ$ can be written as a Green's function, by summing over all possible walks:

$$H_u(e) = \sum_{\chi \in \mathcal{W}(u, e^\partial)} \mathbb{P}[(\eta(t))_{t=0}^\tau = \chi] = \sum_{\chi \in \mathcal{W}(u, e^\partial)} w(\chi) = G(u, e^\partial).$$

In particular, the random walk excursion kernel can be written as

$$K(e_{\text{in}}, e_{\text{out}}) = H_{e_{\text{in}}}^\circ(e_{\text{out}}) = G(e_{\text{in}}^\circ, e_{\text{out}}^\partial).$$

There is more than a superficial resemblance between Theorem 3.7 and Lemma 3.6. In fact, when the endpoints v_1, \dots, v_N are boundary vertices and the weights are chosen as in (3.5), the inner sums on the right-hand side in Theorem 3.7 are connectivity probabilities in the uniform spanning tree.

Lemma 3.8. *Let $e_1, \dots, e_N \in \partial \mathcal{E}$ be distinct boundary edges, and $u_1, \dots, u_N \in \mathcal{V}^\circ$ distinct interior vertices. Then the probability that in the uniform spanning tree, the N boundary branches from u_1, \dots, u_N connect to the boundary via the edges e_1, \dots, e_N , respectively, equals*

$$\mathbb{P}\left[\bigcap_{j=1}^N \{u_j \rightsquigarrow e_j\}\right] = \sum_{\substack{\chi^1, \dots, \chi^N \\ \chi^j \in \mathcal{W}(u_j, e_j^\partial) \\ \forall i < j : \chi^j \cap \text{LE}(\chi^i) = \emptyset}} w(\chi^1) \cdots w(\chi^N),$$

where the weights w are as in (3.5).

Proof. Let η^j be a symmetric random walk started from u_j and stopped upon reaching the boundary. For any given path χ^j which starts from u_j and ends on the boundary, we have $\mathbb{P}[\eta^j = \chi^j] = w(\chi^j)$. The assertion now follows from Lemma 3.6, by writing the probability concerning the random walks η^1, \dots, η^N as the sum of probabilities that the random walks take the specific trajectories χ^1, \dots, χ^N . \square

Rewriting the terms on the right-hand side of Fomin's formula as connectivity probabilities of branches, we arrive at the following interpretation for the uniform spanning tree.

Proposition 3.9. *Let $e_1, \dots, e_N \in \partial \mathcal{E}$ be distinct boundary edges, and $u_1, \dots, u_N \in \mathcal{V}^\circ$ distinct interior vertices. Then, for the uniform spanning tree with wired boundary conditions, we have*

$$(3.6) \quad \sum_{\sigma \in \mathfrak{S}_N} \text{sgn}(\sigma) \mathbb{P}\left[\bigcap_{\ell=1}^N \{u_\ell \rightsquigarrow e_{\sigma(\ell)}\}\right] = \det \left(H_{u_k}(e_\ell) \right)_{k,\ell=1}^N,$$

where $H_u(e)$ is the harmonic measure of $e \in \partial \mathcal{E}$ seen from $u \in \mathcal{V}$.

Proof. Apply Theorem 3.7 with sources u_k , for $k = 1, \dots, N$, and targets $v_\ell = e_\ell^\partial$, for $\ell = 1, \dots, N$. Simplify the inner summations with Lemma 3.8, and observe that when the target points are on the boundary, $v_\ell = e_\ell^\partial$, the Green's functions in the determinant are harmonic measures, $G(u_k, e_\ell^\partial) = H_{u_k}(e_\ell)$. \square

In general, the difficulty in applying Fomin's formula to the uniform spanning tree connectivity probabilities is that the formula contains simultaneously connectivities from the starting points u_1, \dots, u_N to the end points e_1, \dots, e_N in all possible permutations σ . Fomin also noted [Fom01, Theorem 6.4], however, that if the graph and the choice of points is such that it is only possible to connect the starting points to the end points in one order without intersections of the trajectories, then the sum over permutations only contains one term. In this situation, it is possible to compute the sum over paths in Lemma 3.8 as a determinant of the much simpler Green's functions. This happens most naturally in the planar setup, if the points $u_1, \dots, u_N, v_N, \dots, v_1$ are ordered counterclockwise (or clockwise) along the boundary. This special case has become quite well known in the two-dimensional statistical physics research. In particular, the following consequence has been observed by many authors, for instance [Dub06a, KL07]. We include the proof, because some of our further results then become transparent generalizations.

Corollary 3.10. *Let \mathcal{G} be a graph embedded in a Jordan domain as in Section 3.1, and let $e_1, \dots, e_{2N} \in \partial\mathcal{E}$ distinct boundary edges ordered counterclockwise along the boundary of the domain. Consider the uniform spanning tree with wired boundary conditions on \mathcal{G} . Then the probability of the rainbow connectivity $e_1 \rightsquigarrow e_{2N}, e_2 \rightsquigarrow e_{2N-1}, \dots, e_N \rightsquigarrow e_{N+1}$ of the N boundary branches is given by the determinant*

$$\mathbb{P}\left[\bigcap_{\ell=1}^N \{e_\ell \rightsquigarrow e_{2N+1-\ell}\}\right] = \det\left(\mathbb{K}(e_k, e_{2N+1-\ell})\right)_{k,\ell=1}^N,$$

where \mathbb{K} is the random walk excursion kernel on \mathcal{G} .

Proof. Apply Proposition 3.9 with sources $u_\ell = e_\ell^\circ$, for $\ell = 1, \dots, N$, and targets $v_k = e_{2N+1-k}^\partial$, for $k = 1, \dots, N$. Note that the connectivity probability

$$\mathbb{P}\left[\bigcap_{\ell=1}^N \{e_\ell \rightsquigarrow e_{2N+1-\sigma(\ell)}\}\right]$$

vanishes unless σ is the identity permutation, since the boundary branches $\gamma_{e_1}, \dots, \gamma_{e_N}$ cannot cross each other in the planar domain. The left-hand side of (3.6) thus contains only one non-vanishing term,

$$\mathbb{P}\left[\bigcap_{\ell=1}^N \{e_\ell \rightsquigarrow e_{2N+1-\ell}\}\right] = \det\left(H_{e_k^\circ}(e_{2N+1-\ell})\right)_{k,\ell=1}^N.$$

It remains to recognize the harmonic measures seen from boundary points as random walk excursion kernels: $H_{e_k^\circ}(e_{2N+1-\ell}) = \mathbb{K}(e_k, e_{2N+1-\ell})$. \square

3.5. Solution of the connectivity partition functions. The well-known Corollary 3.10 of Fomin's formula is particular first because of planarity, and second because of the maximally nested rainbow connectivity that it describes, encoded in the link pattern $\underline{\mathbb{m}}_N$ (see Figure 2.2).

Let us keep the planar graph embedded in the Jordan domain and marked boundary edges e_1, \dots, e_{2N} counterclockwise along the boundary of the domain, but generalize the choice of the N source points u_ℓ , for $\ell = 1, \dots, N$ among $e_1^\circ, \dots, e_{2N}^\circ$. Each term in Fomin's formula can still be interpreted as a connectivity probability, up to a sign, but the determinant is a sum of various possibilities.

As in Section 2.6, for a link pattern $\alpha \in \text{LP}_N$ with the left-to-right orientation $((a_\ell, b_\ell))_{\ell=1}^N$, denote by

$$(3.7) \quad \Delta_\alpha^K(e_1, \dots, e_{2N}) := \det\left(\mathbb{K}(e_{a_k}, e_{b_\ell})\right)_{k,\ell=1}^N$$

the determinant of α with the random walk excursion kernel \mathbf{K} . Recalling the definition (3.1) of partition functions as the probabilities of connectivities, the conclusion of Corollary 3.10 can be written as

$$Z_{\underline{\alpha}_N}(e_1, \dots, e_{2N}) = \Delta_{\underline{\alpha}_N}^{\mathbf{K}}(e_1, \dots, e_{2N}).$$

With the choice of sources $u_\ell = e_{a_\ell}^\circ$, for $\ell = 1, \dots, N$, and targets $v_k = e_{b_k}^\partial$, for $k = 1, \dots, N$, the conclusion of the more general Proposition 3.9 becomes

$$(3.8) \quad \Delta_\alpha^{\mathbf{K}}(e_1, \dots, e_{2N}) = \sum_{\sigma \in \mathfrak{S}_N} \text{sgn}(\sigma) \mathbf{P} \left[\bigcap_{\ell=1}^N \{e_{a_\ell} \rightsquigarrow e_{b_{\sigma(\ell)}}\} \right].$$

Although there is, in general, more than one non-vanishing term in the sum over permutations σ , planarity still puts certain constraints on them. In fact, we have the following.

Proposition 3.11. *Let $\alpha \in \text{LP}_N$ be a link pattern. We have*

$$(3.9) \quad \Delta_\alpha^{\mathbf{K}}(e_1, \dots, e_{2N}) = \sum_{\beta \in \text{LP}_N} \mathcal{M}_{\alpha, \beta} Z_\beta(e_1, \dots, e_{2N}),$$

where \mathcal{M} is the unit weight incidence matrix (2.4) of the parenthesis reversal relation $\stackrel{\circ}{\leftarrow}$, explicitly given in Example 2.10.

Proof. Keep the link pattern α fixed throughout. To get the asserted formula (3.9), we just simplify Equation (3.8) for the same determinant $\Delta_\alpha^{\mathbf{K}}$. Consider a permutation $\sigma \in \mathfrak{S}_N$ of the exit points. Then, the connectivity probability $\mathbf{P} \left[\bigcap_{\ell=1}^N \{e_{a_\ell} \rightsquigarrow e_{b_{\sigma(\ell)}}\} \right]$ vanishes unless this connectivity determined by σ is planar, i.e., $((a_\ell, b_{\sigma(\ell)}))_{\ell=1}^N$ is an orientation of some link pattern β . By Example 2.10, for any link pattern $\beta \in \text{LP}_N$, we have $\mathcal{M}_{\alpha, \beta} = \text{sgn}(\sigma)$ if β is obtained from α by a permutation σ of exits, and $\mathcal{M}_{\alpha, \beta} = 0$ if no such permutation exists. The formula (3.9) follows. \square

The matrix \mathcal{M} is invertible, and a formula for the inverse is explicitly given in Example 2.10, as a special case of Theorem 2.9. We can therefore solve (3.9) for the partition functions of connectivities.

Theorem 3.12. *Let $\alpha \in \text{LP}_N$ be a link pattern. We have*

$$(3.10) \quad Z_\alpha(e_1, \dots, e_{2N}) = \sum_{\beta \succeq \alpha} \mathcal{M}_{\alpha, \beta}^{-1} \Delta_\beta^{\mathbf{K}}(e_1, \dots, e_{2N}),$$

where \mathcal{M}^{-1} is explicitly given in (2.5) in Example 2.10.

Proof. Multiply Equation (3.9) by $\mathcal{M}_{\gamma, \alpha}^{-1}$ and sum over $\alpha \in \text{LP}_N$ to get $Z_\gamma(e_1, \dots, e_{2N})$. \square

Recall from Section 3.2.2 that the boundary visit probabilities of a UST branch from e_{in} to e_{out} can be expressed in terms of the connectivity partition function Z_α by Lemma 3.2, and therefore, Theorem 3.12 also leads to explicit determinantal formulas for them. Since the law of the UST boundary branch is that of a loop-erased random walk, we get also the boundary visit probabilities for a loop-erased random walk. We state the result in this form.

Corollary 3.13. *Let $e_{\text{in}}, e_{\text{out}} \in \partial \mathcal{E}$ be two boundary edges and let $\hat{e}_1, \dots, \hat{e}_{N'}$ be edges at unit distance from the boundary. Associate to them the boundary edges $e_1, \dots, e_{2N} \in \partial \mathcal{E}$ and the link pattern $\alpha(\omega)$, as in Section 3.2.2. Then, the boundary visit probability for the loop-erasure $\lambda = \text{LE}(\eta)$ of a random walk η on \mathcal{G} from e_{in}° , conditioned to reach the boundary $\partial \mathcal{V}$ via e_{out} , is given by*

$$\mathbf{P}_{e_{\text{in}}, e_{\text{out}}} [\lambda \text{ uses } \hat{e}_1, \dots, \hat{e}_{N'} \text{ in this order}] = \frac{Z_{\alpha(\omega)}(e_1, \dots, e_{2N})}{Z(e_{\text{in}}, e_{\text{out}})} = \sum_{\beta \succeq \alpha} \mathcal{M}_{\alpha, \beta}^{-1} \frac{\Delta_\beta^{\mathbf{K}}(e_1, \dots, e_{2N})}{\mathbf{K}(e_{\text{in}}, e_{\text{out}})}.$$

Proof. This is a direct consequence of Corollary 3.5, Lemma 3.2, and Theorem 3.12. \square

Remark 3.14. The boundary visit probability is given by the formula on the right-hand side of Corollary 3.13 even if the distinct boundary edges $\hat{e}_1, \dots, \hat{e}_{N'}$ share some vertices, i.e., not all edges e_1, \dots, e_{2N} are distinct. The partition function expression for this probability, however, has no immediate interpretation in such degenerate cases.

3.6. Random spanning trees on weighted graphs. For simplicity, we have formulated the results above for a spanning tree chosen uniformly at random. The arguments however generalize to other natural random spanning trees, where the edges e of the graph have weights $c(e) > 0$, and the natural random walk has the transition probabilities

$$w_{v,v'} = \frac{c(\langle v, v' \rangle)}{\sum_u c(\langle v, u \rangle)}.$$

Using Wilson's algorithm, the natural random spanning tree on \mathcal{G}/∂ is obtained from the loop-erasures of these weighted random walks. The probabilities of the spanning tree are [Wil96]

$$\mathbb{P}[\{\mathcal{T}\}] \propto \prod_{e \in \mathcal{T}} c(e).$$

Let $\alpha \in \text{LP}_N$ be a link pattern with any orientation $((a_\ell, b_\ell))_{\ell=1}^N$, and let e_1, \dots, e_{2N} be distinct boundary edges. Associate to them the partition function

$$Z_\alpha(e_1, \dots, e_{2N}) = \left(\prod_{\ell=1}^N c(e_{a_\ell}) \right) \times \mathbb{P}[\{e_{a_1} \rightsquigarrow e_{b_1}\} \cap \dots \cap \{e_{a_N} \rightsquigarrow e_{b_N}\}],$$

which is independent of the chosen orientation by the bijection argument of Lemma 3.1. These connectivity partition functions can be solved by repeating the analysis of Sections 3.3–3.5 with the weighted random walks: let \mathbf{H} denote the harmonic measure of the weighted random walk, and define

$$\mathbf{K}_S(e_{\text{in}}, e_{\text{out}}) = c(e_{\text{in}}) \mathbf{H}_{e_{\text{out}}}(e_{\text{in}}^\circ) = \mathbf{K}_S(e_{\text{out}}, e_{\text{in}}).$$

Then, Theorem 3.12 generalizes to

$$Z_\alpha(e_1, \dots, e_{2N}) = \sum_{\beta \succeq \alpha} \mathcal{M}_{\alpha, \beta}^{-1} \Delta_\beta^{\mathbf{K}_S}(e_1, \dots, e_{2N}),$$

and, analogously, the statements of Corollary 3.13 and Remark 3.14 hold with the formula

$$\mathbb{P}_{e_{\text{in}}, e_{\text{out}}}[\lambda \text{ uses } \hat{e}_1, \dots, \hat{e}_{N'} \text{ in this order}] = \left(\prod_{s=1}^{N'} \frac{c(\hat{e}_s)}{c(\hat{e}_{s;1})c(\hat{e}_{s;2})} \right) \times \sum_{\beta \succeq \alpha} \mathcal{M}_{\alpha, \beta}^{-1} \frac{\Delta_\beta^{\mathbf{K}_S}(e_1, \dots, e_{2N})}{\mathbf{K}_S(e_{\text{in}}, e_{\text{out}})}.$$

By virtue of the robustness of the scaling limit results for random walks and discrete harmonic functions [YY11], some scaling limit results of the next section could be shown to be universal for suitable weighted random spanning trees.

3.7. Scaling limits. So far we have considered the discrete model of uniform spanning tree on a planar graph. We now turn to the question of scaling limits, where a fixed planar domain $\Lambda \subset \mathbb{C}$ is approximated by graphs with increasingly fine mesh and probabilities are renormalized by suitable power laws of the mesh size.

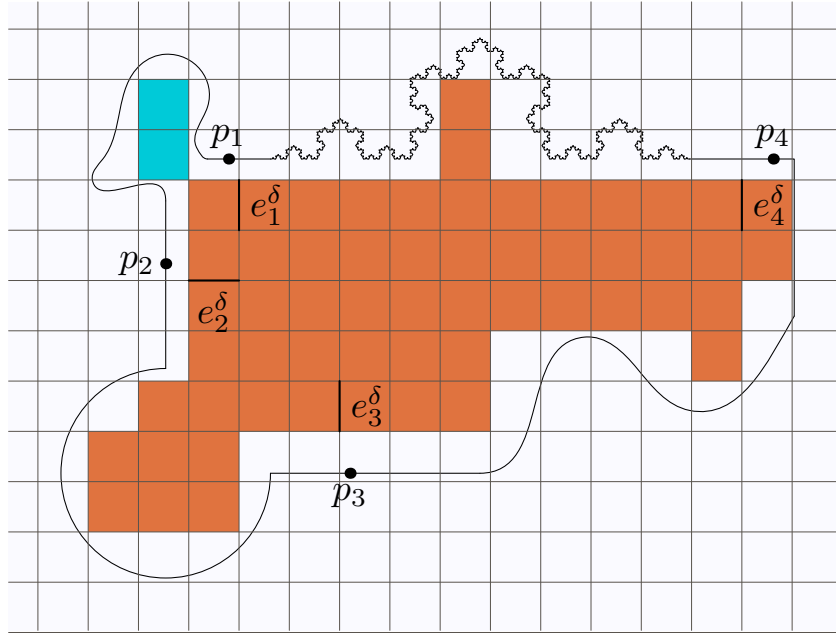


FIGURE 3.7. A Jordan domain with marked boundary points and its square grid approximation.

3.7.1. Finer mesh graphs. For concreteness, when discussing scaling limits, we always take graphs \mathcal{G}^δ which are subgraphs of the regular square lattice $\delta\mathbb{Z}^2$ with mesh size $\delta > 0$, and study the limit $\delta \rightarrow 0$. Our scaling limit results could be extended to more general setups, as long as the random walks on the graphs \mathcal{G}^δ tend to the Brownian motion on Λ and the boundary approximation near the marked points is regular enough so that also suitably renormalized random walk excursion kernels tend to the Brownian excursion kernel — see Lemma 3.15.

Fix the domain Λ , and $2N$ boundary points $p_1, \dots, p_{2N} \in \partial\Lambda$ appearing in counterclockwise order along the boundary $\partial\Lambda$. Assume throughout that locally near each p_j , the boundary is a straight horizontal or vertical line segment. This property is assumed in order to control the scaling limit behavior of the random walk excursion kernels from these marked boundary points.

For a given (small) mesh size $\delta > 0$, we define the *square grid approximation* of the domain Λ as the following graph $\mathcal{G}^\delta = (\mathcal{V}^\delta, \mathcal{E}^\delta)$, illustrated in Figure 3.7. Consider the closed squares $[n\delta, (n+1)\delta] \times [m\delta, (m+1)\delta]$ of the square lattice $\delta\mathbb{Z}^2$ that are contained in Λ . Take a connected component A of the interior of their union, with a maximal number of squares. The graph \mathcal{G}^δ is taken to have vertices $\mathcal{V}^\delta = \overline{A} \cap \delta\mathbb{Z}^2$. The boundary vertices are defined as $\partial\mathcal{V}^\delta = \partial A \cap \delta\mathbb{Z}^2$. The set \mathcal{E}^δ of edges consists of all pairs of vertices at distance δ from each other, such that at least one of the vertices is an interior vertex.

For all j , we denote by $e_j^\delta \in \partial\mathcal{E}^\delta$ a boundary edge nearest to the marked boundary point $p_j \in \partial\Lambda$, that is, an edge $e_j = \langle e_j^\partial, e_j^\circ \rangle$ that contains the boundary vertex e_j^∂ which is the nearest to p_j , and its neighbor e_j° at distance δ to the direction of the inwards normal to the boundary $\partial\Lambda$ (recall that the boundary is assumed locally horizontal or vertical near p_j). The choice of these boundary edges is also illustrated in Figure 3.7.

3.7.2. Scaling limits of excursion kernels. In the scaling limit $\delta \rightarrow 0$, the random walk excursion kernels K^δ on \mathcal{G}^δ can be approximated with the Brownian excursion kernel \mathcal{K}_Λ in the domain Λ , in the sense of Lemma 3.15 below.

We use the simple notation \mathcal{K} for

$$(3.11) \quad \mathcal{K}(x_1, x_2) = \frac{1}{(x_2 - x_1)^2} \quad \text{for } x_1, x_2 \in \mathbb{R}, x_1 \neq x_2,$$

which is a constant multiple of the Brownian excursion kernel in the upper half-plane \mathbb{H} . In any simply connected domain Λ , with two boundary points $p_1, p_2 \in \partial\Lambda$ on straight boundary segments, the Brownian excursion kernel \mathcal{K}_Λ is expressed in terms of \mathcal{K} by conformal covariance:

$$(3.12) \quad \mathcal{K}_\Lambda(p_1, p_2) = \frac{1}{\pi} |\phi'(p_1)| |\phi'(p_2)| \mathcal{K}(\phi(p_1), \phi(p_2)),$$

where $\phi: \Lambda \rightarrow \mathbb{H}$ is any conformal map from Λ to \mathbb{H} such that $\phi(p_1) \neq \infty$ and $\phi(p_2) \neq \infty$.

Let e_{1+}^δ be the boundary edge one lattice unit from e_1^δ to the counterclockwise direction, and define the discrete tangential derivative of the excursion kernel with respect to the first variable as

$$D_{\tau;1}^\delta \mathcal{K}^\delta := \frac{\mathcal{K}^\delta(e_{1+}^\delta, e_2^\delta) - \mathcal{K}^\delta(e_1^\delta, e_2^\delta)}{\delta}.$$

The discrete derivatives $D_{\tau;2}^\delta \mathcal{K}^\delta$ and $D_{\tau;1}^\delta D_{\tau;2}^\delta \mathcal{K}^\delta$ are defined similarly in terms of differences. We also denote by $\partial_{\tau;i}$ the usual counterclockwise tangential derivative with respect to the i :th argument.

Lemma 3.15. *As $\delta \rightarrow 0$, we have*

$$\mathcal{K}^\delta(e_1^\delta, e_2^\delta) = \delta^2 \mathcal{K}_\Lambda(p_1, p_2) + o(\delta^2),$$

and

$$\begin{aligned} D_{\tau;i}^\delta \mathcal{K}^\delta &= \delta^2 \partial_{\tau;i} \mathcal{K}_\Lambda(p_1, p_2) + o(\delta^2) & \text{for } i = 1, 2 \\ D_{\tau;1}^\delta D_{\tau;2}^\delta \mathcal{K}^\delta &= \delta^2 \partial_{\tau;1} \partial_{\tau;2} \mathcal{K}_\Lambda(p_1, p_2) + o(\delta^2). \end{aligned}$$

Proof. This follows from known convergence results of discrete harmonic functions. The renormalized harmonic measure $v \mapsto \frac{1}{\delta} H_v^\delta(e_2^\delta)$ is a discrete harmonic function on \mathcal{V}^δ . It is known to converge to the Poisson kernel when e_2^δ is on a straight boundary segment, see e.g. [CS11]. The convergence of the discrete harmonic function and all its discrete derivatives is uniform on compact subsets of the domain Λ [CFL28, CS11]. But, by Schwarz reflection, the convergence of the function and its discrete derivatives also holds when v is taken to some straight part of the boundary. It remains to note that $\mathcal{K}^\delta(e_1^\delta, e_2^\delta)$ is δ^2 times the discrete normal derivative of $v \mapsto \frac{1}{\delta} H_v^\delta(e_2^\delta)$ at e_1^δ . \square

3.7.3. Scaling limits of partition functions for connectivities. To prepare for the scaling limit statement, we first give two definitions for the continuum setup. For a link pattern α with the left-to-right orientation $((a_\ell, b_\ell))_{\ell=1}^N$, and for any $x_1 < x_2 < \dots < x_{2N}$, we set

$$(3.13) \quad \Delta_\alpha^\mathcal{K}(x_1, \dots, x_{2N}) := \det \left(\mathcal{K}(x_{a_k}, x_{b_\ell}) \right)_{k,\ell=1}^N = \det \left(\frac{1}{(x_{b_\ell} - x_{a_k})^2} \right)_{k,\ell=1}^N,$$

analogously to (3.7), with the kernel $\mathcal{K}(x_1, x_2) = (x_2 - x_1)^{-2}$ in the place of the random walk excursion kernel $\mathcal{K}(e_1, e_2)$. Analogously to (3.10), we also set

$$(3.14) \quad \mathcal{Z}_\alpha(x_1, \dots, x_{2N}) = \sum_{\beta \succeq \alpha} \mathcal{M}_{\alpha,\beta}^{-1} \Delta_\beta^\mathcal{K}(x_1, \dots, x_{2N}).$$

In the scaling limit setup of Section 3.7.1, we get the following limiting formula for the partition functions.

Theorem 3.16. *Let $\alpha \in \text{LP}_N$, and for all $\delta > 0$ denote by $Z_\alpha^{\mathcal{G}^\delta}(e_1^\delta, \dots, e_{2N}^\delta)$ the corresponding connectivity partition function for the UST on the square grid approximation \mathcal{G}^δ of the domain Λ . Then in the scaling limit $\delta \rightarrow 0$, we have*

$$\frac{1}{\delta^{2N}} Z_\alpha^{\mathcal{G}^\delta}(e_1^\delta, \dots, e_{2N}^\delta) \longrightarrow \frac{1}{\pi^N} \times \prod_{j=1}^{2N} |\phi'(p_j)| \times \mathcal{Z}_\alpha(\phi(p_1), \dots, \phi(p_{2N})),$$

where $\phi: \Lambda \rightarrow \mathbb{H}$ is any conformal map such that $\phi(p_1) < \dots < \phi(p_{2N})$.

Proof. This follows by combining Theorem 3.12 with the first statement of Lemma 3.15. \square

In Section 4, we will furthermore prove that the limit function \mathcal{Z}_α above is a positive solution to a system of second order partial differential equations of conformal field theory, see Theorem 4.1.

3.7.4. Scaling limits of boundary visit probabilities. The formulas of Corollary 3.13 for boundary visit probabilities are also amenable to a scaling limit analysis, although this case is considerably more involved than that of Section 3.7.3. The difficulties arise because among the arguments e_1, \dots, e_{2N} of the determinant expressions, N' pairs of edges $\hat{e}_{s;1}, \hat{e}_{s;2}$ are separated by just one lattice unit δ , and we are letting $\delta \rightarrow 0$. We state below the conclusion of the analysis, which will be done in Sections 5.1–5.3.

Theorem 3.17. *Fix a domain Λ and distinct boundary points $p_{\text{in}}, p_{\text{out}}, \hat{p}_1, \dots, \hat{p}_{N'}$ on horizontal or vertical boundary segments. Take a square grid approximation \mathcal{G}^δ of Λ , with $e_{\text{in}}^\delta, e_{\text{out}}^\delta \in \partial\mathcal{E}^\delta$ and $\hat{e}_1^\delta, \dots, \hat{e}_{N'}^\delta$ nearest to $p_{\text{in}}, p_{\text{out}}$ and $\hat{p}_1, \dots, \hat{p}_{N'}$, respectively. Let λ^δ be the loop-erasure $\lambda^\delta = \text{LE}(\eta^\delta)$ of a random walk η^δ on \mathcal{G}^δ from $(e_{\text{in}}^\delta)^\circ$, conditioned to reach the boundary $\partial\mathcal{V}^\delta$ via e_{out}^δ . Then, in the scaling limit as $\delta \rightarrow 0$, we have*

$$\begin{aligned} & \frac{1}{\delta^{3N'}} \mathbb{P}_{e_{\text{in}}^\delta, e_{\text{out}}^\delta} \left[\lambda^\delta \text{ uses } \hat{e}_1^\delta, \dots, \hat{e}_{N'}^\delta \text{ in this order} \right] \\ & \longrightarrow \frac{1}{\pi^{N'}} \times \prod_{s=1}^{N'} |\phi'(\hat{p}_s)|^3 \times \frac{\zeta_\omega(\phi(p_{\text{in}}); \phi(\hat{p}_1), \dots, \phi(\hat{p}_{N'}); \phi(p_{\text{out}}))}{(\phi(p_{\text{out}}) - \phi(p_{\text{in}}))^{-2}}, \end{aligned}$$

where $\phi: \Lambda \rightarrow \mathbb{H}$ is any conformal map such that $\phi(p_{\text{in}}) < \phi(p_{\text{out}})$ and $\phi(p_{\text{in}}) < \phi(\hat{p}_j)$ for all j , and ζ_ω is a function that satisfies two second order PDEs (5.15) and N' third order PDEs (5.16).

The proof is summarized in Section 5.3. It will also be shown (Proposition 5.7) that ζ_ω is positive unless the order of visits ω to the given edges at unit distance from the boundary is already impossible for curves on the planar graphs \mathcal{G}^δ .

3.8. Generalizations of the main results. We finish this section by mentioning further results for uniform spanning trees that generalize or are closely related to the above main results, and which can still be proved with the same techniques. Trusting that the reader can modify our arguments appropriately to cover these generalizations, we choose not to provide full details of their proofs.

3.8.1. Joint boundary visit and connectivity probabilities. Theorem 3.12 gives the connectivity probability of boundary branches in a wired UST, and Lemma 3.2 gives the boundary visit probabilities of one boundary branch. Theorems 3.16 and 3.17 give the scaling limits of these respective probabilities. It is straightforward to generalize Lemma 3.2 to obtain formulas for the probability that any given boundary points are connected by UST branches and that these branches visit any given edges at unit distance from the boundary. Furthermore, this probability can be properly renormalized to have a nontrivial scaling limit. More precisely, we have the following.

Theorem 3.18. *Fix a domain Λ and distinct boundary points $p_1, \dots, p_{2N}, \hat{p}_1^{(1)}, \dots, \hat{p}_{N'_1}^{(1)}, \dots, \hat{p}_1^{(N)}, \dots, \hat{p}_{N'_N}^{(N)}$ on horizontal or vertical boundary segments. Take a square grid approximation \mathcal{G}^δ of Λ , with boundary edges $e_1, \dots, e_{2N} \in \partial\mathcal{E}^\delta$ nearest to p_1, \dots, p_{2N} and, for $\ell = 1, \dots, N$, edges $\hat{e}_1^{(\ell)}, \dots, \hat{e}_{N'_\ell}^{(\ell)}$ at unit distance from the boundary nearest to $\hat{p}_1^{(\ell)}, \dots, \hat{p}_{N'_\ell}^{(\ell)}$, respectively. Let $\alpha \in \text{LP}_N$ be a link pattern with any orientation $(a_\ell, b_\ell)_{\ell=1}^N$ and denote by $\gamma^{(\ell)}$ the boundary branch from e_{a_ℓ} . Then, denoting $N' = \sum_{\ell=1}^N N'_\ell$, in the scaling limit as $\delta \rightarrow 0$, we have*

$$\frac{1}{\delta^{2N+3N'}} \mathbb{P} \left[e_{a_\ell} \rightsquigarrow e_{b_\ell} \text{ and } \gamma^{(\ell)} \text{ uses } \hat{e}_1^{(\ell)}, \dots, \hat{e}_{N'_\ell}^{(\ell)} \text{ in this order, for each } \ell = 1, \dots, N \right] \longrightarrow F^\Lambda(\mathbf{p}; \hat{\mathbf{p}}),$$

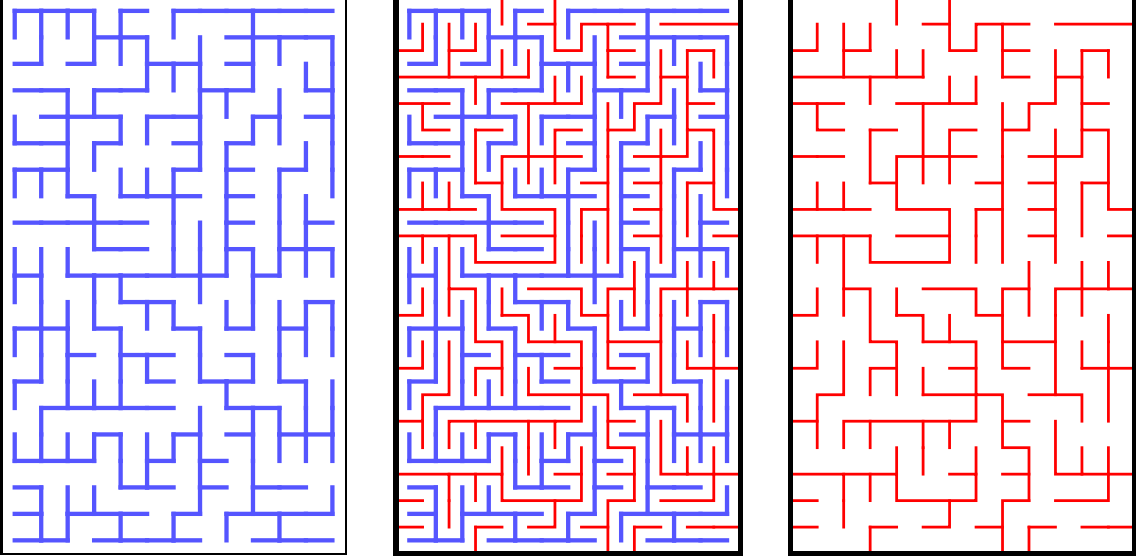


FIGURE 3.8. The uniform spanning tree with free boundary conditions (left figure) is dual to the uniform spanning tree with wired boundary conditions (right figure) as illustrated here (middle figure).

where F^Λ is a conformally covariant function of $2N + N'$ boundary points of Λ , which satisfies $2N$ second order and N' third order PDEs of conformal field theory, of the form given in Section 5.2.

3.8.2. Boundary touching subtrees in a free uniform spanning tree. So far we have discussed the uniform spanning tree only with wired boundary conditions (*wired UST*), meaning that we collapsed the boundary $\partial\mathcal{V} \subset \mathcal{V}$ into a single vertex. In contrast, the uniform spanning tree with free boundary conditions (*free UST*) is just the uniformly randomly chosen spanning tree of the given graph, without any collapsing of boundary. We now present some results for the free UST on square lattice graph approximations of a domain in the plane.

Let \mathcal{G} be a square grid approximation of a Jordan domain Λ as in Section 3.7.1, with mesh size $\delta > 0$ that we keep implicit in the notation below. In order to relate the results to earlier ones in a transparent manner, for the free UST the graph approximation of Λ is taken to be the dual graph $\mathcal{G}^* = (\mathcal{V}^*, \mathcal{E}^*)$ of \mathcal{G}/∂ : the vertices $v^* \in \mathcal{V}^*$ are the square faces of \mathcal{G} and the edges $e^* = \langle v_1^*, v_2^* \rangle \in \mathcal{E}^*$ join two square faces v_1^*, v_2^* that share one side with each other. There is a natural notion of boundary also in \mathcal{G}^* . A face $v^* \in \mathcal{V}^*$ is said to be a *boundary face* if at least one of the corners of the square face v^* is a boundary vertex of \mathcal{G} . A dual edge $e^* \in \mathcal{E}^*$ is said to be a *boundary dual edge* if the edge e which it crosses is a boundary edge, $e \in \partial\mathcal{E}$.

A well-known simple fact is that the free UST \mathcal{T}^* on \mathcal{G}^* can be obtained from the wired UST \mathcal{T} on \mathcal{G} by the duality (illustrated in Figure 3.8):

$$e \in \mathcal{T} \iff e^* \notin \mathcal{T}^* \text{ for the dual edge } e^* \text{ which crosses the edge } e.$$

In the free UST model, the most naive analogue of our earlier questions would be the boundary visits of a boundary-to-boundary branch, illustrated in Figure 3.9. Formally, given two boundary faces v_1^* and v_2^* , and a boundary dual edge e^* on the counterclockwise dual boundary segment $\partial\mathcal{E}_+^*$ from v_1^* to v_2^* : what is the probability that the unique branch of \mathcal{T}^* connecting v_1^* to v_2^* passes through e^* ? By duality, this occurs if and only if the boundary branch of e in \mathcal{T} connects to the primal boundary $\partial\mathcal{V}$ so that it

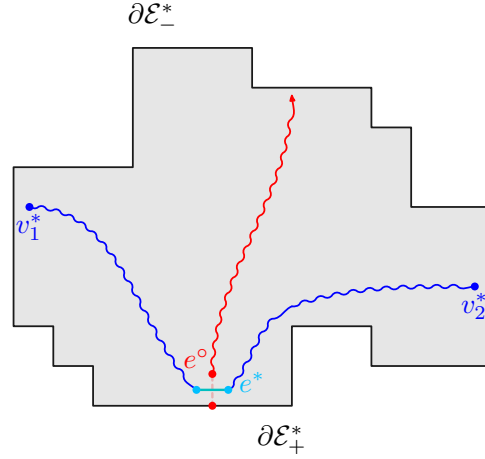


FIGURE 3.9. Schematic illustration of a boundary-to-boundary branch of the free UST \mathcal{T}^* using the boundary dual edge e^* (blue), and the boundary branch of the edge e in the wired UST \mathcal{T} on the primal graph (red).

crosses the clockwise dual boundary segment $\partial\mathcal{E}_-^*$ from v_1^* to v_2^* , as depicted in Figure 3.9. By Wilson's algorithm, the probability of this event is given by the harmonic measure in \mathcal{G} of the boundary edges crossing $\partial\mathcal{E}_-^*$ seen from e° . This gives the discrete boundary visit probability in the free UST.

The scaling limit behavior of the probability of such a boundary visit event is then an easy consequence of the convergence of discrete harmonic measures and their derivatives to the corresponding continuum objects (see, e.g., [CS11]). Assume that \mathcal{G} , v_1^* , v_2^* , and e^* are an approximation of the domain Λ with three boundary points p_1 , p_2 , and \hat{p} , and suppose that \hat{p} lies on a horizontal or vertical boundary segment. The free UST branch from v_1^* to v_2^* visits e^* with probability $\mathcal{O}(\delta)$, where δ is the mesh size of the graph approximation. Renormalized by δ^{-1} , this probability converges to the normal derivative at \hat{p} of the continuum harmonic measure of the clockwise arc from p_1 to p_2 . The limit function is known to be conformally covariant and to satisfy a second order PDE of conformal field theory. This is to be contrasted with the third order PDEs and probability $\mathcal{O}(\delta^3)$ of boundary visits in the wired UST. In summary, the boundary visit probability in the free UST model is considerably easier than in the wired UST, and essentially different in terms of its scaling exponent and PDEs.

The more interesting counterpart is the opposite question: what is the probability that two boundary faces are connected by a path not visiting the boundary in the free UST? More precisely, we consider the following problem of boundary touching subtrees in the free UST \mathcal{T}^* . The *interior forest* of \mathcal{T}^* is the subgraph obtained by removing all boundary dual edges from \mathcal{T}^* . The connected components $\tau_1^*, \dots, \tau_M^*$ of the interior forest are trees, and we ask whether there is a component which intersects the boundary exactly at some given faces $v_1^*, \dots, v_N^* \in \partial\mathcal{V}^*$.

Theorem 3.19. *Let $v_1^*, \dots, v_N^* \in \partial\mathcal{V}^*$ be non-neighboring distinct boundary faces in counterclockwise order along $\partial\mathcal{V}^*$, and let $e_1, \dots, e_{2N} \in \partial\mathcal{E}$ be the (unique) $2N$ boundary edges adjacent to these faces, enumerated counterclockwise starting from v_1^* . Then the probability that some component τ_m^* of the interior forest of \mathcal{T}^* intersects the boundary $\partial\mathcal{V}^*$ exactly at the faces v_1^*, \dots, v_N^* is given by*

$$\mathbb{P}\left[\exists m \text{ such that } \tau_m^* \cap \partial\mathcal{V}^* = \{v_1^*, \dots, v_N^*\}\right] = 2^N Z_{\square\square_N}(e_1, \dots, e_{2N}),$$

where $\square\square_N \in \text{LP}_N$ is the completely unnested link pattern.

The key to the proof is illustrated in Figure 3.10. By duality, the components of the interior forest are separated by boundary-to-boundary branches of the primal wired UST. The event that one component contains exactly the boundary faces v_1^*, \dots, v_N^* is a completely unnested connectivity event of

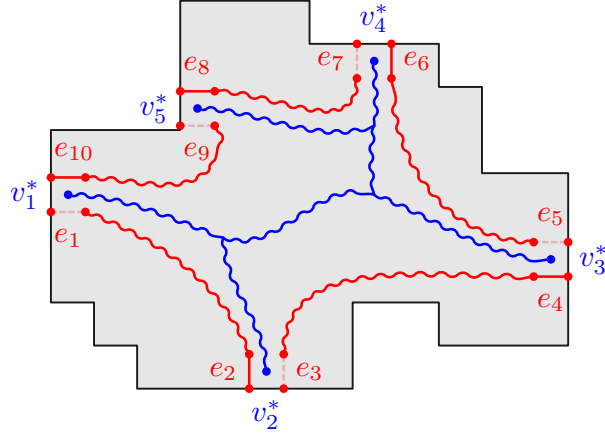


FIGURE 3.10. Schematic illustration of a boundary touching subtree in the interior forest of the free UST \mathcal{T}^* (blue), and the corresponding completely unnested connectivity in the wired UST \mathcal{T} on the primal graph (red).

the boundary edges $e_1, \dots, e_{2N} \in \partial\mathcal{E}$ chosen as in the statement of the theorem. There are 2^N possible orientations of the N branches, each contributing equally.

Among the boundary edges $e_1, \dots, e_{2N} \in \partial\mathcal{E}$ as above, there are N pairs separated by just one lattice unit, and none of these pairs is connected in the completely unnested pattern $\sqcap \sqcap_N$. The scaling limit of connectivity probabilities in such a setup is treated in Section 5. The following scaling limit result for boundary touching subtrees of the free UST can be straightforwardly inferred.

Theorem 3.20. *Fix a domain Λ , and let $\hat{p}_1, \dots, \hat{p}_N \in \partial\Lambda$ be distinct boundary points on horizontal or vertical boundary segments. Let $v_1^*, \dots, v_N^* \in \partial\mathcal{V}^*$ be boundary faces closest to $\hat{p}_1, \dots, \hat{p}_N$, respectively. Then in the scaling limit as $\delta \rightarrow 0$, the probability that some component τ_m^* of the interior forest of \mathcal{T}^* intersects the boundary $\partial\mathcal{V}^*$ exactly at the faces v_1^*, \dots, v_N^* is given by*

$$\frac{1}{\delta^{3N}} \mathbb{P} \left[\exists m \text{ such that } \tau_m^* \cap \partial\mathcal{V}^* = \{v_1^*, \dots, v_N^*\} \right] \longrightarrow F^\Lambda(\hat{\mathbf{p}}),$$

where F^Λ is a conformally covariant function of N boundary points of Λ , which satisfies N third order PDEs of conformal field theory, of the form given in Section 5.2.

4. RELATION TO MULTIPLE SLES

Schramm-Loewner Evolutions (SLE) are random curves in planar domains, whose laws in any two conformally equivalent domains are related to each other via a push-forward by a conformal map. SLE type random curves were originally introduced in [Sch00], motivated in particular by the scaling limits of loop-erased random walks and uniform spanning trees. A number of variants of SLEs exists, each relevant for a slightly different setup, but the most important characteristics of any SLE type curve is captured by one parameter, $\kappa > 0$. For instance, the scaling limits of LERWs and branches in the UST are SLEs with $\kappa = 2$, see [LSW04, Zha08, YY11]. The main new results in this section pertain to that particular value, $\kappa = 2$, and variants of SLEs known as multiple SLEs.

For the purposes of this section, we assume at least superficial familiarity with the most standard SLE variant, the chordal SLE_κ , which is a random curve in a simply connected domain $\Lambda \subset \mathbb{C}$ between two boundary points $p_{\text{in}}, p_{\text{out}} \in \partial\Lambda$. The reader can find the definition, basic properties, and applications of chordal SLE_κ in, e.g., [KN04, RS05, Law05]. We briefly describe the definition of multiple SLEs relying on the chordal SLE, but for the details we again refer to the literature [BBK05, Dub06a, Dub07, KP16].

The description of multiple SLEs is given in Section 4.1, with particular emphasis on their local definition using partition functions. The main result of this section, Theorem 4.1, states that the scaling limits of UST connectivity probabilities given in Theorem 3.16 are the so-called multiple SLE pure partition functions at $\kappa = 2$. As a consequence, we obtain in Theorem 4.2 the existence and extremality of the corresponding local multiple SLE processes at $\kappa = 2$, which for N curves are indexed by link patterns $\alpha \in \text{LP}_N$ of N links. The key ingredients are second order partial differential equations (PDE2), Möbius covariance (COV2), and boundary conditions (ASY2) for the functions \mathcal{Z}_α , whose derivations are given in Section 4.2. We remark that the second order PDEs will also be needed as an intermediate step in the derivation of the third order PDEs in Section 5.

For notational consistency, we introduce the following parameters depending on κ :

$$\begin{aligned} h_{1,2} &= h_{1,2}(\kappa) = \frac{6 - \kappa}{2\kappa} & \Delta &= \Delta(\kappa) = -2h_{1,2}(\kappa) = 1 - \frac{6}{\kappa} \\ h_{1,3} &= h_{1,3}(\kappa) = \frac{8 - \kappa}{\kappa} & \Delta' &= \Delta'(\kappa) = h_{1,3}(\kappa) - 2h_{1,2}(\kappa) = \frac{2}{\kappa}. \end{aligned}$$

For the case of our primary interest, $\kappa = 2$, these parameters are just the following constants:

$$h_{1,2} = 1, \quad h_{1,3} = 3, \quad \Delta = -2, \quad \Delta' = 1.$$

4.1. Multiple SLEs. Multiple SLEs are processes of several interacting random curves. A multiple SLE_κ in a simply connected planar domain consists of N random curves connecting $2N$ distinct points p_1, \dots, p_{2N} on the boundary pairwise without crossing. For example, the joint law of several boundary touching branches of the UST (with wired boundary conditions) should converge in the scaling limit to such a process with $\kappa = 2$, as stated in more detail below in Conjecture 4.3.

The success of the SLE theory relies largely on the growth process description of curves that employs the Loewner chain technique from complex analysis. The growth process description does not directly give a global definition of the curves, but provides a construction of their initial segments. For this reason, we will consider so-called local multiple SLEs in the sense of [BBK05, Dub06a, Dub07, KP16]. A local multiple SLE is constructed by a growth process encoded in a Loewner chain, and the construction relies on a partition function. The definition of local multiple SLEs is given in Section 4.1.2, after some relevant preliminaries about the partition functions in Section 4.1.1.

4.1.1. Partition functions of multiple SLEs. The construction of a local multiple SLE_κ describing N curves from $2N$ marked boundary points, employs a *multiple SLE partition function*

$$\mathcal{Z}: \mathfrak{X}_{2N} \rightarrow \mathbb{R}_{>0},$$

a positive function defined on the chamber

$$\mathfrak{X}_{2N} = \left\{ (x_1, \dots, x_{2N}) \mid x_1 < \dots < x_{2N} \right\},$$

satisfying the following $2N$ partial differential equations of second order:

$$\text{(PDE)} \quad \left[\frac{\kappa}{2} \frac{\partial^2}{\partial x_j^2} + \sum_{i \neq j} \left(\frac{2}{x_i - x_j} \frac{\partial}{\partial x_i} - \frac{2h_{1,2}}{(x_i - x_j)^2} \right) \right] \mathcal{Z}(x_1, \dots, x_{2N}) = 0 \quad \text{for all } j = 1, \dots, 2N,$$

and the covariance under Möbius transformations:

$$\begin{aligned} \text{(COV)} \quad \mathcal{Z}(x_1, \dots, x_{2N}) &= \prod_{j=1}^{2N} \mu'(x_j)^{h_{1,2}} \times \mathcal{Z}(\mu(x_1), \dots, \mu(x_{2N})) \\ \text{for all } \mu(z) &= \frac{az + b}{cz + d}, \quad \text{with } a, b, c, d \in \mathbb{R}, \quad ad - bc > 0, \quad \text{such that } \mu(x_1) < \dots < \mu(x_{2N}). \end{aligned}$$

The solution space of the system (PDE)–(COV) has dimension $C_N = \frac{1}{N+1} \binom{2N}{N}$ (when solutions with at most power-law growth are considered), by the work in [FK15a, FK15b, FK15c]. In [KP16], a set of C_N

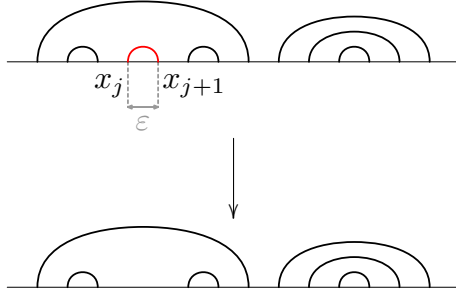


FIGURE 4.1. Schematic illustration of the link patterns in the cascade property (ASY), where the distance ε of the two boundary points x_j and x_{j+1} is taken to zero. The corresponding combinatorial operation is depicted in Figure 2.18.

distinguished linearly independent solutions, the pure partition functions $(\mathcal{Z}_\alpha^{(\kappa)})_{\alpha \in \text{LP}_N}$, were found for generic κ . These were argued to correspond to the extremal multiple SLE_κ probability measures that cannot be written as non-trivial convex combinations in the set of all multiple SLE_κ probability measures. Besides (PDE) and (COV), these distinguished functions satisfy the following specific asymptotics properties on the pairwise diagonals (the codimension one boundary of the chamber domain \mathfrak{X}_{2N}):

$$(ASY) \quad \lim_{x_j, x_{j+1} \rightarrow \xi} \frac{\mathcal{Z}_\alpha^{(\kappa)}(x_1, \dots, x_{2N})}{(x_{j+1} - x_j)^\Delta} = \begin{cases} \mathcal{Z}_{\alpha \setminus \wedge^j}^{(\kappa)}(x_1, \dots, x_{j-1}, x_{j+2}, \dots, x_{2N}) & \text{if } \wedge^j \in \alpha \\ 0 & \text{if } \wedge^j \notin \alpha \end{cases}$$

for all $j \in \{1, \dots, 2N-1\}$ and any $\xi \in (x_{j-1}, x_{j+2})$, where $\mathcal{Z}_\emptyset \equiv 1$ by convention, and the combinatorial notations are as defined in Section 2.4. This asymptotic boundary condition is illustrated in Figure 4.1.

In [KP16], the solutions $\mathcal{Z}_\alpha^{(\kappa)}$ were constructed for $\kappa \in (0, 8) \setminus \mathbb{Q}$. In the present article, we show that the scaling limits \mathcal{Z}_α of uniform spanning tree connectivity probabilities (3.1) satisfy the defining requirements (PDE), (COV) and (ASY) for pure partition functions $\mathcal{Z}_\alpha^{(\kappa)}$ at $\kappa = 2$. At $\kappa = 2$ we can also prove their positivity and conclude the existence of the corresponding local multiple SLE processes, whereas for generic κ , the positivity of the pure partition functions $\mathcal{Z}_\alpha^{(\kappa)}$ has remained conjectural³.

Theorem 4.1. *For any link pattern $\alpha \in \text{LP}_N$, the function $\mathcal{Z}_\alpha: \mathfrak{X}_{2N} \rightarrow \mathbb{R}$ given by (3.14),*

$$\mathcal{Z}_\alpha(x_1, \dots, x_{2N}) = \sum_{\beta \succeq \alpha} \mathcal{M}_{\alpha, \beta}^{-1} \Delta_\beta^K(x_1, \dots, x_{2N}),$$

satisfies (PDE), (COV) and (ASY) at $\kappa = 2$, i.e., we have

$$(PDE2) \quad \left[\frac{\partial^2}{\partial x_j^2} + \sum_{i \neq j} \left(\frac{2}{x_i - x_j} \frac{\partial}{\partial x_i} - \frac{2}{(x_i - x_j)^2} \right) \right] \mathcal{Z}_\alpha(x_1, \dots, x_{2N}) = 0 \quad \text{for all } j = 1, \dots, 2N$$

$$(COV2) \quad \mathcal{Z}_\alpha(x_1, \dots, x_{2N}) = \prod_{j=1}^{2N} \mu'(x_j) \times \mathcal{Z}_\alpha(\mu(x_1), \dots, \mu(x_{2N}))$$

$$\text{for all } \mu(z) = \frac{az + b}{cz + d}, \text{ with } a, b, c, d \in \mathbb{R}, ad - bc > 0, \text{ such that } \mu(x_1) < \dots < \mu(x_{2N})$$

$$(ASY2) \quad \lim_{x_j, x_{j+1} \rightarrow \xi} \frac{\mathcal{Z}_\alpha(x_1, \dots, x_{2N})}{(x_{j+1} - x_j)^{-2}} = \begin{cases} \mathcal{Z}_{\alpha \setminus \wedge^j}(x_1, \dots, x_{j-1}, x_{j+2}, \dots, x_{2N}) & \text{if } \wedge^j \in \alpha \\ 0 & \text{if } \wedge^j \notin \alpha \end{cases}$$

$$\text{for all } j \in \{1, \dots, 2N-1\} \text{ and any } \xi \in (x_{j-1}, x_{j+2}).$$

³The recent works [PW19, Wu18] show the positivity for $\kappa \leq 6$.

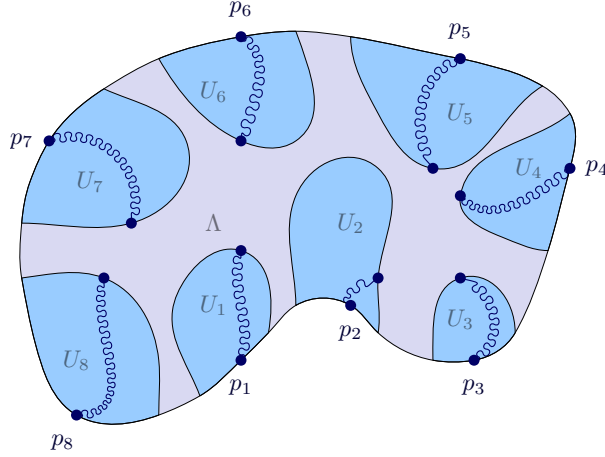


FIGURE 4.2. Schematic illustration of a local multiple SLE.

Moreover, the collection $(\mathcal{Z}_\alpha)_{\alpha \in \text{LP}_N}$ of functions is linearly independent, and each function \mathcal{Z}_α is positive: we have $\mathcal{Z}_\alpha(x_1, \dots, x_{2N}) > 0$ for all $(x_1, \dots, x_{2N}) \in \mathfrak{X}_{2N}$.

The proof of this theorem will be given in Section 4.2.

We remark that in [Dub06a], Dubédat also stated without explicit proof that the determinants Δ_β^κ satisfy the partial differential equations (PDE2), and suggested the problem of finding the appropriate linear combination of the determinants which satisfies the specific boundary conditions (ASY2). Theorem 4.1 above settles this problem.

4.1.2. Local multiple SLEs. In general, for $\kappa > 0$, a local multiple SLE_κ is defined in [KP16, Appendix A] by requiring conformal invariance, a domain Markov property, and absolute continuity of initial segments with respect to the chordal SLE_κ . By [Dub07] and [KP16, Theorem A.4], such local N - SLE_κ processes are classified by multiple SLE partition functions $\mathcal{Z}: \mathfrak{X}_{2N} \rightarrow \mathbb{R}_{>0}$ (modulo multiplicative constant), that is, positive solutions to (PDE)–(COV). For concreteness, we therefore describe below only the local multiple SLE_κ associated with a given partition function \mathcal{Z} .

A local N - SLE_κ associates a probability measure on initial segments of $2N$ random curves to any domain and localization data of the following kind. The domain and localization data consists of a simply connected domain (where the curves live) with $2N$ marked boundary points (the starting points of the curves), and disjoint localization neighborhoods of the marked points (where the initial segments of the curves lie) — see Figure 4.2 for an illustration. More precisely, for any $\kappa > 0$, the local N - SLE_κ is a collection of probability measures indexed by the domain Λ , marked points $p_1, \dots, p_{2N} \in \partial\Lambda$, and their closed localization neighborhoods $U_1, \dots, U_{2N} \subset \bar{\Lambda}$, such that $p_j \in U_j$ for all j , the complements $\Lambda \setminus U_j$ are simply connected, and $U_j \cap U_k = \emptyset$ for $j \neq k$. The probability measures are supported on the set of $2N$ -tuples $(\gamma^{(1)}, \dots, \gamma^{(2N)})$ of oriented non-self-crossing unparametrized curves $\gamma^{(j)}$, traversing from the marked points p_j to the boundary of their localization neighborhoods U_j .

For each $j = 1, \dots, 2N$, the partition function \mathcal{Z} determines the marginal law $\mathbf{P}_{\gamma^{(j)}}$ of the j :th curve $\gamma^{(j)}$ started from p_j , traversing the localization neighborhood U_j , as follows. The curve $\gamma^{(j)}$ is absolutely continuous with respect to the law $\mathbf{P}^{(\Lambda; p_j, p)}$ of an initial segment of the single chordal SLE_κ curve in Λ from p_j to any target point $p \in \partial\Lambda$ outside U_j . The Radon-Nikodym derivative is

$$\frac{d\mathbf{P}_{\gamma^{(j)}}}{d\mathbf{P}^{(\Lambda; p_j, p)}} = \prod_{i \neq j} g'(x_i)^{h_{1,2}} \times \frac{\mathcal{Z}(g(x_1), \dots, g(x_{j-1}), g(\gamma^{(j)}(\tau)), g(x_{j+1}), \dots, g(x_{2N}))}{\mathcal{Z}(x_1, \dots, x_{2N})},$$

where

- $x_j = \phi(p_j)$ for all j , where $\phi: \Lambda \rightarrow \mathbb{H}$ is a conformal map such that $\phi(p) = \infty$,
- $g: H_\tau^{(j)} \rightarrow \mathbb{H}$ is the unique conformal isomorphism from the unbounded component $H_\tau^{(j)}$ of the complement $\mathbb{H} \setminus \phi(\gamma^{(j)}[0, \tau])$ of the conformal image of the curve $\gamma^{(j)}$ to the upper-half plane \mathbb{H} , normalized so that $g(z) = z + o(1)$ as $z \rightarrow \infty$,
- τ is the hitting time of the curve $\gamma^{(j)}$ to the boundary of its localization neighborhood U_j .

Together with the domain Markov property, these marginals on the individual curve segments $\gamma^{(j)}$ in fact determine the joint probability measure of all $2N$ curve segments, see [KP16, Appendix A].

It is also very natural to form convex combinations of probability measures, such as the localizations of a local multiple SLE. Appropriately accounting for conformal transformation properties, one gets a convex structure on the space of local multiple SLEs, see [KP16, Theorem A.4(c)] for details.

In the case $\kappa = 2$, our partition functions \mathcal{Z}_α can be used to construct local multiple SLE₂ processes:

Theorem 4.2. *For each link pattern $\alpha \in \text{LP}_N$, there exists a local N -SLE $_\kappa$ with $\kappa = 2$, associated with the partition function \mathcal{Z}_α as in Theorem 4.1 and Equation (3.14). Moreover, the convex hull of the local N -SLEs corresponding to \mathcal{Z}_α for $\alpha \in \text{LP}_N$ is of dimension $C_N - 1$ and the C_N local N -SLEs corresponding to \mathcal{Z}_α are the extremal points of this convex set.*

Proof. The first assertion follows from the properties of the functions \mathcal{Z}_α established in Theorem 4.1, combined with the classification of local multiple SLEs [KP16, Theorem A.4(a)] at $\kappa = 2$. By [KP16, Theorem A.4(c)], convex combinations of local N -SLEs correspond to positive linear combinations of their partition functions modulo multiplicative constants. The second assertion then follows from the linear independence of $(\mathcal{Z}_\alpha)_{\alpha \in \text{LP}_N}$ and the fact that a linear combination $\mathcal{Z} = \sum_\alpha c_\alpha \mathcal{Z}_\alpha$ is non-negative only if $c_\alpha \geq 0$ for all α , as can be shown by expressing each c_α as a suitable limit of the partition function \mathcal{Z} as in [KP16, Proposition 4.2]. \square

The partition functions \mathcal{Z}_α are the scaling limits of connectivity probabilities of branches in the uniform spanning tree, by Theorem 3.16. The local multiple SLE curves determined by them should of course be closely related to the branches of the UST. Let \mathcal{G}^δ be the square grid approximation of the simply connected domain $\Lambda \subset \mathbb{C}$ with mesh size $\delta > 0$, as in Section 3.7.1. For $2N$ boundary points $p_1, \dots, p_{2N} \in \partial\Lambda$, let $e_1^\delta, \dots, e_{2N}^\delta \in \partial\mathcal{E}$ be boundary edges of the square grid graph \mathcal{G}^δ nearest to them. Assume that the points appear in counterclockwise order along the boundary.

Conjecture 4.3. *Let $\alpha \in \text{LP}_N$ be a link pattern with any orientation $((a_\ell, b_\ell))_{\ell=1}^N$. In the uniform spanning tree on \mathcal{G}^δ with wired boundary conditions, conditioned on the connectivity event $\bigcap_{\ell=1}^N \{e_{a_\ell}^\delta \rightsquigarrow e_{b_\ell}^\delta\}$, the law of the N boundary branches $(\gamma_{e_{a_1}^\delta}^\delta, \dots, \gamma_{e_{a_N}^\delta}^\delta)$ converges in the scaling limit as $\delta \rightarrow 0$ to a process of N curves, whose localization in any non-overlapping closed neighborhoods (U_1, \dots, U_{2N}) of the points (p_1, \dots, p_{2N}) is the local N -SLE₂ determined by the partition function \mathcal{Z}_α .*

Update. In light of some recent developments, several approaches to establish this conjecture are possible. For the tightness of the boundary branches, see [Kar19]. For the identification, using the convergence of a single UST branch to chordal SLE₂ [Zha08] and recent classification results of global multiple SLEs [MS16, BPW18], the scaling limit of multiple UST branches can be identified as a global multiple SLE, whose localizations are local multiple SLEs [PW19]. Alternatively, requiring some more investigation of the discrete model but only basic SLE theory, one can use the results of the present article to generalize the observable approach used in the single UST branch convergence proofs [LSW04, Zha08]; see [Kar19].

4.2. Proof of Theorem 4.1. We prove the asserted properties of the functions \mathcal{Z}_α separately, and conclude the proof of Theorem 4.1 in Section 4.2.4. The Möbius covariance (COV2) and the partial differential equations (PDE2) are linear conditions, so it suffices to establish them for the determinant functions Δ_α^K appearing in the formula (3.14) which defines the functions \mathcal{Z}_α . The proof of property (ASY2) concerning the asymptotics of the functions requires in addition specific combinatorial tools from Section 2.6.

4.2.1. **Möbius covariance.** We first check the Möbius covariance property (COV2) for the determinants Δ_α^κ given by Equation (3.13).

Lemma 4.4. *Let $\mu(z) = \frac{az+b}{cz+d}$ be as in (COV2). Then, for any $(x_1, \dots, x_{2N}) \in \mathfrak{X}_{2N}$, we have*

$$\Delta_\alpha^\kappa(x_1, \dots, x_{2N}) = \prod_{j=1}^{2N} \mu'(x_j) \times \Delta_\alpha^\kappa(\mu(x_1), \dots, \mu(x_{2N})).$$

Proof. It is straightforward to check that $\frac{\mu(z)-\mu(w)}{z-w} = \sqrt{\mu'(z)}\sqrt{\mu'(w)}$ for any $z, w \in \mathbb{C}$, see e.g. [KP16, Lemma 4.7]. This identity can be used in the matrix elements of the determinant function Δ_α^κ ,

$$\frac{1}{(x_{a_k} - x_{b_\ell})^2} = \frac{\mu'(x_{a_k})\mu'(x_{b_\ell})}{(\mu(x_{a_k}) - \mu(x_{b_\ell}))^2}.$$

The asserted covariance property follows by multilinearity of the determinant. \square

4.2.2. **Partial differential equations.** We next check the partial differential equations (PDE2) for the determinants Δ_α^κ .

Lemma 4.5. *The function $\Delta_\alpha^\kappa(x_1, \dots, x_{2N})$ satisfies the partial differential equations (PDE2).*

Proof. The proof is a direct computation. To simplify notation, we denote $x_{a_k} = A_k$ and $x_{b_\ell} = B_\ell$, and write

$$(4.1) \quad \Delta_\alpha^\kappa(x_1, \dots, x_{2N}) = \det \left(\frac{1}{(A_k - B_\ell)^2} \right)_{k, \ell=1}^N = \sum_{\sigma \in \mathfrak{S}_N} \text{sgn}(\sigma) \prod_{m=1}^N \frac{1}{(A_m - B_{\sigma(m)})^2}.$$

It suffices to consider the partial differential equation in (PDE2) with $j = 1$. We write the differential operator as

$$(4.2) \quad \begin{aligned} \mathcal{D}_1 &= \frac{\partial^2}{\partial x_1^2} + \sum_{i \neq 1} \left(\frac{2}{x_i - x_1} \frac{\partial}{\partial x_i} - \frac{2}{(x_i - x_1)^2} \right) \\ &= \frac{\partial^2}{\partial A_1^2} + \frac{2}{B_{\sigma(1)} - A_1} \frac{\partial}{\partial B_{\sigma(1)}} - \frac{2}{(B_{\sigma(1)} - A_1)^2} \\ &\quad + \sum_{k=2}^N \left(\frac{2}{A_k - A_1} \frac{\partial}{\partial A_k} - \frac{2}{(A_k - A_1)^2} + \frac{2}{B_{\sigma(k)} - A_1} \frac{\partial}{\partial B_{\sigma(k)}} - \frac{2}{(B_{\sigma(k)} - A_1)^2} \right) \end{aligned}$$

where we re-arranged the terms containing the variable $B_\ell = x_{b_\ell}$ by a permutation $\sigma \in \mathfrak{S}_N$.

By linearity, let us first study the action of the partial differential operator (4.2) on one term in the determinant (4.1). Straightforward differentiation yields

$$\begin{aligned} &\mathcal{D}_1 \left(\prod_{m=1}^N \frac{1}{(A_m - B_{\sigma(m)})^2} \right) \\ &= \left(\prod_{m=1}^N \frac{1}{(A_m - B_{\sigma(m)})^2} \right) \left[\frac{6}{(A_1 - B_{\sigma(1)})^2} - \frac{4}{(A_1 - B_{\sigma(1)})^2} - \frac{2}{(A_1 - B_{\sigma(1)})^2} \right. \\ &\quad \left. + \sum_{k=2}^N \left(\frac{-4}{(A_k - A_1)(A_k - B_{\sigma(k)})} - \frac{2}{(A_k - A_1)^2} + \frac{4}{(B_{\sigma(k)} - A_1)(A_k - B_{\sigma(k)})} - \frac{2}{(B_{\sigma(k)} - A_1)^2} \right) \right]. \end{aligned}$$

Using the identities

$$\frac{-4}{(A_k - A_1)(A_k - B_{\sigma(k)})} + \frac{4}{(B_{\sigma(k)} - A_1)(A_k - B_{\sigma(k)})} = \frac{4}{(A_k - A_1)(B_{\sigma(k)} - A_1)}$$

and

$$-2 \left(\frac{1}{(B_{\sigma(k)} - A_1)} - \frac{1}{(A_k - A_1)} \right)^2 = -\frac{2(B_{\sigma(k)} - A_k)^2}{(A_k - A_1)^2(B_{\sigma(k)} - A_1)^2},$$

we simplify

$$\mathcal{D}_1 \left(\prod_{m=1}^N \frac{1}{(A_m - B_{\sigma(m)})^2} \right) = -2 \sum_{k=2}^N \frac{1}{(A_k - A_1)^2} \left(\prod_{m \neq k} \frac{1}{(A_m - B_{\sigma(m)})^2} \right) \frac{1}{(B_{\sigma(k)} - A_1)^2}.$$

By linearity, \mathcal{D}_1 now acts on the determinant (4.1) by

$$\begin{aligned} \mathcal{D}_1 \Delta_\alpha^\mathcal{K}(x_1, \dots, x_{2N}) &= \sum_{\sigma \in \mathfrak{S}_N} \text{sgn}(\sigma) \times \mathcal{D}_1 \left(\prod_{m=1}^N \frac{1}{(A_m - B_{\sigma(m)})^2} \right) \\ &= -2 \sum_{k=2}^N \frac{1}{(A_k - A_1)^2} \left[\sum_{\sigma \in \mathfrak{S}_N} \text{sgn}(\sigma) \left(\prod_{m \neq k} \frac{1}{(A_m - B_{\sigma(m)})^2} \right) \frac{1}{(B_{\sigma(k)} - A_1)^2} \right]. \end{aligned}$$

Now, the sum in the square brackets is the determinant of the matrix

$$\left(\frac{1}{(\tilde{A}_m - B_n)^2} \right)_{m,n=1}^N,$$

where $\tilde{A}_m = A_m$ if $m \neq k$ and $\tilde{A}_k = A_1$. The first and k :th rows of this matrix are hence identical, so the determinant is zero, and we obtain the desired property $\mathcal{D}_1 \Delta_\alpha^\mathcal{K}(x_1, \dots, x_{2N}) = 0$. \square

4.2.3. Asymptotics. To obtain the asymptotics of the partition functions \mathcal{Z}_α , we rely on results from Section 2.6. The asymptotics of the partition functions can be derived by considering the asymptotics of the determinants $\Delta_\alpha^\mathcal{K}$, which are somewhat simpler. Moreover, the asymptotics of $\Delta_\alpha^\mathcal{K}$ are closely analogous to the defining properties of the conformal block functions in CFT, see [KKP19].

Proposition 4.6. *For all $j = 1, \dots, 2N - 1$, the determinant function $\Delta_\alpha^\mathcal{K}: \mathfrak{X}_{2N} \rightarrow \mathbb{R}$ satisfies*

$$(\Delta\text{-ASY}) \quad (x_{j+1} - x_j)^2 \Delta_\alpha^\mathcal{K}(x_1, \dots, x_{2N}) \longrightarrow \begin{cases} 0 & \text{if } \times_j \in \alpha \\ \Delta_{\alpha \setminus \wedge^j}^\mathcal{K}(x_1, \dots, x_{j-1}, x_{j+2}, \dots, x_{2N}) & \text{if } \wedge^j \in \alpha \\ -\Delta_{\alpha \setminus \vee^j}^\mathcal{K}(x_1, \dots, x_{j-1}, x_{j+2}, \dots, x_{2N}) & \text{if } \vee^j \in \alpha, \end{cases}$$

as $x_j, x_{j+1} \rightarrow \xi$, for any $\xi \in (x_{j-1}, x_{j+2})$, where $\Delta_\emptyset^\mathcal{K} \equiv 1$ by convention, and the combinatorial notations are as defined in Section 2.4.

Proof. Notice that $\Delta_\alpha^\mathcal{K}$ is an example of a link pattern determinant $\Delta_\alpha^\mathfrak{K}$ studied in Section 2.6, with the kernel $\mathfrak{K}(i, j) = \mathcal{K}(x_i, x_j) = (x_i - x_j)^{-2}$. In the limit $x_j, x_{j+1} \rightarrow \xi$, all kernel entries except $\mathfrak{K}(j, j+1)$ remain bounded, so the renormalized limit $(\Delta\text{-ASY})$ picks the coefficient $[\Delta_\alpha^\mathfrak{K}]_{j,j+1}$ of $\mathfrak{K}(j, j+1)$ in the determinant $\Delta_\alpha^\mathfrak{K}$. This coefficient is given in Lemma 2.20. The asserted limits follow. \square

Proposition 4.7. *The function $\mathcal{Z}_\alpha: \mathfrak{X}_{2N} \rightarrow \mathbb{R}$ defined in (3.14) satisfies the asymptotics (ASY2).*

Proof. The partition function \mathcal{Z}_α is an inverse Fomin type sum $\mathfrak{Z}_\alpha^\mathfrak{K}$ studied in Section 2.6, with the kernel $\mathfrak{K}(i, j) = \mathcal{K}(x_i, x_j) = (x_i - x_j)^{-2}$. The renormalized limit in (ASY2) picks the coefficient $[\mathfrak{Z}_\alpha^\mathfrak{K}]_{j,j+1}$ of $\mathfrak{K}(j, j+1)$ in $\mathfrak{Z}_\alpha^\mathfrak{K}$. This coefficient is given in Proposition 2.18(c) and Proposition 2.21. \square

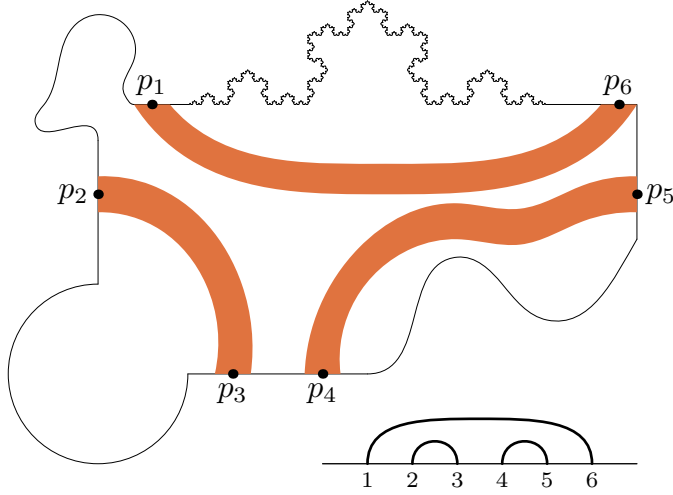


FIGURE 4.3. Illustration of the choice of non-overlapping subdomains $\Lambda_\ell \subset \Lambda$ in the proof of positivity of \mathcal{Z}_α .

4.2.4. Finishing the proof of Theorem 4.1. We now collect the results of Sections 4.2.1–4.2.3 to prove Theorem 4.1. By Lemma 4.4 and linearity, it follows that \mathcal{Z}_α satisfies the Möbius covariance condition (COV2). Similarly, by Lemma 4.5 and linearity, it follows that \mathcal{Z}_α satisfies the partial differential equations (PDE2). Proposition 4.7 contains the asserted asymptotics (ASY2). Linear independence of the collection $(\mathcal{Z}_\alpha)_{\alpha \in \text{LP}_N}$ can be deduced from the asymptotics by arguments presented, e.g., in [KP16, Proposition 4.2] or [FK15c]. It remains only to verify the positivity of the functions \mathcal{Z}_α .

By Theorem 3.16, $\mathcal{Z}_\alpha(x_1, \dots, x_{2N})$ equals a positive constant times the limit of the non-negative quantities $\delta^{-2N} Z_\alpha^{\mathcal{G}^\delta}(e_1^\delta, \dots, e_{2N}^\delta)$ as $\delta \rightarrow 0$, and as such, $\mathcal{Z}_\alpha(x_1, \dots, x_{2N}) \geq 0$. There are many ways to promote the non-negativity to positivity. One, purely analytical option, is to use the ellipticity of the PDEs and a maximum principle. A probabilistic option that uses results from Section 3 is the following: we can argue that for fixed $x_1 < \dots < x_{2N}$ the quantities $\delta^{-2N} Z_\alpha^{\mathcal{G}^\delta}(e_1^\delta, \dots, e_{2N}^\delta)$ are uniformly lower bounded in δ , which implies positivity: $\mathcal{Z}_\alpha(x_1, \dots, x_{2N}) > 0$. The uniform lower bound only essentially relies on the observation that for one UST branch (i.e., a LERW), δ^{-2} times the probability to connect two given boundary points in a given domain tends to a positive limit as $\delta \rightarrow 0$, see Equation (3.3) and Lemma 3.15. Now fix a domain Λ , marked points p_1, \dots, p_{2N} , and a connectivity $\alpha = \{\{a_1, b_1\}, \dots, \{a_N, b_N\}\} \in \text{LP}_N$. Then, for $\ell = 1, \dots, N$, choose non-overlapping subdomains $\Lambda_\ell \subset \Lambda$ such that Λ_ℓ contains neighborhoods of the boundary points p_{a_ℓ} and p_{b_ℓ} — such subdomains, illustrated in Figure 4.3, exist since the connectivity α is planar. Construct the UST branches from $e_{a_\ell}^\delta$ by Wilson’s algorithm as LERWs. A lower bound for the probability of $\bigcap_{\ell=1}^N \{e_{a_\ell}^\delta \rightsquigarrow e_{b_\ell}^\delta\}$ is the product over ℓ of the LERW connectivity probabilities in the subdomains Λ_ℓ from $e_{a_\ell}^\delta$ to $e_{b_\ell}^\delta$. These, in turn, when divided by δ^2 each, are lower bounded by positive quantities, since they have positive limits as $\delta \rightarrow 0$. This proves positivity: $\mathcal{Z}_\alpha(x_1, \dots, x_{2N}) > 0$. \square

5. BOUNDARY VISIT PROBABILITIES AND THIRD ORDER PDES

This section addresses the convergence in the scaling limit of the loop-erased random walk boundary visit probabilities, as well as the partial differential equations and boundary conditions satisfied by the limit functions. The main purpose is thus to finish the proof of Theorem 3.17 about the boundary visit probabilities.

As in Section 3.2.2, let $\omega \in \{+, -\}^{N'}$ be a specification of an order of boundary visits for a chordal curve and let $\alpha(\omega)$ be the link pattern obtained by opening up the curve at each boundary visit, as illustrated in Figure 3.4. Recall from Corollary 3.13 that the boundary visit probability of a LERW in the order ω can be expressed in terms of a connectivity probability $Z_{\alpha(\omega)}$ for multiple branches of the UST. In this section, we study the scaling limit $\delta \rightarrow 0$ of this probability. Note that the proof of our previous scaling limit result, Theorem 3.16 for the connectivity probabilities $Z_{\alpha}^{\mathcal{G}^{\delta}}(e_1^{\delta}, \dots, e_{2N}^{\delta})$, does not directly apply to the case of the boundary visit probability, since now some pairs of consecutive boundary edges $e_j^{\delta}, e_{j+1}^{\delta}$ tend to the same point in the scaling limit. Therefore, significantly more care is needed to establish Theorem 3.17.

We begin in Section 5.1 with a refined treatment of the connectivity probabilities $Z_{\alpha}^{\mathcal{G}^{\delta}}(e_1^{\delta}, \dots, e_{2N}^{\delta})$ in the scaling limit, applicable also when some boundary edges $e_j^{\delta}, e_{j+1}^{\delta}$ are at one lattice unit away from each other. The combinatorial techniques of Section 2.6 are used to derive Theorems 5.1 and 5.2, which show that the renormalized discrete boundary visit probability has scaling limit ζ_{ω} , which can moreover be expressed as a limit of the continuum partition function $Z_{\alpha(\omega)}$.

Section 5.2 takes care of the remaining claim in Theorem 3.17: the second and third order partial differential equations for ζ_{ω} , predicted by conformal field theory. Once we have been able to exchange the order of the scaling limit with another limit by Theorem 5.2, these PDEs can be proved by a fusion argument parallel to one in [Dub15b], see Lemma 5.6.

The proof of Theorem 3.17 is then summarized in Section 5.3.

Finally, Section 5.4 is a supplement to the content of Theorem 3.17: in Propositions 5.8 and 5.9 we establish the predicted asymptotic behaviors for the scaling limit functions, which together with the system of PDEs has been conjectured to uniquely determine them [JJK16].

5.1. Scaling limit of boundary visit probabilities. Throughout this section, we adopt the following assumptions and notation. A link pattern $\alpha \in \text{LP}_N$ is fixed, and among $2N$ counterclockwise ordered boundary edges $e_1^{\delta}, \dots, e_{2N}^{\delta}$, some consecutive pairs are one lattice unit apart. Let $N' \leq N$ denote the number of such pairs, and for $1 \leq s \leq N'$, denote the indices of the pairs by $j_s, j_s + 1$. The link pattern α must not have any links formed by these pairs, i.e., $\wedge^{j_s} \notin \alpha$. As in Section 3.2.2, in this setup there is then an edge \hat{e}_s^{δ} at unit distance from the boundary which joins the interior vertices of the two boundary edges $e_{j_s}^{\delta}$ and $e_{j_s+1}^{\delta}$, see Figure 3.3 (the two boundary edges $e_{j_s}^{\delta}, e_{j_s+1}^{\delta}$ are then the edges $\hat{e}_{s;1}^{\delta}, \hat{e}_{s;2}^{\delta}$ in the figure).

The graphs \mathcal{G}^{δ} form a square grid approximation of a domain Λ , and the boundary $\partial\Lambda$ is locally a vertical or horizontal line near the points

$$p_j = \lim_{\delta \rightarrow 0} e_j^{\delta} \quad \text{and} \quad \hat{p}_s = \lim_{\delta \rightarrow 0} \hat{e}_s^{\delta} = \lim_{\delta \rightarrow 0} e_{j_s}^{\delta} = \lim_{\delta \rightarrow 0} e_{j_s+1}^{\delta}.$$

The limit points p_j , for $j \notin \{j_1, j_1 + 1, \dots, j_{N'}, j_{N'} + 1\}$, and \hat{p}_s , for $s \in \{1, 2, \dots, N'\}$, are assumed to be distinct. In the reference domain \mathbb{H} , we denote the boundary points by $x_1 < x_2 < \dots < x_{2N}$, as in Section 3.7.3.

Theorem 5.1. *Let $\alpha \in \text{LP}_N$ and let $((j_s, j_s + 1))_{s=1}^{N'}$ be a collection of N' disjoint pairs such that $\wedge^{j_s} \notin \alpha$ holds for all s . Let Z_{α} be the function defined in Equation (3.14). Then, the iterated limit*

$$(5.1) \quad \lim_{x_{j_1}, x_{j_1+1} \rightarrow \hat{x}_1} \frac{1}{x_{j_1+1} - x_{j_1}} \cdots \lim_{x_{j_{N'}}, x_{j_{N'}+1} \rightarrow \hat{x}_{N'}} \frac{1}{x_{j_{N'}+1} - x_{j_{N'}}} Z_{\alpha}(x_1, \dots, x_{2N})$$

exists, is finite, explicitly given by the replacing algorithm 5.3 below, and independent of the order of the limits.

In particular, in the case where $\alpha = \alpha(\omega)$ for some boundary visit order ω , this limit function is denoted by $\zeta_{\omega}(x_{\text{in}}; \hat{x}_1, \dots, \hat{x}_{N'}; x_{\text{out}})$, where $x_{\text{in}} = x_i$ and $x_{\text{out}} = x_j$ for the only indices i, j not in the pairs $(j_s, j_s + 1)$ — see Equation (5.6) and Figure 5.1. In Proposition 5.7, the function ζ_{ω} will be shown to

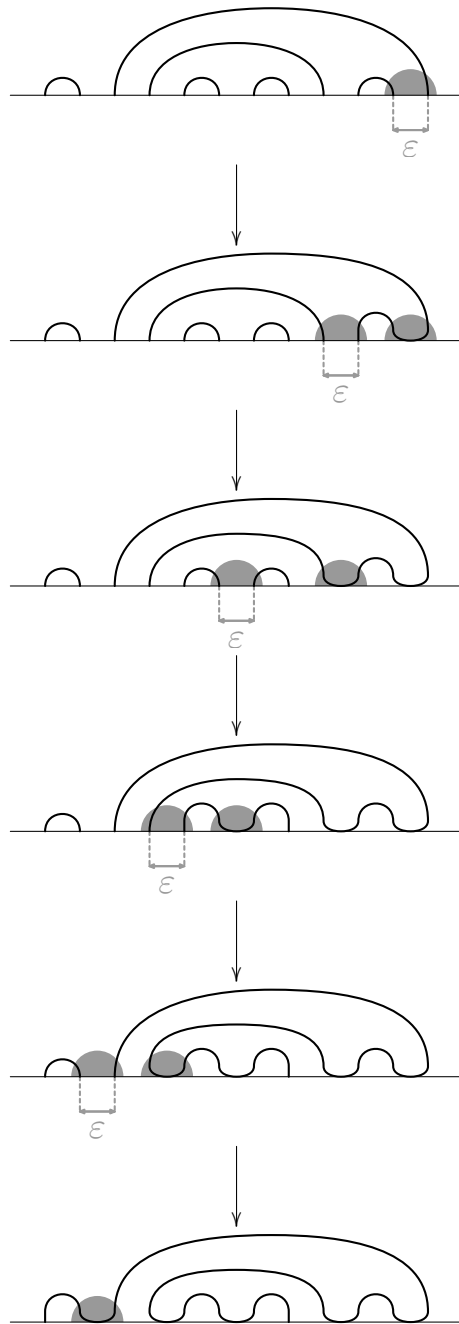


FIGURE 5.1. Schematic illustration of the iterated limits (5.1) in Theorem 5.1.

be a positive solution to the second and third order PDEs predicted for SLE boundary visit amplitudes in [JJK16].

It is in fact natural to associate such functions to each domain Λ by conformal covariance. Let $\phi: \Lambda \rightarrow \mathbb{H}$ be a conformal map. We assume below that the boundary is a straight segment locally near all boundary points where derivatives of ϕ are needed.

First of all, the Brownian excursion kernel \mathcal{K}_Λ in the domain Λ is given by

$$(5.2) \quad \mathcal{K}_\Lambda(p_1, p_2) = \frac{1}{\pi} |\phi'(p_1)| |\phi'(p_2)| \mathcal{K}(\phi(p_1), \phi(p_2)),$$

where $\mathcal{K}(x_1, x_2) = (x_2 - x_1)^{-2}$. Second, the limit of the connectivity probabilities of Theorem 3.16 in the domain Λ is a determinant of the Brownian excursion kernels, given by

$$\mathcal{Z}_\alpha^\Lambda(p_1, \dots, p_{2N}) := \frac{1}{\pi^N} \times \prod_{j=1}^{2N} |\phi'(p_j)| \times \mathcal{Z}_\alpha(\phi(p_1), \dots, \phi(p_{2N})).$$

Let S be a set of indices s specifying the pairs $(j_s, j_s + 1)$, and let $J = \{1, \dots, 2N\} \setminus \bigcup_{s \in S} \{j_s, j_s + 1\}$ be the set of all the other indices. Let $\mathbf{x} = (x_j)_{j \in J}$ and $\hat{\mathbf{x}} = (\hat{x}_s)_{s \in S}$ denote the corresponding real variables as in Theorem 5.1. The limit (5.1) in the statement of the theorem is a function

$$F(\mathbf{x}; \hat{\mathbf{x}}).$$

In any other domain Λ , we can form a similar limit

$$(5.3) \quad F^\Lambda(\mathbf{p}; \hat{\mathbf{p}}) := \lim_{p_{j_1}, p_{j_1+1} \rightarrow \hat{p}_1} \frac{1}{|p_{j_1+1} - p_{j_1}|} \cdots \lim_{p_{j_{N'}}, p_{j_{N'}+1} \rightarrow \hat{p}_{N'}} \frac{1}{|p_{j_{N'}+1} - p_{j_{N'}}|} \mathcal{Z}_\alpha^\Lambda(p_1, \dots, p_{2N}).$$

This limit can then be related to the limit (5.1) by the conformal covariance property

$$(5.4) \quad F^\Lambda(\mathbf{p}; \hat{\mathbf{p}}) = \frac{1}{\pi^N} \times \prod_{j \in J} |\phi'(p_j)| \times \prod_{s \in S} |\phi'(\hat{p}_s)|^3 \times F(\phi(\mathbf{p}); \phi(\hat{\mathbf{p}})),$$

where, for each point \hat{p}_s , two powers of $|\phi'(\hat{p}_s)|$ originate from the factors $|\phi'(p_{j_s})|$ and $|\phi'(p_{j_s+1})|$ in the conformal covariance rule (5.2) of the functions $\mathcal{Z}_\alpha^\Lambda$, and one additional power comes from the factor $\frac{1}{|p_{j_s+1} - p_{j_s}|} \approx \frac{|\phi'(\hat{p}_s)|}{|\phi(p_{j_s+1}) - \phi(p_{j_s})|}$. The constant factors including π are included for convenience in the domain specific notations \mathcal{K}_Λ , $\mathcal{Z}_\alpha^\Lambda$ and F^Λ , but are not included for simplicity in the functions \mathcal{K} , \mathcal{Z}_α , and F , defined on real variables.

The following theorem is a key ingredient in the proof of Theorem 3.17. Informally, the content is that we can exchange the order of the scaling limit $\delta \rightarrow 0$ with the limit (5.3) that collapses pairs of link endpoints to boundary visit locations as in Figure 5.1. The importance of this is twofold: first of all, it gives an explicit formula for the scaling limit of boundary visit probabilities, and secondly, for limits of type (5.3) higher order partial differential equations can be proved by a fusion argument.

Theorem 5.2. *Let $\alpha \in \text{LP}_N$, and let $((j_s, j_s + 1))_{s \in S}$ be a collection of disjoint pairs such that $\wedge_s^j \notin \alpha$ holds for all $s \in S$. Let the boundary edges $e_1^\delta, \dots, e_{2N}^\delta \in \partial \mathcal{E}^\delta$ be as above. Then, the UST connectivity probability*

$$Z_\alpha^{\mathcal{G}^\delta}(e_1^\delta, \dots, e_{2N}^\delta)$$

is, for each fixed δ , explicitly given by the replacing algorithm 5.5 below. Its scaling limit as $\delta \rightarrow 0$ is given by Equation (5.3):

$$\lim_{\delta \rightarrow 0} \frac{1}{\delta^{N'+2N}} Z_\alpha^{\mathcal{G}^\delta}(e_1^\delta, \dots, e_{2N}^\delta) = F^\Lambda(\mathbf{p}; \hat{\mathbf{p}}).$$

The proofs the Theorems 5.1 and 5.2 are based on the replacing algorithms 5.3 and 5.5 below. Recall from Section 3 that we denote by $D_{\tau; i}^\delta$ the discrete tangential derivative with respect to the i :th variable,

and by $\partial_{\tau;i}$ the usual tangential derivative with respect to the i :th variable, taken in the counterclockwise direction. For a function $f: \mathcal{V}^\delta \rightarrow \mathbb{C}$, the discrete tangential derivative is defined at $\hat{e}_s = \langle e_{j_s}^\circ, e_{j_s+1}^\circ \rangle$ by

$$(D_\tau^\delta f)(\hat{e}_s) = (D_\tau^\delta f)(\langle e_{j_s}^\circ, e_{j_s+1}^\circ \rangle) := \frac{f(e_{j_s+1}^\circ) - f(e_{j_s}^\circ)}{\delta}.$$

Algorithm 5.3 (Replacing algorithm for Theorem 5.1). *Under the notation and assumptions of Theorem 5.1, the following procedure of replacements gives an explicit expression for the limit (5.1).*

0. Start from the expression (3.14) of the partition function,

$$\mathcal{Z}_\alpha(x_1, \dots, x_{2N}) = \sum_{\beta \succeq \alpha} \mathcal{C}(\alpha/\beta) \Delta_\beta^K(x_1, \dots, x_{2N}).$$

1. Replace all the kernel entries $\mathcal{K}(x_{j_s}, x_{j_s+1})$ and $\mathcal{K}(x_{j_s+1}, x_{j_s})$, for $s = 1, \dots, N'$, by zero in all the determinants Δ_β^K in the above sum.
2. For all $s = N', N'-1, \dots, 2, 1$, in all the (now modified) determinants, replace the (unique) row or column that is a function of x_{j_s+1} by its derivative at \hat{x}_s , and in the (unique) row or column that is a function of x_{j_s} , replace all appearances of x_{j_s} by \hat{x}_s .

Remark 5.4. A procedure analogous to the replacing algorithm 5.3 can also be applied to the limit (5.3) in any domain Λ with boundary points on straight boundary segments so that the conformal covariance formula (5.4) is valid. The only changes are replacing \mathcal{K} by \mathcal{K}_Λ , and derivatives in step 2 by counterclockwise tangential derivatives.

Algorithm 5.5 (Replacing algorithm for Theorem 5.2). *Under the notation and assumptions of Theorem 5.2, the following procedure of replacements gives an explicit expression for the UST connectivity probability $\mathcal{Z}_\alpha^{\mathcal{G}^\delta}$.*

0. Start from the expression (3.10) of the connectivity probability,

$$\mathcal{Z}_\alpha^{\mathcal{G}^\delta}(e_1^\delta, \dots, e_{2N}^\delta) = \sum_{\beta \succeq \alpha} \mathcal{C}(\alpha/\beta) \Delta_\beta^K(e_1^\delta, \dots, e_{2N}^\delta).$$

1. Replace all the kernel entries $\mathcal{K}(e_{j_s}^\delta, e_{j_s+1}^\delta)$ and $\mathcal{K}(e_{j_s+1}^\delta, e_{j_s}^\delta)$ by zero in all the determinants Δ_β^K in the above sum.
2. For all $s = N', N'-1, \dots, 2, 1$, in all the (now modified) determinants, replace the (unique) row or column that is a function of $e_{j_s+1}^\delta$ by its discrete tangential derivative at \hat{e}_s^δ and add a factor δ in front of the modified connectivity probability.

Proof for Algorithm 5.3. The proof is based on repeated application of the computation rules for inverse Fomin type sums listed in Proposition 2.18 of Section 2.6.

Step 0 starts from the inverse Fomin type sum $\mathcal{Z}_\alpha(x_1, \dots, x_{2N}) = \sum_{\beta \succeq \alpha} \mathcal{C}(\alpha/\beta) \Delta_\beta^K(x_1, \dots, x_{2N})$.

Step 1 applies Proposition 2.18(c) to obtain another inverse Fomin type sum with the same value.

In Step 2, each value of s takes care of one renormalized limit of Equation (5.1). For example, in the first step $s = N'$, we expand the kernel entries with index $j_{N'} + 1$ as

$$(5.5) \quad \mathcal{K}(x_{j_{N'}+1}, x_i) = \mathcal{K}(x_{j_{N'}}, x_i) + (x_{j_{N'}+1} - x_{j_{N'}}) \partial_{\tau;1} \mathcal{K}(x_{j_{N'}}, x_i) + o(|x_{j_{N'}+1} - x_{j_{N'}}|)$$

for $i \neq j_{N'}, j_{N'} + 1$. (Other values of s are handled identically, except that derivatives of \mathcal{K} might appear here.) Then, by the multilinearity of determinants, we can split the inverse Fomin type sum into three different inverse Fomin type sums, with the kernel entries $\mathfrak{K}(j_{N'}+1, i)$ given by one term of the above expansion. The first one, corresponding to the first term in (5.5), has a kernel satisfying the property denoted $\mathfrak{K}(j_{N'}, \cdot) = \mathfrak{K}(j_{N'} + 1, \cdot)$, i.e.,

$$\mathfrak{K}(j_{N'}, i) = \mathcal{K}(x_{j_{N'}}, x_i) = \mathfrak{K}(j_{N'} + 1, i).$$

This inverse Fomin type sum is zero by Proposition 2.18(b). The inverse Fomin type sum corresponding to the third term of (5.5) vanishes in the renormalized limit. The second term yields the asserted replacing algorithm. \square

Proof for Algorithm 5.5. The proof is practically identical to the previous one. The only difference between the proofs is that when writing the discrete Taylor expansion, there is no error term since the discrete tangential derivative is a difference: for any function $f: \mathcal{V}^\delta \rightarrow \mathbb{C}$, we have

$$f(e_{j_s+1}^\circ) = f(e_{j_s}^\circ) + \delta (D_\tau^\delta f)(\hat{e}_s).$$

By multilinearity arguments identical to the case of algorithm 5.3, we cancel the first term of this expansion, and extract the coefficient δ from the determinant. This leaves a determinant with the discrete tangential derivatives, as desired. \square

Using the replacing algorithms 5.3 and 5.5, we can now prove Theorems 5.1 and 5.2.

Proof of Theorem 5.1. Above we saw that the replacing algorithm 5.3 gives the limit (5.1). The multiple limit is independent of the order of limits, since the replacing algorithm is. \square

Proof of Theorem 5.2. The replacing algorithm 5.5 guarantees that we can omit the exponent N' in the expression $\frac{1}{\delta^{N'+2N}} Z_\alpha^\delta(e_1^\delta, \dots, e_{2N}^\delta)$, and replace in the UST connectivity probability

$$Z_\alpha^\delta(e_1^\delta, \dots, e_{2N}^\delta) = \sum_{\beta \succeq \alpha} \# \mathcal{C}(\alpha/\beta) \Delta_\beta^K(e_1^\delta, \dots, e_{2N}^\delta)$$

any kernel entries involving $e_{j_s+1}^\delta$ by the discrete tangential derivatives at \hat{e}_s^δ . By Lemma 3.15, the random walk excursion kernels and their discrete derivatives, normalized by δ^{-2} , converge to the Brownian excursion kernels and their derivatives. Hence, by the similarity of the replacing algorithms 5.3 and 5.5 and Remark 5.4, $\frac{1}{\delta^{N'+2N}} Z_\alpha^\delta(e_1^\delta, \dots, e_{2N}^\delta)$ tends to the limit given by Equation (5.3). \square

5.2. Third order partial differential equations through fusion. We now prove the third order PDEs predicted by CFT for the functions ζ_ω of Theorem 3.17. The proof needs two crucial inputs, discussed below.

Fix a boundary visit order $\omega \in \{+, -\}^{N'}$, and let $\alpha = \alpha(\omega)$ be the link pattern associated to this boundary visit order as in Section 3.2.2 and in Figure 3.4. In this case, we have $N = N' + 1$. As the first input to the proof, we use the iterated limit expression for ζ_ω obtained from Theorems 5.1 and 5.2:

$$(5.6) \quad \zeta_\omega(x_{\text{in}}; \hat{x}_1, \dots, \hat{x}_{N'}; x_{\text{out}}) = \lim_{\substack{x_{j_1}, x_{j_1+1} \rightarrow \hat{x}_1 \\ \vdots \\ x_{j_{N'}}, x_{j_{N'}+1} \rightarrow \hat{x}_{N'}}} \prod_{s=1}^{N'} \frac{1}{x_{j_s+1} - x_{j_s}} \times \mathcal{Z}_{\alpha(\omega)}(x_1, \dots, x_{2N}),$$

where the limits are taken in a specific order: first $x_{j_1}, x_{j_1+1} \rightarrow \hat{x}_1$, then $x_{j_2}, x_{j_2+1} \rightarrow \hat{x}_2$, and so on. The order of the limits does not matter for the result, but we rely on taking the limits one at a time.

As the second input, we use the $2N$ second order partial differential equations (PDE2) for the partition functions \mathcal{Z}_α , which were verified by an explicit calculation in Lemma 4.5 of Section 4.

The strategy of the proof is as follows. We take the limits in (5.6) one at a time, and check recursively that after taking r limits, the resulting function of $2N - r$ variables satisfies $2N - 2r$ PDEs of second order and r PDEs of third order. This recursion step is proven with a fusion procedure described by Dubédat in [Dub15b]. A version of this fusion procedure sufficient for our purposes is Lemma 5.6 below. Technical assumptions in the lemma could be relaxed (see [Dub15b]), but since our explicit functions clearly admit well-behaved Frobenius expansions, we prefer the approach that only invokes direct calculations.

To make a clear distinction, the variables that have not yet been involved in limits will be denoted x_j , and the variables that have been involved in some limit will be denoted \hat{x}_s , with indices j and s in index

sets that are appropriate subsets $J \subset \{1, \dots, 2N\}$ and $S \subset \{1, \dots, N'\}$ depending on how many limits have been taken. We will thus consider functions

$$F(\mathbf{x}; \hat{\mathbf{x}})$$

of variables $\mathbf{x} = (x_j)_{j \in J}$ and $\hat{\mathbf{x}} = (\hat{x}_s)_{s \in S}$.

Let us now write down the second and third order PDEs in the general form, which applies likewise to the input function \mathcal{Z}_α , the final answer ζ_ω , and all the intermediate steps. Without additional difficulty we first work with general $\kappa > 0$, and afterwards specialize to $\kappa = 2$ to derive the main results of this section. We thus use the conformal weight parameters $h = h_{1,2}(\kappa) = \frac{6-\kappa}{2\kappa}$ and $\hat{h} = h_{1,3}(\kappa) = \frac{8-\kappa}{\kappa}$, which at $\kappa = 2$ become $h = 1$ and $\hat{h} = 3$. We express the differential equations in terms of the following first order differential operators:

$$\mathcal{L}_{-n}^{(j)} = \sum_{k \in J \setminus \{j\}} \left(\frac{(n-1)h}{(x_k - x_j)^n} - \frac{1}{(x_k - x_j)^{n-1}} \frac{\partial}{\partial x_k} \right) + \sum_{t \in S} \left(\frac{(n-1)\hat{h}}{(\hat{x}_t - x_j)^n} - \frac{1}{(\hat{x}_t - x_j)^{n-1}} \frac{\partial}{\partial \hat{x}_t} \right)$$

for $n \in \mathbb{Z}_{>0}$ and $j \in J$, and

$$\hat{\mathcal{L}}_{-n}^{(s)} = \sum_{k \in J} \left(\frac{(n-1)h}{(x_k - \hat{x}_s)^n} - \frac{1}{(x_k - \hat{x}_s)^{n-1}} \frac{\partial}{\partial x_k} \right) + \sum_{t \in S \setminus \{s\}} \left(\frac{(n-1)\hat{h}}{(\hat{x}_t - \hat{x}_s)^n} - \frac{1}{(\hat{x}_t - \hat{x}_s)^{n-1}} \frac{\partial}{\partial \hat{x}_t} \right)$$

for $n \in \mathbb{Z}_{>0}$ and $s \in S$. Although we keep it implicit in the notation, note that $\mathcal{L}_{-n}^{(j)}$ and $\hat{\mathcal{L}}_{-n}^{(s)}$ depend on J and S , and they thus denote different operators at different intermediate stages. The second order PDEs will always be of the form

$$(5.7) \quad \mathcal{D}^{(j)} F(\mathbf{x}; \hat{\mathbf{x}}) = 0 \quad \text{where } j \in J \text{ and} \quad \mathcal{D}^{(j)} = \frac{\partial^2}{\partial x_j^2} - \frac{4}{\kappa} \mathcal{L}_{-2}^{(j)}$$

and the third order PDEs will always be of the form

$$(5.8) \quad \hat{\mathcal{D}}^{(s)} F(\mathbf{x}; \hat{\mathbf{x}}) = 0 \quad \text{where } s \in S \text{ and} \quad \hat{\mathcal{D}}^{(s)} = \frac{\partial^3}{\partial \hat{x}_s^3} - \frac{16}{\kappa} \hat{\mathcal{L}}_{-2}^{(s)} \frac{\partial}{\partial \hat{x}_s} + \frac{8(8-\kappa)}{\kappa^2} \hat{\mathcal{L}}_{-3}^{(s)}.$$

Both are special cases of the partial differential equations of conformal field theory introduced by Belavin, Polyakov, and Zamolodchikov in [BPZ84a, BPZ84b], and specifically within the family for which explicit formulas were given by Benoit and Saint-Aubin in [BSA88]. Note that at $\kappa = 2$ and $J = \{1, \dots, 2N\}$ and $S = \emptyset$, Equation (5.7) is nothing but the system (PDE2).

The next key result pertains to fusion in conformal field theory, and it achieves the r :th recursive step of our procedure. In the limit $x_{j_r}, x_{j_r+1} \rightarrow \hat{x}_r$ of interest, solutions to the PDEs (5.7) above can have power law behavior with two possible exponents: the roots $\Delta = -2h = \frac{\kappa-6}{\kappa}$ and $\Delta' = \hat{h} - 2h = \frac{2}{\kappa}$ of the indicial equation of a Frobenius series (see the proof of Lemma 5.6 below). The result specifically addresses the coefficient of the subleading power law behavior, with exponent⁴ Δ' . The argument follows ideas in [Dub15b]. We include the proof, because this is a key step towards our main results.

Lemma 5.6. *Let $J \subset \{1, \dots, 2N\}$ be a subset of size $\#J = 2N - 2(r-1)$ and let $S = \{1, \dots, r-1\}$. Let also $j_r, j_r+1 \in J$ be two consecutive indices, and $J' = J \setminus \{j_r, j_r+1\}$ and $S' = \{1, \dots, r\}$. Denote*

$$\hat{x}_r = \frac{1}{2}(x_{j_r+1} + x_{j_r}) \quad \text{and} \quad \varepsilon = x_{j_r+1} - x_{j_r}.$$

Let $F(\mathbf{x}; \hat{\mathbf{x}})$ be a function which satisfies Equations (5.7) for all $j \in J$ and Equations (5.8) for all $s \in S$, and which for any $\mathbf{x}' = (x_j)_{j \in J'}$ and $\hat{\mathbf{x}}' = (\hat{x}_s)_{s \in S'}$ and small positive ε has the Frobenius series expansion

$$(5.9) \quad F(\mathbf{x}; \hat{\mathbf{x}}) = \sum_{m=0}^{\infty} \varepsilon^{\Delta'+m} F^{(m)}(\mathbf{x}'; \hat{\mathbf{x}}')$$

⁴For $\kappa < 8$ we have $\Delta < \Delta'$, whence the terminology leading and subleading for Δ and Δ' , respectively.

with exponent $\Delta' = \frac{2}{\kappa}$. Assume that the coefficients $F^{(m)}$ are smooth functions of $(\mathbf{x}'; \hat{\mathbf{x}}')$, and that for any compact subset K of the domain of their definition and for any multi-index α , there exist positive constants $r_{K;\alpha}, C_{K;\alpha}$ such that the bound on partial derivatives,

$$\left| \partial^\alpha F^{(m)}(\mathbf{x}'; \hat{\mathbf{x}}') \right| \leq C_{K;\alpha} r_{K;\alpha}^{-m},$$

holds for all $m \in \mathbb{N}$ and $(\mathbf{x}'; \hat{\mathbf{x}}') \in K$. Then the limit

$$F_{\text{lim}}(\mathbf{x}'; \hat{\mathbf{x}}') := \lim_{x_{j_r}, x_{j_r+1} \rightarrow \hat{x}_r} \frac{1}{(x_{j_r+1} - x_{j_r})^{\Delta'}} F(\mathbf{x}; \hat{\mathbf{x}})$$

defines a function $F_{\text{lim}} = F^{(0)}$ of $\mathbf{x}' = (x_j)_{j \in J'}$ and $\hat{\mathbf{x}}' = (\hat{x}_s)_{s \in S'}$, which satisfies all the second and third order PDEs (5.10) and (5.11) associated with the index sets J' and S' and the corresponding variables.

Proof. Paying attention to the dependence of the differential operators on the index sets, the precise claim is that the limit function $F_{\text{lim}}(\mathbf{x}'; \hat{\mathbf{x}}') = F^{(0)}(\mathbf{x}'; \hat{\mathbf{x}}')$ satisfies the differential equations

$$(5.10) \quad \mathcal{D}'^{(j)} F^{(0)}(\mathbf{x}'; \hat{\mathbf{x}}') = 0 \quad \text{for all } j \in J' \text{ and} \quad \mathcal{D}'^{(j)} = \frac{\partial^2}{\partial x_j^2} - \frac{4}{\kappa} \mathcal{L}'_{-2}^{(j)},$$

where

$$\mathcal{L}'_{-n}^{(j)} = \sum_{k \in J' \setminus \{j\}} \left(\frac{(n-1)h}{(x_k - x_j)^n} - \frac{1}{(x_k - x_j)^{n-1}} \frac{\partial}{\partial x_k} \right) + \sum_{t \in S'} \left(\frac{(n-1)\hat{h}}{(\hat{x}_t - x_j)^n} - \frac{1}{(\hat{x}_t - x_j)^{n-1}} \frac{\partial}{\partial \hat{x}_t} \right)$$

and

$$(5.11) \quad \widehat{\mathcal{D}}'^{(s)} F^{(0)}(\mathbf{x}'; \hat{\mathbf{x}}') = 0 \quad \text{for all } s \in S' \text{ and} \quad \widehat{\mathcal{D}}'^{(s)} = \frac{\partial^3}{\partial \hat{x}_s^3} - \frac{16}{\kappa} \widehat{\mathcal{L}}'^{(s)}_{-2} \frac{\partial}{\partial \hat{x}_s} + \frac{8(8-\kappa)}{\kappa^2} \widehat{\mathcal{L}}'^{(s)}_{-3},$$

where

$$\widehat{\mathcal{L}}'^{(s)}_{-n} = \sum_{k \in J'} \left(\frac{(n-1)h}{(x_k - \hat{x}_s)^n} - \frac{1}{(x_k - \hat{x}_s)^{n-1}} \frac{\partial}{\partial x_k} \right) + \sum_{t \in S' \setminus \{s\}} \left(\frac{(n-1)\hat{h}}{(\hat{x}_t - \hat{x}_s)^n} - \frac{1}{(\hat{x}_t - \hat{x}_s)^{n-1}} \frac{\partial}{\partial \hat{x}_t} \right).$$

The proof is divided to three separate cases, each establishing some of the asserted PDEs for $F^{(0)}$:

- (i) $\mathcal{D}'^{(j)} F^{(0)}(\mathbf{x}'; \hat{\mathbf{x}}') = 0$ for $j \in J' = J \setminus \{j_r, j_r + 1\}$
- (ii) $\widehat{\mathcal{D}}'^{(s)} F^{(0)}(\mathbf{x}; \hat{\mathbf{x}}) = 0$ for $s \neq r$
- (iii) $\widehat{\mathcal{D}}'^{(r)} F^{(0)}(\mathbf{x}; \hat{\mathbf{x}}) = 0$.

The verifications of the PDEs (i) and (ii) are in principle straightforward, although the number of terms renders the calculations somewhat lengthy. The truly interesting part is (iii), where we have the appearance of the new third order PDE $\widehat{\mathcal{D}}'^{(r)} F^{(0)}(\mathbf{x}; \hat{\mathbf{x}}) = 0$ via fusion from two second order PDEs.

Case (i), second order PDEs in the limit: We begin by verifying the straightforward second order PDEs $\mathcal{D}'^{(j)} F^{(0)}(\mathbf{x}'; \hat{\mathbf{x}}') = 0$ for $j \in J'$. From the original variables $(\mathbf{x}; \hat{\mathbf{x}})$ we change to new variables $(\mathbf{x}'; \hat{\mathbf{x}}'; \varepsilon)$ as in the statement of the lemma. The assumed original PDE $\mathcal{D}^{(j)} F(\mathbf{x}; \hat{\mathbf{x}}) = 0$ becomes, after changing the order of differentiation and summation in the Frobenius series (5.9),

$$(5.12) \quad \sum_{m=0}^{\infty} \mathcal{D}^{(j)} \left(\varepsilon^{\Delta'+m} F^{(m)}(\mathbf{x}'; \hat{\mathbf{x}}') \right) = 0.$$

The exchange of the order of differentiation and summation is justified by the assumed locally uniform bounds on the series coefficients and their partial derivatives.

Let us consider the various terms appearing in $\mathcal{D}^{(j)} (\varepsilon^{\Delta'+m} F^{(m)}(\mathbf{x}'; \hat{\mathbf{x}}'))$. We split the differential operator $\mathcal{D}^{(j)}$ to the following parts:

- (a): $\frac{\partial^2}{\partial x_j^2}$
- (b): $-\frac{4}{\kappa} \frac{h}{(x_k - x_j)^2} + \frac{4}{\kappa} \frac{1}{x_k - x_j} \frac{\partial}{\partial x_k}$ for $k \in J' = J \setminus \{j_r, j_r + 1\}$

$$\begin{aligned}
\text{(c): } & -\frac{4}{\kappa} \frac{\hat{h}}{(\hat{x}_t - x_j)^2} + \frac{4}{\kappa} \frac{1}{\hat{x}_t - x_j} \frac{\partial}{\partial \hat{x}_t} \text{ for } t \in S \\
\text{(d): } & -\frac{4}{\kappa} \frac{h}{(x_{j_r} - x_j)^2} + \frac{4}{\kappa} \frac{1}{x_{j_r} - x_j} \frac{\partial}{\partial x_{j_r}} \\
\text{(e): } & -\frac{4}{\kappa} \frac{h}{(x_{j_r+1} - x_j)^2} + \frac{4}{\kappa} \frac{1}{x_{j_r+1} - x_j} \frac{\partial}{\partial x_{j_r+1}}.
\end{aligned}$$

The chain rule expresses the derivatives in the old variables appearing in $\mathcal{D}^{(j)}$ in terms of the new variables as $\frac{\partial}{\partial x_{j_r}} = -\frac{\partial}{\partial \varepsilon} + \frac{1}{2} \frac{\partial}{\partial \hat{x}_r}$ and $\frac{\partial}{\partial x_{j_r+1}} = +\frac{\partial}{\partial \varepsilon} + \frac{1}{2} \frac{\partial}{\partial \hat{x}_r}$. The variables x_j, x_k for $k \in J'$, and \hat{x}_t for $t \in S$ are not affected by the change of variables, so the terms (a), (b), and (c) simply become

$$(5.12a) \quad \varepsilon^{\Delta'+m} \frac{\partial^2}{\partial x_j^2} F^{(m)}(\mathbf{x}'; \hat{\mathbf{x}}'),$$

$$(5.12b) \quad \varepsilon^{\Delta'+m} \frac{4}{\kappa} \left(\frac{1}{x_k - x_j} \frac{\partial}{\partial x_k} F^{(m)}(\mathbf{x}'; \hat{\mathbf{x}}') - \frac{h}{(x_k - x_j)^2} F^{(m)}(\mathbf{x}'; \hat{\mathbf{x}}') \right),$$

$$(5.12c) \quad \varepsilon^{\Delta'+m} \frac{4}{\kappa} \left(\frac{1}{\hat{x}_t - x_j} \frac{\partial}{\partial \hat{x}_t} F^{(m)}(\mathbf{x}'; \hat{\mathbf{x}}') - \frac{\hat{h}}{(\hat{x}_t - x_j)^2} F^{(m)}(\mathbf{x}'; \hat{\mathbf{x}}') \right).$$

The remaining terms (d) and (e) involve one of the original variables x_{j_r} or x_{j_r+1} , which we express in terms of \hat{x}_r and ε . Noticing $x_{j_r} - x_j = \hat{x}_r - x_j - \frac{\varepsilon}{2}$, we get the expansions

$$\frac{1}{x_{j_r} - x_j} = \frac{1}{\hat{x}_r - x_j} \sum_{\ell=0}^{\infty} \frac{\varepsilon^\ell}{2^\ell (\hat{x}_r - x_j)^\ell} \quad \text{and} \quad \frac{h}{(x_{j_r} - x_j)^2} = \frac{h}{(\hat{x}_r - x_j)^2} \sum_{\ell=0}^{\infty} \frac{(\ell+1) \varepsilon^\ell}{2^\ell (\hat{x}_r - x_j)^\ell}.$$

Now use the chain rule to write the terms in (d) as

$$(5.12d) \quad \varepsilon^{\Delta'+m} \frac{4}{\kappa} \left(\left(\frac{1}{2} \frac{\partial}{\partial \hat{x}_r} F^{(m)}(\mathbf{x}'; \hat{\mathbf{x}}') - \frac{\Delta' + m}{\varepsilon} F^{(m)}(\mathbf{x}'; \hat{\mathbf{x}}') \right) \frac{1}{\hat{x}_r - x_j} \sum_{\ell=0}^{\infty} \frac{\varepsilon^\ell}{2^\ell (\hat{x}_r - x_j)^\ell} \right. \\ \left. - F^{(m)}(\mathbf{x}'; \hat{\mathbf{x}}') \frac{h}{(\hat{x}_r - x_j)^2} \sum_{\ell=0}^{\infty} \frac{(\ell+1) \varepsilon^\ell}{2^\ell (\hat{x}_r - x_j)^\ell} \right).$$

Proceeding similarly, the terms in (e) are written as

$$(5.12e) \quad \varepsilon^{\Delta'+m} \frac{4}{\kappa} \left(\left(\frac{1}{2} \frac{\partial}{\partial \hat{x}_r} F^{(m)}(\mathbf{x}'; \hat{\mathbf{x}}') + \frac{\Delta' + m}{\varepsilon} F^{(m)}(\mathbf{x}'; \hat{\mathbf{x}}') \right) \frac{1}{\hat{x}_r - x_j} \sum_{\ell=0}^{\infty} \frac{(-\varepsilon)^\ell}{2^\ell (\hat{x}_r - x_j)^\ell} \right. \\ \left. - F^{(m)}(\mathbf{x}'; \hat{\mathbf{x}}') \frac{h}{(\hat{x}_r - x_j)^2} \sum_{\ell=0}^{\infty} \frac{(\ell+1) (-\varepsilon)^\ell}{2^\ell (\hat{x}_r - x_j)^\ell} \right).$$

From expressions (5.12a), (5.12b), (5.12c), (5.12d), and (5.12e), we can read the ε -expansion of $\mathcal{D}^{(j)} F(\mathbf{x}; \hat{\mathbf{x}})$. Note that terms of order $\varepsilon^{\Delta'-1}$ cancel in (5.12d) and (5.12e), and the leading order of $\mathcal{D}^{(j)} F(\mathbf{x}; \hat{\mathbf{x}})$ is

$$\begin{aligned}
\varepsilon^{\Delta'} & \left(\frac{\partial^2}{\partial x_j^2} F^{(0)}(\mathbf{x}'; \hat{\mathbf{x}}') + \frac{4}{\kappa} \sum_{k \in J'} \frac{1}{x_k - x_j} \frac{\partial}{\partial x_k} F^{(0)}(\mathbf{x}'; \hat{\mathbf{x}}') - \frac{4}{\kappa} \sum_{k \in J'} \frac{h}{(x_k - x_j)^2} F^{(0)}(\mathbf{x}'; \hat{\mathbf{x}}') \right. \\
& + \frac{4}{\kappa} \sum_{t \in S} \frac{1}{\hat{x}_t - x_j} \frac{\partial}{\partial \hat{x}_t} F^{(0)}(\mathbf{x}'; \hat{\mathbf{x}}') - \frac{4}{\kappa} \sum_{t \in S} \frac{\hat{h}}{(\hat{x}_t - x_j)^2} F^{(0)}(\mathbf{x}'; \hat{\mathbf{x}}') \\
& \left. + \frac{4}{\kappa} \frac{1}{\hat{x}_r - x_j} \frac{\partial}{\partial \hat{x}_r} F^{(0)}(\mathbf{x}'; \hat{\mathbf{x}}') - \frac{4}{\kappa} \frac{\Delta' + 2h}{(\hat{x}_r - x_j)^2} F^{(0)}(\mathbf{x}'; \hat{\mathbf{x}}') \right).
\end{aligned}$$

By the assumed original PDE $\mathcal{D}^{(j)} F(\mathbf{x}; \hat{\mathbf{x}}) = 0$, the above expression must vanish. Taking into account the relation $\Delta' + 2h = \hat{h}$, this implies the asserted second order PDE for the limit function,

$$\mathcal{D}^{(j)} F^{(0)}(\mathbf{x}'; \hat{\mathbf{x}}') = \left(\frac{\partial^2}{\partial x_j^2} - \frac{4}{\kappa} \mathcal{L}'^{(j)} \right) F^{(0)}(\mathbf{x}'; \hat{\mathbf{x}}') = 0.$$

Case (ii), third order PDEs in the limit: We leave it for the reader to verify these third order PDEs for the limit function. No new ideas are needed, and the calculations are similar to case (i).

Case (iii), new third order PDEs via fusion: Let us finally turn to how the recursion makes new third order PDEs appear. The starting point is either of the two second order PDEs $\mathcal{D}^{(j_r)}F(\mathbf{x}; \hat{\mathbf{x}}) = 0$ or $\mathcal{D}^{(j_r+1)}F(\mathbf{x}; \hat{\mathbf{x}}) = 0$ for the original function. We again differentiate the Frobenius series (5.9) term by term, and after some straightforward calculations, we obtain

$$(5.13) \quad \begin{aligned} \mathcal{D}^{(j_r)}F(\mathbf{x}; \hat{\mathbf{x}}) = & \varepsilon^{\Delta'-2} \left(\Delta'(\Delta' - 1) + \frac{4}{\kappa}(\Delta' - h) \right) F^{(0)}(\mathbf{x}'; \hat{\mathbf{x}}') \\ & + \varepsilon^{\Delta'-1} \left(\left(\frac{2}{\kappa} - \Delta' \right) \frac{\partial}{\partial \hat{x}_r} F^{(0)}(\mathbf{x}'; \hat{\mathbf{x}}') + ((\Delta' + 1)\Delta' + \frac{4}{\kappa}(\Delta' + 1 - h)) F^{(1)}(\mathbf{x}'; \hat{\mathbf{x}}') \right) \\ & + \mathcal{O}(\varepsilon^{\Delta'}). \end{aligned}$$

We will in fact below need to calculate two further coefficients of this expansion, but they can be significantly simplified by conclusions drawn from the above.

The coefficient of $\varepsilon^{\Delta'-2}$ in (5.13) vanishes simply because $\Delta' = \hat{h} - 2h = \frac{2}{\kappa}$ is a solution of the indicial equation

$$\Delta'(\Delta' - 1) + \frac{4}{\kappa}(\Delta' - \frac{6-\kappa}{2\kappa}) = 0$$

of the Frobenius series (the other solution is $\Delta = -2h = \frac{\kappa-6}{\kappa}$). In the higher order terms we can also perform the related simplification $(\Delta' + m)(\Delta' + m - 1) + \frac{4}{\kappa}(\Delta' + m - \frac{6-\kappa}{2\kappa}) = m^2 - m + 2m\Delta' + m\frac{4}{\kappa} = m^2 + m\frac{8-\kappa}{\kappa}$.

Next consider the coefficient of $\varepsilon^{\Delta'-1}$ in (5.13), which must also vanish because of the assumed original partial differential equation $\mathcal{D}^{(j_r)}F(\mathbf{x}; \hat{\mathbf{x}}) = 0$. Since $\frac{2}{\kappa} - \Delta' = 0$ and $(\Delta' + 1)\Delta' + \frac{4}{\kappa}(\Delta' + 1 - \frac{6-\kappa}{2\kappa}) \neq 0$, the vanishing of this coefficient is equivalent to $F^{(1)}(\mathbf{x}'; \hat{\mathbf{x}}') = 0$. In other words, the next-to-leading order coefficient in the Frobenius series (5.9) is necessarily zero.

These observations can be used to simplify the result of the calculation of $\mathcal{D}^{(j_r)}F(\mathbf{x}; \hat{\mathbf{x}})$ up to order $\varepsilon^{\Delta'}$ to the following form:

$$(5.13') \quad \begin{aligned} \mathcal{D}^{(j_r)}F(\mathbf{x}; \hat{\mathbf{x}}) = & 0 \times \varepsilon^{\Delta'-2} + 0 \times \varepsilon^{\Delta'-1} \\ & + \varepsilon^{\Delta'} \left(\frac{1}{4} \frac{\partial^2}{\partial \hat{x}_r^2} F^{(0)}(\mathbf{x}'; \hat{\mathbf{x}}') + \left(4 + 2\frac{8-\kappa}{\kappa} \right) F^{(2)}(\mathbf{x}'; \hat{\mathbf{x}}') \right. \\ & + \frac{4}{\kappa} \sum_{k \in J'} \frac{1}{x_k - \hat{x}_r} \frac{\partial}{\partial x_k} F^{(0)}(\mathbf{x}'; \hat{\mathbf{x}}') + \frac{4}{\kappa} \sum_{t \in S} \frac{1}{\hat{x}_t - \hat{x}_r} \frac{\partial}{\partial \hat{x}_t} F^{(0)}(\mathbf{x}'; \hat{\mathbf{x}}') \\ & \left. - \frac{4}{\kappa} \sum_{k \in J'} \frac{h}{(x_k - \hat{x}_r)^2} F^{(0)}(\mathbf{x}'; \hat{\mathbf{x}}') - \frac{4}{\kappa} \sum_{t \in S} \frac{\hat{h}}{(\hat{x}_t - \hat{x}_r)^2} F^{(0)}(\mathbf{x}'; \hat{\mathbf{x}}') \right) \\ & + \mathcal{O}(\varepsilon^{\Delta'+1}). \end{aligned}$$

Using the assumption $\mathcal{D}^{(j_r)}F(\mathbf{x}; \hat{\mathbf{x}}) = 0$, the coefficient of $\varepsilon^{\Delta'}$ in (5.13') must vanish, and we can solve for the next term $F^{(2)}(\mathbf{x}'; \hat{\mathbf{x}}')$ in the Frobenius series (5.9) in terms of the leading term $F^{(0)}(\mathbf{x}'; \hat{\mathbf{x}}')$:

$$(5.14) \quad F^{(2)}(\mathbf{x}'; \hat{\mathbf{x}}') = \frac{\kappa}{8 + \kappa} \left(\frac{2}{\kappa} \hat{\mathcal{L}}_{-2}^{(r)} F^{(0)}(\mathbf{x}'; \hat{\mathbf{x}}') - \frac{1}{8} \frac{\partial^2}{\partial \hat{x}_r^2} F^{(0)}(\mathbf{x}'; \hat{\mathbf{x}}') \right).$$

It remains to inspect $\mathcal{D}^{(j_r)}F(\mathbf{x}; \hat{\mathbf{x}})$ up to order $\varepsilon^{\Delta'+1}$,

$$\begin{aligned}
(5.13'') \quad \mathcal{D}^{(j_r)}F(\mathbf{x}; \hat{\mathbf{x}}) = & 0 \times \varepsilon^{\Delta'-2} + 0 \times \varepsilon^{\Delta'-1} + 0 \times \varepsilon^{\Delta'} \\
& + \varepsilon^{\Delta'+1} \left(-2 \frac{\partial}{\partial \hat{x}_r} F^{(2)}(\mathbf{x}'; \hat{\mathbf{x}}') \right. \\
& - \frac{2}{\kappa} \sum_{k \in J'} \frac{1}{(x_k - \hat{x}_r)^2} \frac{\partial}{\partial x_k} F^{(0)}(\mathbf{x}'; \hat{\mathbf{x}}') - \frac{2}{\kappa} \sum_{t \in S} \frac{1}{(\hat{x}_t - \hat{x}_r)^2} \frac{\partial}{\partial \hat{x}_t} F^{(0)}(\mathbf{x}'; \hat{\mathbf{x}}') \\
& + \frac{4}{\kappa} \sum_{k \in J'} \frac{h}{(x_k - \hat{x}_r)^3} F^{(0)}(\mathbf{x}'; \hat{\mathbf{x}}') + \frac{4}{\kappa} \sum_{t \in S} \frac{\hat{h}}{(\hat{x}_t - \hat{x}_r)^3} F^{(0)}(\mathbf{x}'; \hat{\mathbf{x}}') \Big) \\
& + \mathcal{O}(\varepsilon^{\Delta'+2}).
\end{aligned}$$

From the vanishing of the coefficient of $\varepsilon^{\Delta'+1}$ in (5.13''), we solve

$$\frac{\partial}{\partial \hat{x}_r} F^{(2)}(\mathbf{x}'; \hat{\mathbf{x}}') = \frac{1}{\kappa} \widehat{\mathcal{L}}_{-3}^{(r)} F^{(0)}(\mathbf{x}'; \hat{\mathbf{x}}').$$

Substituting here the expression (5.14) for $F^{(2)}(\mathbf{x}'; \hat{\mathbf{x}}')$, we arrive at the third order PDE

$$-\frac{\kappa}{8(8+\kappa)} \frac{\partial^3}{\partial \hat{x}_r^3} F^{(0)}(\mathbf{x}'; \hat{\mathbf{x}}') + \frac{2}{8+\kappa} \frac{\partial}{\partial \hat{x}_r} \widehat{\mathcal{L}}_{-2}^{(r)} F^{(0)}(\mathbf{x}'; \hat{\mathbf{x}}') = \frac{1}{\kappa} \widehat{\mathcal{L}}_{-3}^{(r)} F^{(0)}(\mathbf{x}'; \hat{\mathbf{x}}')$$

for the leading coefficient $F^{(0)}(\mathbf{x}'; \hat{\mathbf{x}}')$ of the Frobenius series (5.9). Finally, using the commutation relation $\frac{\partial}{\partial \hat{x}_r} \widehat{\mathcal{L}}_{-2}^{(r)} - \widehat{\mathcal{L}}_{-2}^{(r)} \frac{\partial}{\partial \hat{x}_r} = \widehat{\mathcal{L}}_{-3}^{(r)}$, we get the nontrivial third order PDE that we wanted to establish:

$$0 = \frac{\partial^3}{\partial \hat{x}_r^3} F^{(0)}(\mathbf{x}'; \hat{\mathbf{x}}') - \frac{16}{\kappa} \widehat{\mathcal{L}}_{-2}^{(r)} \frac{\partial}{\partial \hat{x}_r} F^{(0)}(\mathbf{x}'; \hat{\mathbf{x}}') + \frac{8(8-\kappa)}{\kappa^2} \widehat{\mathcal{L}}_{-3}^{(r)} F^{(0)}(\mathbf{x}'; \hat{\mathbf{x}}').$$

□

Using Lemma 5.6 recursively, we now prove the third order partial differential equations for the function ζ_ω given by the iterated limit (5.6).

Proposition 5.7. *The function $\zeta_\omega(x_1; \hat{x}_1, \dots, \hat{x}_{N'}; x_2)$ satisfies the two second order PDEs, for $j \in J = \{1, 2\}$,*

$$(5.15) \quad \mathcal{D}^{(j)} \zeta_\omega(x_1; \hat{x}_1, \dots, \hat{x}_{N'}; x_2) = 0, \quad \text{where} \quad \mathcal{D}^{(j)} = \frac{\partial^2}{\partial x_j^2} - 2 \mathcal{L}_{-2}^{(j)}$$

and the N' third order PDEs, for $s \in S = \{1, \dots, N'\}$,

$$(5.16) \quad \widehat{\mathcal{D}}^{(s)} \zeta_\omega(x_1; \hat{x}_1, \dots, \hat{x}_{N'}; x_2) = 0, \quad \text{where} \quad \widehat{\mathcal{D}}^{(s)} = \frac{\partial^3}{\partial \hat{x}_s^3} - 8 \widehat{\mathcal{L}}_{-2}^{(s)} \frac{\partial}{\partial \hat{x}_s} + 12 \widehat{\mathcal{L}}_{-3}^{(s)}.$$

Moreover, the function $\zeta_\omega(x_1; \hat{x}_1, \dots, \hat{x}_{N'}; x_2)$ is positive.

Proof. Start from the function

$$F_0(x_1, \dots, x_{2N}) := \mathcal{Z}_\alpha(x_1, \dots, x_{2N})$$

with $\alpha = \alpha(\omega)$. At $\kappa = 2$, the system of second order PDEs (5.7) for F_0 is nothing but the system (PDE2) for \mathcal{Z}_α , which is satisfied by virtue of Lemma 4.5 (and at this stage there are no third order PDEs). By iterated limits, recursively define new functions for $r = 1, 2, \dots, N'$,

$$F_r(\mathbf{x}'; \hat{\mathbf{x}}') := \lim_{x_{j_r}, x_{j_r+1} \rightarrow \hat{x}_r} \frac{1}{(x_{j_r+1} - x_{j_r})^{\Delta'}} F_{r-1}(\mathbf{x}; \hat{\mathbf{x}}).$$

By the replacing algorithm 5.3, each function F_{r-1} is a linear combination of certain determinants, whose Taylor series expansion is a Frobenius series of the required form. Therefore, by Lemma 5.6, each

F_r satisfies the corresponding joint system of second and third order PDEs. Finally, with $r = N'$ we obtain the function

$$F_{N'}(x_1, \hat{x}_1, \dots, \hat{x}_{N'}, x_2) = \zeta_\omega(x_1, \hat{x}_1, \dots, \hat{x}_{N'}, x_2),$$

according to the expression (5.6). The asserted partial differential equations thus follow.

Positivity is shown by the same recursive argument. First of all, $F_0 = \mathcal{Z}_\alpha$ is positive by Theorem 4.1. Each iterated limit F_r is therefore non-negative. It remains to show that F_r is pointwise non-vanishing. The value of $F_r(\mathbf{x}'; \hat{\mathbf{x}}')$ is the coefficient of $(x_{j_r+1} - x_{j_r})^{-\Delta'}$ in the Frobenius series expansion of $F_{r-1}(\mathbf{x}; \hat{\mathbf{x}})$. The coefficient of the leading term $(x_{j_r+1} - x_{j_r})^{-\Delta}$ is vanishing, so if also $F_r(\mathbf{x}'; \hat{\mathbf{x}}')$ were vanishing, the function $F_{r-1}(\mathbf{x}; \hat{\mathbf{x}})$ would have to be zero. Non-vanishingness then follows recursively. \square

5.3. Proof of Theorem 3.17. Let us now conclude the proof of one of our main results, Theorem 3.17, about the scaling limit of boundary visit probabilities of the loop-erased random walk. The starting point is the formula of Corollary 3.13 for the probability that a LERW λ^δ on \mathcal{G}^δ from e_{in}^δ to e_{out}^δ uses edges $\hat{e}_1^\delta, \dots, \hat{e}_{N'}^\delta$ at unit distance from the boundary in an order specified by ω ,

$$\mathbb{P}_{e_{\text{in}}^\delta, e_{\text{out}}^\delta} [\lambda^\delta \text{ uses } \hat{e}_1^\delta, \dots, \hat{e}_{N'}^\delta \text{ in the order } \omega] = \frac{Z_{\alpha(\omega)}^{\mathcal{G}^\delta}(e_1^\delta, \dots, e_{2N}^\delta)}{Z^{\mathcal{G}^\delta}(e_{\text{in}}^\delta, e_{\text{out}}^\delta)}.$$

In the setup of Theorem 3.17, \mathcal{G}^δ is a square grid approximation of a domain Λ , and the edges $e_{\text{in}}^\delta, e_{\text{out}}^\delta, \hat{e}_1^\delta, \dots, \hat{e}_{N'}^\delta$ are the nearest to the marked points $p_{\text{in}}, p_{\text{out}}, \hat{p}_1, \dots, \hat{p}_{N'}$, which lie on horizontal or vertical boundary segments. Then Theorem 5.2 applied to the numerator and Lemma 3.15 to the denominator give the existence of the limit

$$\lim_{\delta \rightarrow 0} \frac{\mathbb{P}_{e_{\text{in}}^\delta, e_{\text{out}}^\delta} [\lambda^\delta \text{ uses } \hat{e}_1^\delta, \dots, \hat{e}_{N'}^\delta \text{ in the order } \omega]}{\delta^{3N'}}.$$

Moreover, with Equation (5.4), this limit is explicitly expressed as

$$\pi^{-N'} \times \prod_{s=1}^{N'} |\phi'(\hat{p}_s)|^3 \times \frac{\zeta_\omega(\phi(p_{\text{in}}), \phi(p_{\text{out}}); \phi(\hat{\mathbf{p}}))}{\mathcal{K}(\phi(p_{\text{in}}), \phi(p_{\text{out}}))},$$

where ζ_ω is given by Equation (5.6) and $\mathcal{K}(x_{\text{in}}, x_{\text{out}}) = (x_{\text{out}} - x_{\text{in}})^{-2}$. Finally, in Proposition 5.7, we verified the asserted two second order and N' third order partial differential equations for ζ_ω . This concludes the proof. \square

5.4. Asymptotics of the scaling limits of the boundary visit probabilities. To finish this section, we prove asymptotics properties for the boundary visit probabilities, predicted in [JJK16].

Proposition 5.8. *Let $\omega = (\omega_1, \dots, \omega_{N'}) \in \{\pm 1\}^{N'}$ be an order of boundary visits, and let \hat{x}_s be the boundary visit point closest to x_{in} on either side of x_{in} . Then, as $\hat{x}_s, x_{\text{in}} \rightarrow x'_{\text{in}}$, we have the following asymptotics of ζ_ω :*

$$(5.17) \quad \lim_{\hat{x}_s, x_{\text{in}} \rightarrow x'_{\text{in}}} |\hat{x}_s - x_{\text{in}}|^3 \zeta_\omega(x_{\text{in}}; \hat{x}_1, \hat{x}_2, \dots, \hat{x}_{N'}; x_{\text{out}}) \\ = \begin{cases} 0 & \text{if } \hat{x}_s \text{ is not the first boundary visit, i.e., } \omega_1 \neq \text{sgn}(\hat{x}_s - x_{\text{in}}) \\ 2 \zeta_{\omega'}(x'_{\text{in}}; \hat{x}_2, \dots, \hat{x}_{N'}; x_{\text{out}}) & \text{if } \hat{x}_s \text{ is the first boundary visit, i.e., } \omega_1 = \text{sgn}(\hat{x}_s - x_{\text{in}}), \end{cases}$$

where $\omega' = (\omega_2, \dots, \omega_{N'}) \in \{\pm 1\}^{N'-1}$ is obtained from ω by omitting the first boundary visit, as illustrated in Figure 5.2.

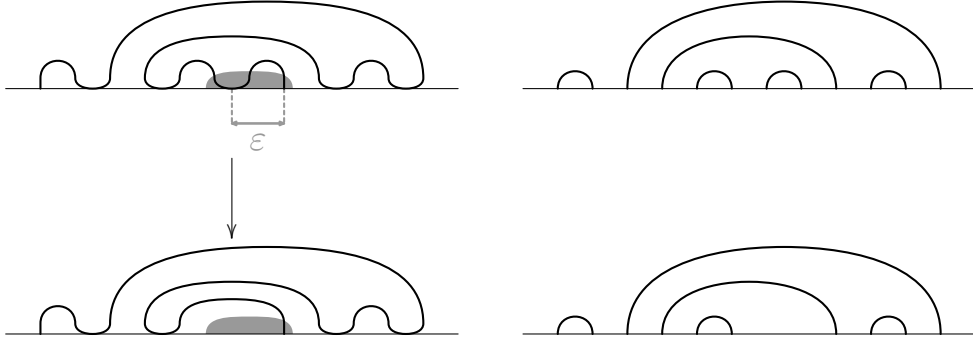


FIGURE 5.2. Illustration of the asymptotics property in Proposition 5.8: collapsing the first visited point with the starting point. The boundary visit orders ω and ω' are shown on the top left and bottom left, and the corresponding link patterns $\alpha(\omega)$ and $\alpha(\omega')$ on the top right and bottom right, respectively.

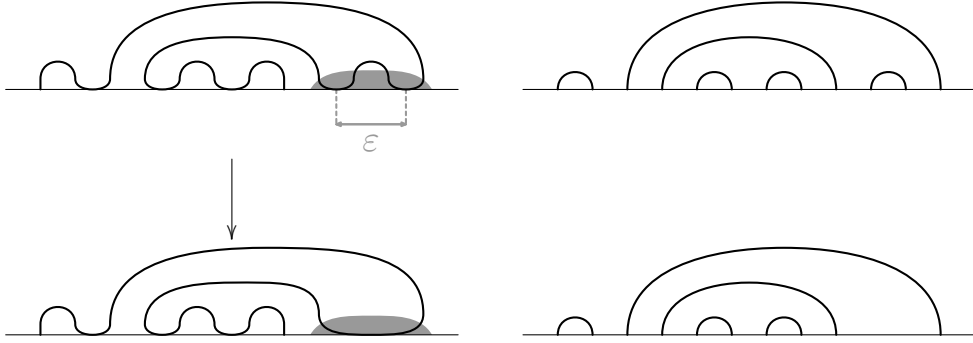


FIGURE 5.3. Illustration of the asymptotics property in Proposition 5.9: collapsing two successively visited points. The boundary visit orders ω and ω' are shown on the top left and bottom left, and the corresponding link patterns $\alpha(\omega)$ and $\alpha(\omega')$ on the top right and bottom right, respectively.

Proposition 5.9. *Let $\omega \in \{\pm 1\}^{N'}$ be an order of boundary visits, and let \hat{x}_s and \hat{x}_{s+1} be two consecutive boundary visit points. Then, as $\hat{x}_s, \hat{x}_{s+1} \rightarrow \hat{x}'$, we have the following asymptotics of ζ_ω :*

$$(5.18) \quad \lim_{\hat{x}_s, \hat{x}_{s+1} \rightarrow \hat{x}'} |\hat{x}_{s+1} - \hat{x}_s|^3 \zeta_\omega(x_{\text{in}}; \dots, \hat{x}_{s-1}, \hat{x}_s, \hat{x}_{s+1}, \hat{x}_{s+2}, \dots; x_{\text{out}}) \\ = \begin{cases} 0 & \text{if } \hat{x}_s \text{ and } \hat{x}_{s+1} \text{ are not successively visited,} \\ 10 \zeta_{\omega'}(x_{\text{in}}; \dots, \hat{x}_{s-1}, \hat{x}', \hat{x}_{s+2}, \dots; x_{\text{out}}) & \text{if } \hat{x}_s \text{ and } \hat{x}_{s+1} \text{ are successively visited,} \end{cases}$$

where $\omega' \in \{\pm 1\}^{N'-1}$ is obtained from $\omega \in \{\pm 1\}^{N'}$ by omitting the boundary visits corresponding to \hat{x}_{s+1} , as illustrated in Figure 5.3.

Remark 5.10. *The above asymptotics of ζ_ω , including their multiplicative constants, coincide with what one gets from the case of generic κ treated in [KP16] by letting $\kappa \rightarrow 2$. Namely, if $\zeta_\omega^{(\kappa)}$ is defined as the limit of $\prod_{s=1}^{N'} |x_{j_s+1} - x_{j_s}|^{-2/\kappa} \times \mathcal{Z}_{\alpha(\omega)}^{(\kappa)}$, generalizing our definition (5.6), then we have the following analogues of the above propositions. The non-zero asymptotics of Proposition 5.8 gets replaced by $\zeta_\omega^{(\kappa)} \sim C_1 |\hat{x}_s - x_{\text{in}}|^{\frac{\kappa-8}{\kappa}} \zeta_{\omega'}^{(\kappa)}$ with $C_1 = \frac{4 \cos^2(\frac{4}{\kappa}\pi)}{1+2 \cos(\frac{8}{\kappa}\pi)} \frac{\Gamma(1-\frac{8}{\kappa}) \Gamma(2-\frac{8}{\kappa})}{\Gamma(1-\frac{4}{\kappa}) \Gamma(2-\frac{12}{\kappa})}$. In the limit $\kappa \rightarrow 2$, we have $C_1 \rightarrow 2$, in*



FIGURE 5.4. In the setup of Proposition 5.8, the first boundary visit is on the left of x_{in} if and only if there is a link $\{j, j+1\}$ in the link pattern $\alpha(\omega)$ and $j+1$ is the index corresponding to the point x_{in} .



FIGURE 5.5. In the setup of Proposition 5.9, the visits to \hat{x}_s and \hat{x}_{s+1} are successive if and only if the link pattern $\alpha(\omega)$ contains the link $\{j+1, j+2\}$.

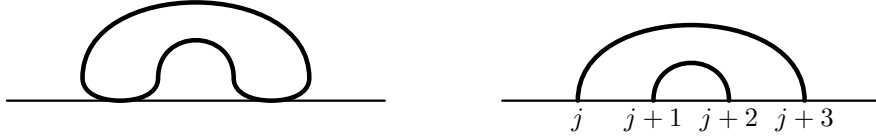


FIGURE 5.6. This cannot happen in the setup of Proposition 5.9.

accordance with Equation (5.17). Likewise, the non-zero asymptotics of Proposition 5.9 gets replaced by $\zeta_{\omega}^{(\kappa)} \sim C_2 |\hat{x}_{s+1} - \hat{x}_s|^{\frac{\kappa-8}{\kappa}} \zeta_{\omega'}^{(\kappa)}$ with $C_2 = \frac{2 \cos^2(\frac{4}{\kappa} \pi)}{\cos(\frac{8}{\kappa} \pi)} \frac{\Gamma(1-\frac{8}{\kappa})^2 \Gamma(2-\frac{8}{\kappa})}{\Gamma(1-\frac{4}{\kappa})^2 \Gamma(2-\frac{16}{\kappa})}$. In the limit $\kappa \rightarrow 2$, we have $C_2 \rightarrow 10$, in accordance with Equation (5.18).

In proving the above propositions, we make use of the combinatorial properties of inverse Fomin type sums listed in Propositions 2.18 and 2.21 in Section 2.6. Note that the replacing algorithm 5.3 yields an expression for ζ_{ω} as an inverse Fomin type sum.

Proof of Proposition 5.8. Assume for definiteness that \hat{x}_s is on the left side of x_{in} . Now, in the link pattern $\alpha(\omega)$ associated to the boundary visit order ω , the point \hat{x}_s corresponds to some consecutive indices $j-1, j$ and x_{in} to $j+1$. As illustrated in Figure 5.4, \hat{x}_s is the first boundary visit of ω if and only if there is a link $\{j, j+1\}$ in the link pattern $\alpha(\omega)$, that is, $\wedge^j \in \alpha(\omega)$. By the replacing algorithm 5.3, the kernel entries of the inverse Fomin type sum giving $\zeta_{\omega} = \mathfrak{Z}_{\alpha(\omega)}$ are for these indices

$$\mathfrak{K}(j-1, j) = 0, \quad \mathfrak{K}(j-1, j+1) = \frac{1}{|x_{\text{in}} - \hat{x}_s|^2}, \quad \text{and} \quad \mathfrak{K}(j, j+1) = \frac{2}{|x_{\text{in}} - \hat{x}_s|^3}.$$

All other kernel entries remain bounded in the limit $|x_{\text{in}} - \hat{x}_s| \rightarrow 0$. Hence, the desired asymptotics (5.17) is twice the coefficient of $\mathfrak{K}(j, j+1)$ in the inverse Fomin type sum $\zeta_{\omega} = \mathfrak{Z}_{\alpha(\omega)}$, because the product $\mathfrak{K}(j, j+1) \mathfrak{K}(j-1, j+1)$ does not appear. By Proposition 2.18(c), this coefficient is zero if $\wedge^j \notin \alpha(\omega)$ and by Proposition 2.21, it equals $\mathfrak{Z}_{\alpha(\omega) \setminus \wedge^j}^{\mathfrak{K} \setminus \diamond_j}$ if $\wedge^j \in \alpha(\omega)$. These two possibilities correspond to the two cases in the assertion (5.17). It remains to observe that $\mathfrak{Z}_{\alpha(\omega) \setminus \wedge^j}^{\mathfrak{K} \setminus \diamond_j} = \zeta_{\omega'}$, by the replacing algorithm 5.3. \square

Proof of Proposition 5.9. In the link pattern $\alpha(\omega)$ associated to the boundary visit order ω , the consecutive points \hat{x}_s and \hat{x}_{s+1} correspond to some pairs of consecutive indices $j, j+1$ and $j+2, j+3$, respectively. As illustrated in Figure 5.5, the boundary visits are successive if and only if there is a link $\{j+1, j+2\}$ in $\alpha(\omega)$, that is, $\wedge^{j+1} \in \alpha$. We again list the kernel entries at the indices of interest for

the inverse Fomin type sum $\zeta_\omega = \mathfrak{Z}_{\alpha(\omega)}$:

$$\begin{aligned}
 \mathfrak{K}(j, j+1) &= 0 & \mathfrak{K}(j+1, j+2) &= \frac{2}{|\hat{x}_{s+1} - \hat{x}_s|^3} \\
 \mathfrak{K}(j, j+2) &= \frac{1}{|\hat{x}_{s+1} - \hat{x}_s|^2} & \mathfrak{K}(j+1, j+3) &= \frac{-6}{|\hat{x}_{s+1} - \hat{x}_s|^4} \\
 \mathfrak{K}(j, j+3) &= \frac{-2}{|\hat{x}_{s+1} - \hat{x}_s|^3} & \mathfrak{K}(j+2, j+3) &= 0.
 \end{aligned}
 \tag{5.19}$$

All other kernel entries remain bounded in the limit $|\hat{x}_{s+1} - \hat{x}_s| \rightarrow 0$. Hence, as for Proposition 5.8, the asymptotics (5.18) can be read off from the coefficients of the four diverging kernels above.

Assume first that the boundary visits are not successive, or equivalently, $\wedge^{j+1} \notin \alpha$. Then, by Proposition 2.18(c), the coefficient of $\mathfrak{K}(j+1, j+2)$ is zero in $\zeta_\omega = \mathfrak{Z}_{\alpha(\omega)}$. By construction, in the link pattern $\alpha(\omega)$ there are no links $\{j, j+1\}$ or $\{j+2, j+3\}$, that is, $\wedge^j, \wedge^{j+2} \notin \alpha$. In such a situation, we can apply the interchange operation of Proposition 2.18(a) to verify that the coefficients of $\mathfrak{K}(j, j+2)$, $\mathfrak{K}(j+1, j+3)$, and $\mathfrak{K}(j, j+3)$ are also zero. Indeed, the first of these coefficients is obtained from the coefficient of $\mathfrak{K}(j+1, j+2)$ by interchanging the pair of indices $j, j+1$, the second by interchanging the pair $j+2, j+3$, and the third by interchanging both pairs. We conclude that all the kernel entries in (5.19) that diverge in the limit $|\hat{x}_{s+1} - \hat{x}_s| \rightarrow 0$ cancel out in the inverse Fomin type sum $\zeta_\omega = \mathfrak{Z}_{\alpha(\omega)}$. This proves the first case in Equation (5.18).

Assume then that the boundary visits are successive, or equivalently, $\wedge^{j+1} \in \alpha$. We first claim that no product of the non-zero kernel entries listed in (5.19) appears in the inverse Fomin type sum $\zeta_\omega = \mathfrak{Z}_{\alpha(\omega)}$. To see this, by Proposition 2.21, the coefficient of $\mathfrak{K}(j+1, j+2)$ is $\mathfrak{Z}_{\alpha(\omega) \setminus \wedge^{j+1}}^{\mathfrak{K} \setminus \diamond_{j+1}}$. Next, as illustrated in Figure 5.6, the link $\{j, j+3\}$ cannot belong to $\alpha(\omega)$, which implies $\wedge^j \notin \alpha(\omega) \setminus \wedge^{j+1}$. Then, Proposition 2.18(c) implies that the coefficient of $\mathfrak{K}(j, j+3)$ is zero in $\mathfrak{Z}_{\alpha(\omega) \setminus \wedge^{j+1}}^{\mathfrak{K} \setminus \diamond_{j+1}}$. Thus, the product $\mathfrak{K}(j+1, j+2) \mathfrak{K}(j, j+3)$ does not appear in the inverse Fomin type sum $\zeta_\omega = \mathfrak{Z}_{\alpha(\omega)}$. Other similar products are then excluded by repeated application of the interchange operation of Proposition 2.18(a) with the pairs of indices $j, j+1$ or $j+2, j+3$.

Now we can compute the limit of interest (5.18) simply by adding up the contributions of the individual divergent kernel entries in Equation (5.19). The entry $\mathfrak{K}(j, j+2)$ has too mild a divergence to contribute, so there are in fact only three contributions to consider. We already saw that the coefficient of $\mathfrak{K}(j+1, j+2)$ is $\mathfrak{Z}_{\alpha(\omega) \setminus \wedge^{j+1}}^{\mathfrak{K} \setminus \diamond_{j+1}}$, and by the replacing algorithm 5.3, we have $\mathfrak{Z}_{\alpha(\omega) \setminus \wedge^{j+1}}^{\mathfrak{K} \setminus \diamond_{j+1}} = \zeta_{\omega'}$. The entry $\mathfrak{K}(j+1, j+2)$ thus contributes

$$2 \zeta_{\omega'}(x_{\text{in}}; \dots, \hat{x}_{s-1}, \hat{x}', \hat{x}_{s+2}, \dots; x_{\text{out}}).
 \tag{5.20}$$

Next, applying twice the antisymmetry under the interchange operation of Proposition 2.18(a) gives the coefficient of $\mathfrak{K}(j, j+3)$ in terms of the previous one. Note, in addition, that comparing the coefficient of $\mathfrak{K}(j, j+3)$ to the replacing algorithm 5.3 to yield $\zeta_{\omega'}$, we have instead of x_{j+2} differentiated with respect to x_{j+1} , i.e., the smaller of the two real points x_{j+1} and x_{j+2} that now correspond to the collapsed boundary visit in ω' . Thus, we use Proposition 2.18(a) a third time to interchange $j+1$ and $j+2$, and obtain $\zeta_{\omega'}$. Thus, the entry $\mathfrak{K}(j, j+3)$ contributes

$$(-1)^3 \times (-2) \zeta_{\omega'}(x_{\text{in}}; \dots, \hat{x}_{s-1}, \hat{x}', \hat{x}_{s+2}, \dots; x_{\text{out}}).
 \tag{5.21}$$

We are only left with finding the coefficient of $\mathfrak{K}(j+1, j+3)$. Proposition 2.18(a) relates this to the coefficient of $\mathfrak{K}(j+1, j+2)$, which is $\zeta_{\omega'}$, and we see that the coefficient of $\mathfrak{K}(j+1, j+3)$ is an inverse Fomin type sum otherwise similar to $\zeta_{\omega'}$, except that we have not differentiated with respect to either one of the boundary points x_j and x_{j+2} related to the collapsed boundary visit in ω' . An argument identical to the proof of the replacing algorithm 5.3 allows us to differentiate with respect to x_{j+2} and

cancel one power of $|\hat{x}_{s+1} - \hat{x}_s|$. The contribution of $\mathfrak{R}(j+1, j+3)$ to the limit (5.18) is thus

$$(5.22) \quad -1 \times (-6) \zeta_{\omega'}(x_{\text{in}}; \dots, \hat{x}_{s-1}, \hat{x}', \hat{x}_{s+2}, \dots; x_{\text{out}}).$$

Summing the contributions given in Equations (5.20), (5.21), and (5.22), we obtain the asserted limit (5.18). This concludes the proof. \square

APPENDIX A. EXAMPLE BOUNDARY VISIT FORMULAS

In this appendix, we provide a few examples of the boundary visit amplitudes ζ and the order-refined amplitudes ζ_{ω} with small numbers of marked points.

A.1. One boundary visit. For one boundary visit, $N' = 1$, there is only one possible order (so we omit ω from the notation). The corresponding amplitude is obtained using replacing algorithm 5.3:

$$\zeta(x_{\text{in}}; \hat{x}; x_{\text{out}}) = \frac{\text{diagram}}{(\hat{x} - x_{\text{in}})^3 (x_{\text{out}} - \hat{x})^3} = \frac{2(x_{\text{out}} - x_{\text{in}})}{(\hat{x} - x_{\text{in}})^3 (x_{\text{out}} - \hat{x})^3}.$$

One can directly check that this function solves the PDE system in Theorem 3.17 and asymptotics properties (5.17).

A.2. Two boundary visits. For two boundary visits, $N' = 2$, there are two essentially different cases: boundary visits on the same side or boundary visits on the opposite sides. As representative examples, we consider the orders $\omega = (-, -)$ and $\omega = (-, +)$.

For the visits on the same side, using replacing algorithm 5.3, we find the solution

$$\begin{aligned} \zeta_{--}(x_{\text{in}}; \hat{x}_1, \hat{x}_2; x_{\text{out}}) &= \frac{\text{diagram}}{(\hat{x}_1 - x_{\text{in}})^2 (\hat{x}_2 - x_{\text{in}})^2 (\hat{x}_2 - x_{\text{out}})^2 (\hat{x}_1 - x_{\text{out}})^2} \\ &= \det \begin{pmatrix} \frac{-2}{(\hat{x}_2 - x_{\text{in}})^3} & \frac{-2}{(\hat{x}_2 - x_{\text{out}})^3} & \frac{-6}{(\hat{x}_2 - \hat{x}_1)^4} \\ \frac{1}{(\hat{x}_1 - x_{\text{in}})^2} & \frac{1}{(\hat{x}_1 - x_{\text{out}})^2} & 0 \\ \frac{1}{(\hat{x}_2 - x_{\text{in}})^2} & \frac{1}{(\hat{x}_2 - x_{\text{out}})^2} & \frac{2}{(\hat{x}_2 - \hat{x}_1)^3} \end{pmatrix} \\ &\quad + \det \begin{pmatrix} \frac{-2}{(\hat{x}_2 - x_{\text{in}})^3} & \frac{-2}{(\hat{x}_2 - x_{\text{out}})^3} & \frac{-2}{(\hat{x}_2 - \hat{x}_1)^3} \\ \frac{1}{(\hat{x}_2 - x_{\text{in}})^2} & \frac{1}{(\hat{x}_2 - x_{\text{out}})^2} & \frac{1}{(\hat{x}_2 - \hat{x}_1)^2} \\ \frac{-2}{(\hat{x}_1 - x_{\text{in}})^3} & \frac{-2}{(\hat{x}_1 - x_{\text{out}})^3} & 0 \end{pmatrix} \\ &= \frac{4\hat{x}_1 + 2\hat{x}_2 - 6x_{\text{in}}}{(\hat{x}_1 - \hat{x}_2)^4 (\hat{x}_1 - x_{\text{out}})^2 (\hat{x}_2 - x_{\text{in}})^3} - \frac{2\hat{x}_1 + 4\hat{x}_2 - 6x_{\text{in}}}{(\hat{x}_1 - \hat{x}_2)^4 (\hat{x}_1 - x_{\text{in}})^3 (\hat{x}_2 - x_{\text{out}})^2} \\ &\quad + \frac{4\hat{x}_1 - 4x_{\text{in}}}{(\hat{x}_1 - \hat{x}_2)^3 (x_{\text{out}} - \hat{x}_1)^3 (\hat{x}_2 - x_{\text{in}})^3} + \frac{4\hat{x}_2 - 4x_{\text{in}}}{(\hat{x}_1 - \hat{x}_2)^3 (\hat{x}_1 - x_{\text{in}})^3 (x_{\text{out}} - \hat{x}_2)^3}. \end{aligned}$$

Up to a coordinate change and an overall multiplicative constant, this formula coincides with the specialization to $\kappa = 2$ of the Schramm-Zhou two-point boundary proximity function of the chordal SLE_{κ} [SZ10], as well as with an SLE_{κ} boundary zig-zag amplitude in [JJ16].

For the visits on opposite sides, using replacing algorithm 5.3, we find the solution

$$\begin{aligned}
\zeta_{-+}(x_{\text{in}}; \hat{x}_1, \hat{x}_2; x_{\text{out}}) &= \text{Diagram} \\
&= \det \begin{pmatrix} \frac{-2}{(\hat{x}_2 - x_{\text{in}})^3} & \frac{-2}{(\hat{x}_2 - \hat{x}_1)^3} & \frac{-6}{(\hat{x}_2 - \hat{x}_1)^4} \\ \frac{1}{(\hat{x}_2 - x_{\text{in}})^2} & \frac{1}{(\hat{x}_2 - \hat{x}_1)^2} & \frac{2}{(\hat{x}_2 - \hat{x}_1)^3} \\ \frac{1}{(x_{\text{out}} - x_{\text{in}})^2} & \frac{1}{(x_{\text{out}} - \hat{x}_1)^2} & \frac{2}{(x_{\text{out}} - \hat{x}_1)^3} \end{pmatrix} \\
&= \frac{2(\hat{x}_1 - x_{\text{in}})^2(\hat{x}_2 - x_{\text{out}})^2(\hat{x}_1\hat{x}_2 - 3\hat{x}_1x_{\text{in}} + 2\hat{x}_1x_{\text{out}} + 2\hat{x}_2x_{\text{in}} - 3\hat{x}_2x_{\text{out}} + x_{\text{in}}x_{\text{out}})}{(\hat{x}_1 - \hat{x}_2)^6(\hat{x}_1 - x_{\text{out}})^3(\hat{x}_2 - x_{\text{in}})^3(x_{\text{in}} - x_{\text{out}})^2}.
\end{aligned}$$

Up to a coordinate change and an overall multiplicative constant, this formula coincides with a specialization to $\kappa = 2$ of an SLE $_{\kappa}$ boundary zig-zag amplitude in [JK16].

Again, one can check that these functions solve the PDE system in Theorem 3.17 and asymptotics properties (5.17) hold.

REFERENCES

- [BB03] M. Bauer and D. Bernard. SLE, CFT and zig-zag probabilities. *Proceedings of the conference ‘Conformal Invariance and Random Spatial Processes’, Edinburgh*, 2003.
- [BBK05] M. Bauer, D. Bernard, and K. Kytölä. Multiple Schramm-Loewner evolutions and statistical mechanics martingales. *J. Stat. Phys.*, 120(5-6):1125–1163, 2005.
- [BPW18] V. Beffara, E. Peltola, and H. Wu. On the uniqueness of global multiple SLEs. Preprint, <http://arxiv.org/abs/1801.07699>, 2018.
- [BPZ84a] A. A. Belavin, A. M. Polyakov, and A. B. Zamolodchikov. Infinite conformal symmetry in two-dimensional quantum field theory *Nucl. Phys. B*, 241(2):333–380, 1984.
- [BPZ84b] A. A. Belavin, A. M. Polyakov, and A. B. Zamolodchikov. Infinite conformal symmetry of critical fluctuations in two dimensions. *J. Stat. Phys.*, 34(5-6):763–774, 1984.
- [BLV16] C. Beneš, G. F. Lawler, and F. Viklund. Scaling limit of the loop-erased random walk Green’s function. *Probab. Theory Related Fields*, 166(1):271–319, 2016.
- [BSA88] L. Benoit and Y. Saint-Aubin. Degenerate conformal field theories and explicit expressions for some null vectors. *Phys. Lett.*, B215(3):517–522, 1988.
- [CS11] D. Chelkak and S. Smirnov. Discrete complex analysis on isoradial graphs. *Adv. Math.*, 228(3):1590–1630, 2011.
- [CS12] D. Chelkak and S. Smirnov. Universality in the 2D Ising model and conformal invariance of fermionic observables. *Invent. Math.*, 189(3):515–580, 2012.
- [CFL28] R. Courant, K. Friedrichs, and H. Lewy. Über die partiellen Differenzengleichungen der mathematischen Physik. *Math. Ann.*, 100(1):32–74, 1928.
- [Dub06a] J. Dubédat. Euler integrals for commuting SLEs. *J. Stat. Phys.*, 123(6):1183–1218, 2006.
- [Dub06b] J. Dubédat. Excursion decompositions for SLE and Watts’ crossing formula. *Probab. Theory Rel. Fields*, 134(3):453–488, 2006.
- [Dub07] J. Dubédat. Commutation relations for SLE. *Comm. Pure Appl. Math.*, 60(12):1792–1847, 2007.
- [Dub15a] J. Dubédat. SLE and Virasoro representations: Localization. *Comm. Math. Phys.*, 336(2):695–760, 2015.
- [Dub15b] J. Dubédat. SLE and Virasoro representations: Fusion. *Comm. Math. Phys.*, 336(2):761–809, 2015.
- [Fel89] G. Felder. BRST approach to minimal models. *Nucl. Phys. B*, 317(1):215–236, 1989. Erratum *ibid.* B, 324(2):548, 1989.
- [FF90] B. L. Feigin and D. B. Fuchs. Representations of the Virasoro algebra. In *Representation of Lie groups and related topics*, volume 7 of *Adv. Stud. Contemp. Math.*, pages 465–554. Gordon and Breach, New York, 1990.
- [FFK89] G. Felder, J. Fröhlich, and G. Keller. Braid matrices and structure constants for minimal conformal models. *Comm. Math. Phys.*, 124(4):647–664, 1989.
- [FP19] S. M. Flores and E. Peltola. Monodromy invariant CFT correlation functions of first column Kac operators. In preparation, 2019.
- [FK15a] S. M. Flores and P. Kleban. A solution space for a system of null-state partial differential equations, Part I. *Comm. Math. Phys.*, 333(1):389–434, 2015.
- [FK15b] S. M. Flores and P. Kleban. A solution space for a system of null-state partial differential equations, Part II. *Comm. Math. Phys.*, 333(1):435–481, 2015.

- [FK15c] S. M. Flores and P. Kleban. A solution space for a system of null-state partial differential equations, Part III. *Comm. Math. Phys.*, 333(2):597–667, 2015.
- [Fom01] S. Fomin. Loop-erased walks and total positivity. *Trans. Amer. Math. Soc.*, 353(9):3363–3583, 2001.
- [DMS97] P. Di Francesco, P. Mathieu, and D. Sénéchal. *Conformal field theory*. Springer Verlag, 1997.
- [GV85] I. Gessel and G. Viennot. Binomial determinants, paths, and hook length formulae. *Adv. Math.*, 58(3):300–321, 1985.
- [IK11] K. Iohara and Y. Koga. *Representation theory of the Virasoro algebra*. Springer Monographs in Mathematics. Springer, 2011.
- [JJK16] N. Jokela, M. Järvinen, and K. Kytölä. SLE boundary visits. *Ann. Henri Poincaré*, 17(6):1263–1330, 2016.
- [Kac78] V. Kac. Highest weight representations of infinite dimensional Lie algebras. *Proceedings of ICM, Helsinki 1978*, pages 299–304, 1980.
- [KN04] W. Kager and B. Nienhuis. A guide to stochastic Löwner evolution and its applications. *J. Stat. Phys.*, 115(5):1149–1229, 2004.
- [KM59] S. Karlin and J. McGregor. Coincidence probabilities. *Pacific J. Math.*, 9(4):1141–1164, 1959.
- [KKP19] A. Karrila, K. Kytölä, and E. Peltola. Conformal blocks, q -combinatorics, and quantum group symmetry. To appear in *Annales de l’Institut Henri Poincaré D*, 2019.
- [Kar19] A. Karrila. Multiple SLE type scaling limits: from local to global. Preprint, <https://arxiv.org/abs/1903.10354>, 2019.
- [Ken00] R. Kenyon. The asymptotic determinant of the discrete Laplacian. *Acta Math.*, 185(2):239–286, 2000.
- [KW11a] R. W. Kenyon and D. B. Wilson. Boundary partitions in trees and dimers. *Trans. Amer. Math. Soc.*, 363(3):1325–1364, 2011.
- [KW11b] R. W. Kenyon and D. B. Wilson. Double-dimer pairings and skew Young diagrams. *Electr. J. Combinatorics*, 18(1):130–142, 2011.
- [KW15] R. W. Kenyon and D. B. Wilson. Spanning trees of graphs on surfaces and the intensity of loop-erased random walk on planar graphs. *J. Amer. Math. Soc.*, 28(4):985–1030, 2015.
- [Kim12] J. S. Kim. Proofs of two conjectures of Kenyon and Wilson on Dyck tilings. *J. Combin. Theory Ser. A*, 119(8):1692–1710, 2012.
- [KMPW14] J. S. Kim, K. Mészáros, G. Panova, D. B. Wilson. Dyck tilings, increasing trees, descents, and inversions. *J. Combin. Theory Ser. A*, 122(C):9–27, 2014.
- [KL07] M. J. Kozdron and G. F. Lawler. The configurational measure on mutually avoiding SLE paths. In *Universality and Renormalization: From Stochastic Evolution to Renormalization of Quantum Fields*, Fields Inst. Commun. Amer. Math. Soc., 2007.
- [KP16] K. Kytölä and E. Peltola. Pure partition functions of multiple SLEs. *Comm. Math. Phys.*, 346(1):237–292, 2016.
- [KP19] K. Kytölä and E. Peltola. Conformally covariant boundary correlation functions with a quantum group. To appear in *J. Eur. Math. Soc.*, 2019.
- [Law05] G. F. Lawler. *Conformally invariant processes in the plane*. American Mathematical Society, 2005.
- [Law91] G. F. Lawler. *Intersections of random walks*. Birkhäuser, 1991.
- [Law14] G. F. Lawler. The probability that planar loop-erased random walk uses a given edge. *Electron. Commun. Probab.*, 19:1–13, 2014.
- [LSW04] G. F. Lawler, O. Schramm, and W. Werner. Conformal invariance of planar loop-erased random walks and uniform spanning trees. *Ann. Probab.*, 32(1B):939–995, 2004.
- [LV16] G. F. Lawler and F. Viklund. Convergence of loop-erased random walk in the natural parametrization. Preprint, <http://arxiv.org/abs/1603.05203>, 2016.
- [LV19] J. Lenells and F. Viklund. Schramm’s formula and the Green’s function for multiple SLE. *J. Stat. Phys.*, 176(4):873–931.
- [Lin73] B. Lindström. On the vector representations of induced matroids. *Bull. Lond. Math. Soc.*, 5(1):85–90, 1973.
- [MS16] J. Miller and S. Sheffield. Imaginary geometry II: Reversibility of $SLE_{\kappa}(\rho_1; \rho_2)$ for $\kappa \in (0, 4)$. *Ann. Probab.*, 44(3):1647–1722, 2016.
- [PW14] G. Panova and D. B. Wilson. Pfaffian formulas for spanning tree probabilities. *Combin. Probab. Comput.*, 26(1):118–137, 2017.
- [Pel19] E. Peltola. Basis for solutions of the Benoit & Saint-Aubin PDEs with particular asymptotic properties. To appear in *Ann. Inst. H. Poincaré D*, 2019.
- [PW19] E. Peltola and H. Wu. Global and Local Multiple SLEs for $\kappa \leq 4$ and Connection Probabilities for Level Lines of GFF. *Comm. Math. Phys.* 366(2):469–536, 2019.
- [Pem91] R. Pemantle. Choosing a spanning tree for the integer lattice uniformly. *Ann. Probab.*, 19(4):1559–1574, 1991.
- [Pon18] A. Poncelet. Schramm’s formula for multiple loop-erased random walks. *J. Stat. Mech.: Theory and Exp.*, 103106, 2018.
- [Rib14] S. Ribault. Conformal field theory on the plane. <http://arxiv.org/abs/1406.4290>, 2014.
- [RS05] S. Rohde and O. Schramm. Basic properties of SLE. *Ann. Math.*, 161(2):883–924, 2005.
- [Sch00] O. Schramm. Scaling limits of loop-erased random walks and uniform spanning trees. *Israel J. Math.*, 118(1):221–288, 2000.

- [SZ10] O. Schramm and W. Zhou. Boundary proximity of SLE. *Probab. Th. Rel. Fields*, 146(3-4):435–450, 2010.
- [SW11] S. Sheffield and D. B. Wilson. Schramm’s proof of Watts’ formula. *Ann. Probab.*, 39(5):1844–1863, 2011.
- [SZ12] K. Shigechi and P. Zinn-Justin. Path representation of maximal parabolic Kazhdan–Lusztig polynomials. *J. Pure Appl. Algebra*, 216(11):2533–2548, 2012.
- [Wil96] D. Wilson. Generating random spanning trees more quickly than the cover time. *Proc. 28th Annual ACM Symposium on the Theory of Computing*, pages 296–303, 1996.
- [Wu18] Hao Wu. Hypergeometric SLE: conformal Markov characterization and applications. Preprint, <http://arxiv.org/abs/1703.02022> (v4), 2018.
- [YY11] A. Yadin and A. Yehudayoff. Loop-erased random walk and Poisson kernel on planar graphs. *Ann. Probab.*, 39(4):1243–1285, 2011.
- [Zha08] D. Zhan. The scaling limits of planar LERW in finitely connected domains. *Ann. Probab.*, 36(2):467–529, 2008.